AD-A071 596 CALIFORNIA UNIV RIVERSIDE DEPT OF PHYSICS F/G 20/8
CALCULATION OF ELECTRON-CARBON MONOXIDE VIBRATIONAL TRANSITION --ETC(U)
APR 79 R T POE, B H CHOI F33615-77-C-2011
UNCLASSIFIED AFAPL-TR-79-2022 NL

1 OF 2
AD A071596

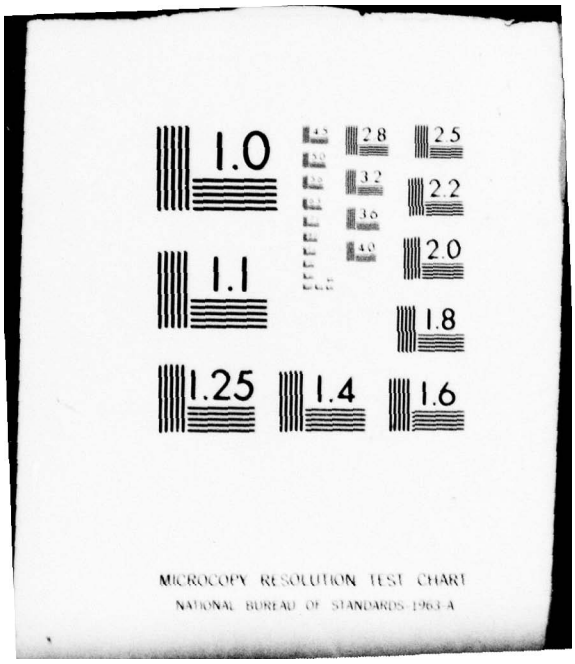
1.0
1.1
1.25
1.4
1.6
1.8
2.0
2.2
2.5
2.8
3.2
3.6
4.0
MICROCOPY RESOLUTION TEST CHART
NATIONAL BUREAU OF STANDARDS-1963-A

(2) LEVEL II

Sc

AFAPL-TR-79-2022

CALCULATION OF ELECTRON-CARBON MONOXIDE VIBRATIONAL TRANSITION CROSS SECTIONS

DEPARTMENT OF PHYSICS
UNIVERSITY OF CALIFORNIA
RIVERSIDE, CALIFORNIA 92521

April 1979

TECHNICAL REPORT AFAPL-TR-79-2022
Interim Report for Period April 1977-January 1979

Approved for public release; distribution unlimited.

AIR FORCE AERO PROPULSION LABORATORY
AIR FORCE WRIGHT AERONAUTICAL LABORATORIES
AIR FORCE SYSTEMS COMMAND
WRIGHT-PATTERSON AIR FORCE BASE, OHIO 45433

NOTICE

When Government drawings, specifications, or other data are used for any purpose other than in connection with a definitely related Government procurement operation, the United States Government thereby incurs no responsibility nor any obligation whatsoever; and the fact that the government may have formulated, furnished, or in any way supplied the said drawings, specifications, or other data, is not to be regarded by implication or otherwise as in any manner licensing the holder or any other person or corporation, or conveying any rights or permission to manufacture, use, or sell any patented invention that may in any way be related thereto.

This report has been reviewed by the Information Office (OI) and is releasable to the National Technical Information Service (NTIS). At NTIS, it will be available to the general public, including foreign nations.

This technical report has been reviewed and is approved for publication.

WILLIAM F. BAILEY, Major, USAF
Research Physicist

PHILIP E. STOVER
Chief, High Power Branch

FOR THE COMMANDER

JAMES D. REAMS
Chief, Aerospace Power Division

"If your address has changed, if you wish to be removed from our mailing list, or if the addressee is no longer employed by your organization please notify AFAPL/POD *, W-PAFB, OH 45433 to help us maintain a current mailing list".*

Copies of this report should not be returned unless return is required by security considerations, contractual obligations, or notice on a specific document.

AIR FORCE/56780/12 July 1979 — 140

SECURITY CLASSIFICATION OF THIS PAGE (When Data Entered)

REPORT DOCUMENTATION PAGE

READ INSTRUCTIONS BEFORE COMPLETING FORM

1. REPORT NUMBER: AFAPL-TR-79-2022	2. GOVT ACCESSION NO.
3. RECIPIENT'S CATALOG NUMBER	
4. TITLE (and Subtitle): CALCULATION OF ELECTRON-CARBON MONOXIDE VIBRATIONAL TRANSITION CROSS SECTIONS.	5. TYPE OF REPORT & PERIOD COVERED: Final Technical Report. 15 April 1977-15 January 1979
	6. PERFORMING ORG. REPORT NUMBER
7. AUTHOR(s): Robert T. Poe, B. H. Choi	8. CONTRACT OR GRANT NUMBER(s): F33615-77-C-2011
9. PERFORMING ORGANIZATION NAME AND ADDRESS: Department of Physics, University of California, Riverside, California 92521	10. PROGRAM ELEMENT, PROJECT, TASK AREA & WORK UNIT NUMBERS: 2301 S2 03
11. CONTROLLING OFFICE NAME AND ADDRESS: Air Force Aero Propulsion Laboratory (POD), Wright-Patterson Air Force Base, Ohio 45433	12. REPORT DATE: April 1979
	13. NUMBER OF PAGES: 120
14. MONITORING AGENCY NAME & ADDRESS (if different from Controlling Office): 126 p.	15. SECURITY CLASS. (of this report): Unclassified
	15a. DECLASSIFICATION/DOWNGRADING SCHEDULE

16. DISTRIBUTION STATEMENT (of this Report)

Approved for public release; distribution unlimited

17. DISTRIBUTION STATEMENT (of the abstract entered in Block 20, if different from Report)

18. SUPPLEMENTARY NOTES

19. KEY WORDS (Continue on reverse side if necessary and identify by block number)

Electron-Carbon Monoxide Scattering
Vibrational Transition Cross Section
Elastic Scattering Cross Section
Hybrid Theory

20. ABSTRACT (Continue on reverse side if necessary and identify by block number)

Critical evaluations of theories used for electron-molecule scattering calculation were made. The hybrid theory appears to be best suited for the calculation of e-CO vibrational transition cross sections. A reformulation of hybrid theory was made in terms of the total angular momentum representation. The vibrational transition cross sections of e-CO scattering were computed in the energy range of 0-10 eV, based on this reformulation. The → next page

DD FORM 1 JAN 73 1473 EDITION OF 1 NOV 65 IS OBSOLETE

SECURITY CLASSIFICATION OF THIS PAGE (When Data Entered)

agreement between the results of present calculation and the experimental measurements for 0-v vibrational transitions were reasonably good. Furthermore, the present calculations predicted the strong resonance peak at 1.4 eV in the 1-2 vibrational transition cross section. In general, the rate of vibrational excitations decreases as the change of vibrational quantum numbers increases.

FOREWORD

This report describes an effort conducted by personnel of the Department of Physics, University of California, Riverside, under Contract F33615-77-C-2011, Project 2301.

The work reported herein was performed during the period 15 April 1977 to 15 October 1978, under the direction of the authors, Dr. Robert T. Poe, principal investigator, and Dr. B. H. Choi, co-investigator. The report was released by the authors in November 1978.

The authors wish to thank Major William F. Bailey and Dr. Alan Garscadden for their valuable discussions. The authors wish to thank Mr. James C. Sun and Mrs. Glenna Paschal for their assistance in preparing this report.

TABLE OF CONTENTS

TABLE OF CONTENTS (cont'd)

LIST OF ILLUSTRATIONS

LIST OF ILLUSTRATIONS (cont'd)

LIST OF TABLES

SECTION I
INTRODUCTION

Present and future efforts in gas discharge laser development, laser fusion, isotope separation, combustion, atmospheric physics, as well as other energy-related fields, rely on a quantitative understanding of electron scattering processes for a variety of small molecules. The need for quantitatively accurate electron-molecule scattering cross sections is putting stringent demands on present theoretical methods. As this need becomes more pressing, it is important to assess the scope of those methods which are presently being used in the study of electron-molecule collisions, to identify the key advantages and limitations of the various methods and to see which techniques are best suited for a quantitative study of the important problems in molecular scattering such as the vibrational transitions.

Straightforward application of the simultaneous vibrotational close-coupling theory to the study of vibrational transitions of electron-molecule scattering has met a severe computational difficulty. The number of channels of the coupled differential equation is so large that it is almost impossible to carry out the calculation with the capacity of the present day computer even when 7-8 vibrational states are included. That is the reason that the hybrid theory was proposed.

In this report, we made critical evaluations of theories used for electron-molecule scattering calculation and found out that the hybrid theory is best suited for the present e-CO project. We further present a reformulation of this theory. The vibrational transition cross sections of e-CO scattering were computed in the energy range of 0-10 eV, based on the present reformulation. The final results are reported.

SECTION II
REVIEW AND EVALUATION OF THEORY

In this Section, we present a review of the theoretical approaches which have been used for the electron-diatomic molecule scattering and discuss the advantages and disadvantages of those approaches.

1. Semiclassical Approach

The calculations of electron-molecule scattering cross section with the semi-classical approach such as the impact parameter method and the binary encounter theory (Ref. 1) are scarce, while they are abundant for atom, ion-atom, molecule scatterings. The reason is that the deBroglie wavelength of the incident electron is too large for the semiclassical approach to be appropriate for the study of electron-molecule scattering.

2. Feshbach Approach and Boomerang Model

These approaches appear to be appropriate for describing the electron-molecule resonance scattering (Refs. 2 and 3). However, it is difficult to obtain rigorous ab initio solutions from these methods. The shape of resonance cross section as a function of the incident (kinetic) energy of the electron is determined through resonance energies and widths. These are treated as the empirical parameters in the present approaches. Thus they become more or less phenomenological for the interpretation of experimental data and do not have the capability of predicting the experimental measurements. There is no doubt that these methods are useful for the physical explanation of a given experiment.

This is the most general and realistic approach for electron-molecule scattering. Only a few calculations for the rotational transition of light molecule exist with the present close-coupling theory (Ref. 11, 12 and 13). The results show that the agreement with the experimental data is indeed very good. However, to carry out the close-coupling calculation for the vibrational and rotational transition cross section is a formidable task, because the dimension of the coupled differential equation is very large in that case. Therefore, this method is impractical for the study of electron-molecule vibrational and rotational transitions.

7. Fixed-Nuclei Approximation

In this approximation, both the separation of two nuclei and the direction of internuclear axis of target molecule are fixed during the collision process. There exist a number of calculations for the vibrationally elastic cross sections of electron-molecule scattering using this approximation (Refs. 14, 15 and 16). In spite of the simplicity of the present approach, the agreement with the experiment is fairly good when the exchange and polarization potentials are properly taken into account.

8. R-matrix Theory

This approach was based on the fixed-nuclei approximation. The wavefunctions of internal region are computed in a similar manner as the bound state approach and those of external region are obtained with the fixed-nuclei close-coupling calculation. Both wave functions are matched on the appropriate boundary. However, in addition to the complexity of this method, it has not yet been fully developed to evaluate the vibrational transition cross sections (Refs. 17 and 18).

9. Adiabatic-Nuclei Approximation for Rotational Transitions

It is not possible to obtain the rotational transitions in the fixed-nuclei approximation. Thus the present scheme was developed. In the adiabatic-nuclei approach, the scattering amplitude for the rotational transitions is obtained from

$$f_{\beta,\alpha}(\theta,\phi) = \int d\Omega \; g_\beta^*(\Omega) f(\theta,\phi,\Omega) g_\alpha(\Omega)$$

Here, $f(\theta,\phi,\Omega)$ is the fixed-nuclei scattering amplitude and $g_\alpha(\Omega)$, $g_\beta(\Omega)$ are the initial and the final rotational wave functions of the target molecule. It should be noted that this approach is much simpler than the rotational close-coupling theory where the rotational states are dynamically coupled. When the SEP (Static + Exchange + Polarization) potential are used for the calculation of cross sections, the agreement with the experimental data are reasonably good. (Refs. 19, 20 and 21).

10. Hybrid Approach

The hybrid theory was derived from the fixed- and adiabatic-nuclei approach to study the vibrational and rotational transitions for electron-molecule scattering. The condition of the fixed internuclear separation in the fixed-nuclei approximation is relaxed and the vibrational states of the target molecule are coupled dynamically. The simultaneous vib-rotational transition of target molecule are obtained by incorporating the adiabatic nuclei procedure (Refs. 22 and 26). For the calculation of vibrational and rotational transition cross sections, the present approach will be most appropriate from the practical point of view. In this approach, it is not too difficult to couple the vibrational states up to ∿10 levels, while that is not possible

in the vib-rotational close-coupling theory. The numerical results of the vibrational and rotational transition cross sections for electron-nitrogen molecule scattering (Ref. 22) show that the agreements with the experimental data are good.

11. Adiabatic-Nuclei Approximation for Vibrational Transitions

This is also called vibrational impulse approximation (Refs. 23 and 24). The elastic transition matrix elements are obtained as functions of the internuclear separations. They are computed through the fixed-nuclei close-coupling calculations performed at each internuclear separation. The vibrational transition matrix elements are then obtained from averaging the above elastic transition matrix elements over initial and final vibrational wave functions. It is seen that this method is simpler than the hybrid approach.

On the other hand, the elastic transition matrix elements are, in general, violently oscillating functions of the internuclear separations for resonant wave, while they are smooth function for non-resonant wave. Therefore, this method is not suitable for evaluating the vibrational transition matrix elements (or cross sections) for resonant wave. However, this approach could be efficient for computing the vibrational transition cross sections in the non-resonant energy region.

12. Multiple Scattering Method

The atoms in the target molecule are treated as independent scattering centers for short range interaction potential. This method is basically similar to the "Two Potential Approach" employed by us (Ref. 45) for studying intermediate and high energy electron-molecule scattering and yields reasonable results in those energy regions. Recently, some workers

applied this method to low energy (0~10 eV) electron-molecule scattering (Ref. 25). The results show that this method does not account for the substructures of the vibrational excitation cross section in the low energy resonance region.

SECTION III
DEVELOPMENT OF THEORY

Our review of theories for electron-molecule scattering indicates that the hybrid theory, as originally proposed by Chandra and Temkin (Ref. 22), will be the most appropriate theoretical approach for the present purpose.

We have reformulated the hybrid theory in terms of the total (electron + target molecule) angular momentum representation. This has not been done in the original formulation of Chandra and Temkin. In our reformulation, the formulae of cross sections become more concise and thus they can be easily programmed into computer code. Furthermore, the relationship with the general and accurate vib-rotational close-coupling theory is transparent because this theory is also in terms of the total angular momentum representation. Therefore, the hybrid theory can be improved systematically through our reformulation in the future. The equations derived according to the formulation of Choi and Poe (Ref. 26) were used in the code programming for the present e-CO project. In the following, we describe this reformulation which is the main theoretical feature of this calculation.

The scattering wave function $\Psi^{(+)}_{vjm_j}(\vec{r},\vec{R})$ of the electron-diatomic molecule system satisfies the following Schrodinger equation

$$H\Psi^{(+)}_{vjm_j}(\vec{r},\vec{R}) = E\Psi^{(+)}_{vjm_j}(\vec{r},\vec{R})$$

with

$$H = -\frac{h^2}{2\mu_e}\nabla_r^2 - \frac{h^2}{2\mu_N}\nabla_R^2 + V(r,R,\gamma) + \varepsilon_o(R)$$

Here, $\vec{r}$ is the position vector of the incident electron relative to the center-of-mass of target nuclei and $\vec{R}$ is the inter-nuclei vector (see Figure1), and

$$\mu_e = \frac{m(M_A+M_B)}{M_A+M_B+m}\ ,\ \mu_N = \frac{M_A M_B}{M_A+M_B}$$

M_A,M_B and m are the masses of nuclei A and B, and electron, respectively. The v is the vibrational quantum number, and j,m_j are the rotational quantum number and its projection. $V(r,R,\gamma)$ is the electron-molecule interaction potential with γ the angle between $\vec{r}$ and $\vec{R}$. $\varepsilon_o(R)$ is the interatomic potential in the ground electronic state of target molecule.

In hybrid theory, the vib-rotational transition cross sections are obtained from a synthesis of close-coupling theory for vibrational states with fixed-nuclei approximation and adiabatic nuclei theory for rotational states. The rotational angular momenta of target molecule are neglected in H, that is,

$$-\frac{h^2}{2\mu_N}\nabla_R^2 = -\frac{\hbar^2}{2\mu_N}\frac{1}{R^2}\frac{\partial}{\partial R}\left(R^2\frac{\partial}{\partial R}\right) - \frac{\hbar^2}{2\mu_N R^2}\left(\vec{R}\times\nabla_R\right)^2$$

$$\approx -\frac{h^2}{2\mu_N}\frac{1}{R^2}\frac{\partial}{\partial R}\left(R^2\frac{\partial}{\partial R}\right) \qquad (1)$$

The radial wave function and energy level, $\phi_v(R)$ and ε_v, are

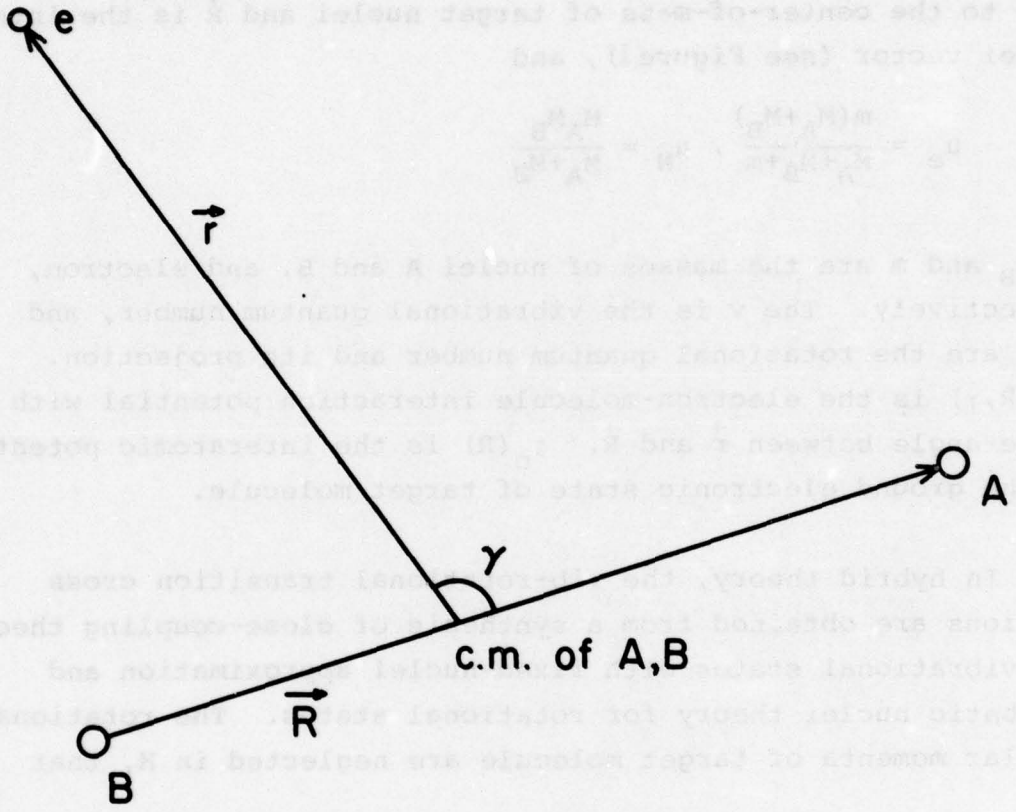

Figure 1. Geometry of the Scattering Between an Atom and a Diatomic Molecule.

obtained from

$$\left(-\frac{\hbar^2}{2\mu_N}\frac{1}{R^2}\frac{\partial}{\partial R}\left(R^2\frac{\partial}{\partial R}\right) + \varepsilon_o(R)\right)\phi_v(R) = \varepsilon_v\,\phi_v(R) \qquad (2)$$

For vibrational transitions, the angular parts of vibrotational wave functions of target molecule are not considered in hybrid theory. Thus the scattering wave function $\psi^{(+)}_{vjm_j}(\vec{r},\vec{R})$ is replaced by $\psi^{(+)}_{v}(\vec{r},\vec{R})$ in the Schrödinger equation and

$$\psi^{(+)}_{v}(\vec{r},\vec{R}) = \frac{4\pi}{k_v r}\sum_{\substack{\ell\ell' v' \\ mm'}} g^{(m')}_{\ell' v',\ell v}(r)\;\phi_{v'}(R)Y_{\ell' m'}(\hat{r}')D^{\ell *}_{mm'}(\hat{R})Y^{*}_{\ell m}(\hat{k}_v)$$

$$\underset{r\to\infty}{\sim} e^{i\vec{k}_v\cdot\vec{r}}\phi_v(R) + \sum_{v'}\frac{e^{ik_{v'}r}}{r}f_{v',v}(\hat{R},\hat{r})\phi_{v'}(R) \qquad (3)$$

Here, $k_v^2 = \frac{2\mu_e}{\hbar^2}(E-\varepsilon_v)$ and $\hat{r}'$ denotes the polar angles of $\hat{r}$ with respect to a coordinate system in which the internuclear axis $\vec{R}$ is chosen to be z-axis. $D^{\ell}_{mm'}(R) = D^{\ell}_{mm'}(\phi_R,\theta_R,0)$ is the rotation matrix element. $\hat{R}$ is treated as parameters in the fixed nuclear approximation or hybrid theory. From Eqs. (1)-(3) and the Schrödinger equation, we have

$$\left[\frac{d^2}{dr^2} - \frac{\ell'(\ell'+1)}{r^2} + k^2_{v'}\right] g^{(m')}_{\ell' v',\ell v}(r)$$

$$= \frac{2\mu_e}{\hbar^2}\sum_{\ell'' v''} V^{(m')}_{\ell' v',\ell'' v''}(r)\; g^{(m')}_{\ell'' v'',\ell v}(r)$$

$$(\ell,\ell',\ell'' \geq |m'|) \qquad (4)$$

and

$$g^{(m')}_{\ell'v',\ell v}(r) \underset{r\to\infty}{\sim}$$

$$i^{\ell'}\left(\frac{k_v}{k_{v'}}\right)^{1/2}\left\{\delta_{\ell',\ell}\delta_{v'v}F_{\ell',v'}(r)+T^{(m')}_{\ell'v',\ell v}(G_{\ell',v'}(r)+iF_{\ell',v'}(r))\right\} \tag{5}$$

Here,

$$V^{(m')}_{\ell'v',\ell''v''}(r)$$

$$= (-1)^{m'}\sum_{\lambda}\frac{1}{2\lambda+1}[(2\ell'+1)(2\ell''+1)]^{1/2}\langle\ell' o\ell'' o|\lambda o\rangle\langle\ell' m'\ell''-m'|\lambda o\rangle V^{\lambda}_{v'v''}(r)$$

$$V^{\lambda}_{v'v''}(r) = \int R^2 dR\,\phi_{v'}(R)V_{\lambda}(r,R)\phi_{v''}(R)$$

$$F_{\ell',v'}(r) = k_{v'}r\,j_{\ell'}(k_{v'}r)$$

$$G_{\ell',v'}(r) = -k_{v'}r\,n_{\ell'}(k_{v'}r) \tag{6}$$

$V_{\lambda}(r,R)$ is the λth harmonic component of $V(r,R,\gamma)$. It is seen that m', the internuclear axis component of incident electronic angular momentum (which is also that component of total electronic angular momentum of electron plus the target molecular compound system), is conserved in hybrid theory or in fixed nuclear approximation. Thus, the coupled differential equation is solved separately for each m' and it is sufficient to consider non-negative m', since

$$V^{(m')}_{\ell'v',\ell''v''}(r) = V^{(-m')}_{\ell'v',\ell''v''}(r),\quad g^{(m')}_{\ell'v',\ell v}(r) = g^{(-m')}_{\ell'v',\ell v}(r)$$

$$T^{(m')}_{\ell'v',\ell v} = T^{(-m')}_{\ell'v',\ell v} \tag{7}$$

$T^{(m')}_{\ell'v',\ell v}$ is the vibrational transition matrix element of hybrid theory. Thus we have scattering amplitude.

$$f_{v',v}(\hat{R},\theta,\phi) = \left(\frac{4\pi}{k_v k_{v'}}\right)^{1/2} \sum_{\ell'\ell m'm} (2\ell+1)^{1/2} T^{(m')}_{\ell'v',\ell v} D^{\ell'}_{mm'}(\hat{R}) D^{\ell\star}_{0m'}(\hat{R}) Y_{\ell'm}(\theta,\phi) \tag{8}$$

The differential, integral and momentum transfer cross sections of the vibrational transitions in the hybrid theory are, then, given by

$$\frac{d\sigma_{v\to v'}}{d\Omega}(\theta) = \frac{k_{v'}}{k_v} \cdot \frac{1}{4\pi} \int d\hat{R} |f_{v',v}(\hat{R},\theta,\phi)|^2$$

$$= \frac{4\pi}{k_v^2} \sum_{\lambda\mu} \frac{1}{2\lambda+1} \Big| \sum_{\ell'\ell m'} (-1)^{m'} (2\ell+1)^{1/2} \langle \ell'\mu\ell 0 | \lambda\mu\rangle \langle \ell' m' \ell -m' | \lambda 0\rangle$$

$$\times T^{(m')}_{\ell'v',\ell v} Y_{\ell'\mu}(\theta,\phi) \Big|^2$$

$$= \frac{1}{k_v^2} \sum_{\lambda} B_\lambda(v\to v') P_\lambda(\cos\theta) \tag{9}$$

$$\sigma_{v\to v'} = \int d\Omega \frac{d\sigma_{v\to v'}}{d\Omega}(\theta)$$

$$= \frac{4\pi}{k_v^2} B_o(v\to v')$$

$$= \frac{4\pi}{k_v^2} \sum_{\ell' m'} |T^{(m')}_{\ell' v', \ell v}|^2 \tag{10}$$

$$\sigma^{(M)}_{v\to v'} = \int d\Omega (1-\cos\theta) \frac{d\sigma_{v\to v'}}{d\Omega}(\theta)$$

$$= \frac{4\pi}{k_v^2} \left(B_o(v\to v') - \frac{1}{3} B_1(v\to v')\right) \tag{11}$$

Here,

$$B_\lambda(v\to v') = \sum_{\substack{\ell\ell' \\ \bar{\ell}\bar{\ell}' \\ \bar{m}'}} \frac{1}{2\lambda+1} \left((2\ell'+1)(2\bar{\ell}'+1)(2\ell+1)(2\bar{\ell}+1)\right)^{1/2}$$

$$\times \langle \ell' o \bar{\ell}' o | \lambda o\rangle \langle \ell o \bar{\ell} o | \lambda o\rangle \langle \ell' m' \bar{\ell}' -\bar{m}' | \lambda m' -\bar{m}'\rangle \langle \ell m' \bar{\ell} -\bar{m}' | \lambda m' -\bar{m}'\rangle$$

$$\times T^{(m')}_{\ell' v', \ell v} T^{(\bar{m}')*}_{\bar{\ell} v', \bar{\ell} v} \tag{12}$$

For deriving the last part of Eq. (9), we have used well-known relations (Ref. 27),

$$\sum_{m_2} \langle j_1 m_1 j_2 m_2 | j_5 m_1+m_2\rangle \langle j_5 m_1+m_2 j_4 m-m_2 | j_3 m_1+m\rangle \langle j_2 m_2 j_4 m-m_2 | j_6 m\rangle$$

$$= (-1)^{j_1+j_2+j_3+j_4} \left((2j_5+1)(2j_6+1)\right)^{1/2} \langle j_1 m_1 j_6 m | j_3 m_1+m\rangle \begin{Bmatrix} j_1 & j_2 & j_5 \\ j_4 & j_3 & j_6 \end{Bmatrix} \tag{13}$$

and

$$\sum_{j_6}((2j_5+1)(2j_6+1))^{1/2}\begin{Bmatrix} j_1 & j_2 & j_5 \\ j_4 & j_3 & j_6 \end{Bmatrix}\langle j_2 m_2 j_4 m_4 | j_6 m_2+m_4\rangle\langle j_1 m_1 j_6 m_2+m_4 | j_3 m_3\rangle$$

$$= (-1)^{j_1+j_2+j_3+j_4}\langle j_1 m_1 j_2 m_2 | j_5 m_1+m_2\rangle\langle j_5 m_1+m_2 j_4 m_4 | j_3 m_3\rangle \tag{14}$$

When solving the coupled differential equation (Eq. (4)), the real (rather than complex) wave functions $f^{(m')}_{\ell'v',\ell v}(r)$, with following real boundary condition

$$f^{(m')}_{\ell'v',\ell v}(r) \underset{r\to\infty}{\sim} \left(\frac{k_v}{k_{v'}}\right)^{1/2}(\delta_{\ell',\ell}\delta_{v'v}F_{\ell'v'}(r) + K^{(m')}_{\ell'v',\ell v}G_{\ell'v'}(r)) \tag{15}$$

are more convenient to use.

Introducing square matrices, $g^{(m')}(r)$, $f^{(m')}(r)$, $T^{(m')}$, $K^{(m')}$, I and Λ as

$$g^{(m')}(r) = (g^{(m')}_{\ell'v',\ell v}(r)),\ f^{(m')}(r) = (f^{(m')}_{\ell'v',\ell v}(r)),\ T^{(m')} = (T^{(m')}_{\ell'v',\ell v})$$

$$K^{(m')} = (K^{(m')}_{\ell'v',\ell v}),\ I = (i^{\ell'}\delta_{\ell',\ell}\delta_{v'v}),\ \Lambda = (k_{v'}^{1/2}\delta_{\ell',\ell}\delta_{v'v}) \tag{16}$$

we obtain

$$g^{(m')}(r) = f^{(m')}(r)\ D^{(m')} \tag{17}$$

$$T^{(m')} = I^{+}\frac{K^{(m')}}{1-iK^{(m')}}\ I \tag{18}$$

with

$$D^{(m')} = I\Lambda^{-1}(1+iT^{(m')})\Lambda \tag{19}$$

$K^{(m')}$ is the reactance matrix and it is real, symmetric, i.e., $K^{(m')}_{\ell'v',\ell v} = K^{(m')}_{\ell v,\ell'v'}$. Thus, $T^{(m')}_{\ell'v',\ell v} = (-1)^{\ell'+\ell} T^{(m')}_{\ell v,\ell'v'}$ and the principle of detailed balance

$$k_v^2 \sigma_{v\to v'} = k_{v'}^2 \sigma_{v'\to v} \tag{20}$$

is satisfied. The numerical procedure of evaluating the reactance matrix is given below. Let $U^{(m')}(r)$ be a square matrix such that each column is a real solution of coupled differential equation (Eq. (4)) with $U^{(m')}(0) = 0$ and all columns are independent. Then,

$$f^{(m')}(r) = U^{(m')}(r)\ C^{(m')} \tag{21}$$

for all r. $C^{(m')}$ is a coefficient matrix not yet known. In the asymptotic region,

$$U^{(m')}(r)\ C^{(m')} = \Lambda^{-1}(F(r) + G(r)K^{(m')})\Lambda \tag{22}$$

as can be seen from Eq. (15). Here

$$F(r) = (F_{\ell'v'}(r)\delta_{\ell'\ell}\delta_{v'v}),\ G(r) = (G_{\ell'v'}(r)\delta_{\ell'\ell}\delta_{v'v}) \tag{23}$$

Differentiating Eq. (22) with respect to r, we have

$$U^{(m')'}(r)C^{(m')} = \Lambda^{-1}(F'(r) + G'(r)K^{(m')})\Lambda \tag{24}$$

Multiplying Eqs. (22) and (24) by G'(r) and G(r) on the left, respectively, and subtracting from each other, we obtain

$$(G'(r)U^{(m')}(r) - G(r)U^{(m')'}(r))C^{(m')} = -\Lambda^2 \tag{25}$$

Here, we have used the relation

$$F(r)G'(r) - F'(r)G(r) = -\Lambda^2 \tag{26}$$

and the fact that all diagonal matrices commute with each other. Multiplying Eqs. (22) and (24) again by F'(r) and F(r) on the left, respectively, and subtracting from each other,

$$(F'(r)U^{(m')}(r) - F(r)U^{(m')'}(r))C^{(m')} = \Lambda K^{(m')}\Lambda \qquad (27)$$

Obtaining $C^{(m')}$ from Eq. (25), we evaluate the reactance matrix from Eq. (27), that is,

$$K^{(m')} = -\Lambda^{-1}(F'(r_o)U^{(m')}(r_o)-F(r_o)U^{(m')'}(r_o))$$

$$\times\ (G'(r_o)U^{(m')}(r_o)-G(r_o)U^{(m')'}(r_o))^{-1}\Lambda \qquad (28)$$

r_o is a point in the asymptotic region. The (partial) cross section

$$\sigma^{(m')}_{v\to v'} = \frac{4\pi}{k_v^2}\sum_{\ell'\ell} |T^{(m')}_{\ell'v',\ell v}|^2 \qquad (29)$$

is used for studying the resonance scattering cross sections.

In hybrid theory, the scattering amplitude $f_{v'j'm'_j,vjm_j}(\Theta,\phi)$ for the simultaneous vib-rotational transition $(vjm_j)\to(v'j'm'_j)$ is obtained from close-coupling scattering amplitude of vibrational transition with fixed nuclear approximation, $f_{v',v}(\hat{R},\Theta,\phi)$, given by Eq. (8) as follows

$$f_{v'j'm'_j,vjm_j}(\Theta,\phi)=\int d\hat{R}\ Y^*_{j'm'_j}(\hat{R})\ f_{v',v}(\hat{R},\Theta,\phi)Y_{jm_j}(\hat{R}) \qquad (30)$$

This is the adiabatic nuclear approach.

Carrying out the integration over $\hat{R}$, we have

$$f_{v'j'm_j',vjm_j}(\theta,\phi) = \left(\frac{4\pi}{k_v k_{v'}}\right)^{1/2} \sum_{J\ell'\ell} (2\ell+1)^{1/2} \langle \ell' m_j - m_j' j' m_j' | J m_j \rangle$$

$$\times \langle \ell o j m_j | J m_j \rangle \, \tilde{T}^J_{v'j'\ell',vj\ell} \, Y_{\ell' m_j - m_j'}(\theta,\phi) \qquad (31)$$

with

$$\tilde{T}^J_{v'j'\ell',vj\ell} = \frac{((2j'+1)(2j+1))^{1/2}}{2J+1} \sum_{m'} \langle \ell' m' j' o | J m' \rangle T^{(m')}_{\ell' v',\ell v} \langle \ell m' j o | J m' \rangle \qquad (32)$$

As can be seen from Eqs. (7) and (32),

$$(-1)^{j'+\ell'+J} = (-1)^{j+\ell+J} \qquad (33)$$

For deriving Eq. (31), we have expresed $Y^*_{j'm_j'}(\hat{R})$, $Y_{jm_j}(\hat{R})$ in terms of rotational matrix elements. Next, the Clebsch-Gordan series for each pair $D^{\ell'}$, $D^{j'}$ and D^{ℓ}, D^{j}, and the orthogonalities of the rotation matrix elements have been used. It is seen that $\tilde{T}^J_{v'j'\ell',vj\ell}$ of hybrid theory corresponds to $\tilde{T}^J_{v'j'\ell',vj\ell'}$ the transition matrix element of total angular momentum representation, of the vib-rotational close-coupling theory. Furthermore, the parity $(-1)^{j'+\ell'+J}$ is known to conserve in that theory. Therefore, the above correspondence provides us with a detailed comparison between vib-rotational close-coupling and hybrid theory. This includes not only cross sections but also transition matrix elements, for electron-diatomic molecule scattering. The differential cross section of vib-rotational transition $vj \to v'j'$ in the hybrid theory is, then, given by

$$\frac{d\sigma_{vj\to v'j'}}{d\Omega}(\theta) = \frac{k_{v'}}{k_v} \frac{1}{2j+1} \sum_{m_j m_j'} |f_{v'j'm_j',vjm_j}(\theta,\phi)|^2 \qquad (34)$$

$$= \frac{1}{k_v^2 (2j+1)} \sum_{\lambda} B_\lambda(vj\to v'j') P_\lambda(\cos\theta)$$

With

$$B_\lambda(vj\to v'j') = (-1)^{j'+j} \sum_{\substack{\ell\bar{\ell}'J \\ \bar{\ell}\ell',\bar{J}}} (2J+1)(2\bar{J}+1)\left((2\ell'+1)(2\bar{\ell}'+1)(2\ell+1)(2\bar{\ell}+1)\right)^{1/2}$$

$$\times \langle \ell' o \bar{\ell}' o | \lambda o\rangle \langle \ell o \bar{\ell} o | \lambda o\rangle \begin{Bmatrix} \lambda & \bar{J} & J \\ j' & \ell' & \bar{\ell}' \end{Bmatrix} \begin{Bmatrix} \lambda \bar{J} J \\ j\ell\bar{\ell} \end{Bmatrix} \tilde{T}^J_{v'j'\ell',vj\ell}\, \tilde{T}^{\bar{J}*}_{v'j'\bar{\ell}',vj\bar{\ell}} \tag{35}$$

Here, we have used Eqs. (13) and (33).
The integral and momentum transfer cross sections for the transition, $vj\to v'j'$, in the hybrid theory are given by

$$\sigma_{vj\to v'j'} = \int d\Omega \frac{d\sigma_{vj\to v'j'}}{d\Omega}(\theta) = \frac{4\pi}{k_v^2(2j+1)} B_o(vj\to v'j')$$

$$= \frac{4\pi}{k_v^2(2j+1)} \sum_{\ell\ell'J} (2J+1)\left|\tilde{T}^J_{v'j'\ell',vj\ell}\right|^2 \tag{36}$$

and

$$\sigma^{(M)}_{vj\to v'j'} = \int d\Omega (1-\cos\theta) \frac{d\sigma_{vj\to v'j'}}{d\Omega}(\theta)$$

$$= \frac{4\pi}{k_v^2(2j+1)} \left(B_o(vj\to v'j') - \tfrac{1}{3} B_1(vj\to v'j')\right) \tag{37}$$

The principle of detailed balance

$$k_v^2(2j+1)\sigma_{vj\to v'j'} = k_{v'}^2(2j'+1)\sigma_{v'j'\to vj} \tag{38}$$

is satisfied, since $\tilde{T}^J_{v'j'\ell',vj\ell} = (-1)^{\ell'+\ell}\, \tilde{T}^J_{vj\ell,v'j'\ell'}$.

From Eqs. (9)-(11), (34), (36), and (37), it is seen that

$$\frac{d\sigma_{v\to v'}}{d\Omega}(\theta) = \sum_{j'} \frac{d\sigma_{vj\to v'j'}}{d\Omega}(\theta) \tag{39}$$

$$\sigma_{v\to v'} = \sum_{j'} \sigma_{vj\to v'j'} \tag{40}$$

$$\sigma^{(M)}_{v\to v'} = \sum_{j'} \sigma^{(M)}_{vj\to v'j'} \tag{41}$$

by applying the closure property of spherical harmonics to Eq. (30). In fact, one can show that

$$B_\lambda(v\to v') = \frac{1}{2j+1} \sum_{j'} B_\lambda(vj\to v'j') \tag{42}$$

using Eq. (14).

SECTION VI

THE PROCEDURES OF COMPUTATION

To carry out the vibrational close-coupling calculation, the information of the input interaction potential is necessary. Therefore, we describe here the computational procedures of the input potentials in the following.

1. Input Potential

The electron-diatomic molecule interaction potential is written as:

$$V = V^{(stat)}(r,R,\gamma) + V^{(pol)}(r,R,\gamma) + V^{(ex)} \qquad (43)$$

Here, $V^{(stat)}(r,R,\gamma)$ is the static electron-molecule potential in the ground electronic state of the target molecule. $V^{(pol)}(r,R,\gamma)$ is the long range polarization potential due to the induced polarizabilities of the molecule in the presence of the incident electron. This potential partly takes into account the electronic distortion of target molecule. $V^{(ex)}$ is the local or non-local exchange potential.

a. Static Potential

This is the sum of Coulomb interactions between the incident electron and the electronic clouds of CO in the ground state

$$(1\sigma^2\ 2\sigma^2\ 3\sigma^2\ 4\sigma^2\ 5\sigma^2\ 1\pi^4)\,^1\Sigma^+ \qquad (44)$$

which is a closed shell configuration, and between the incident electron and nuclei. If one makes the harmonic expansion,

$$V^{(stat)}(r,R,\gamma) = \sum_{\lambda} V_{\lambda}^{(stat)}(r,R) P_{\lambda}(\cos\gamma) \tag{45}$$

then it is seen that

$$V_{\lambda}^{(stat)}(r,R) = e^2 \left\{ \frac{4\pi}{2\lambda+1} \int r'^2 dr' \rho_{\lambda}(r',R) \frac{r_<^{\lambda}}{r_>^{\lambda+1}} - Z_A \frac{r_{b<}^{\lambda}}{r_{b>}^{\lambda+1}} - Z_B(-1)^{\lambda} \frac{r_{a<}^{\lambda}}{r_{a>}^{\lambda+1}} \right\} \tag{46}$$

Here, $\rho_{\lambda}(r',R)$ is again λth harmonic component of the electronic density $\rho(r',\theta',R)$ of CO given by

$$\rho(r',\theta',R) = \sum_{\alpha} |\phi_{\alpha}(r',\theta',\phi',R)|^2 \tag{47}$$

$\phi_{\alpha}(\vec{r}',R) = \phi_{\alpha}(r',\theta',\phi',R)$ is the molecular orbital wave function in terms of single center coordinates with θ',ϕ' the polar angles with respect to $\vec{R}$. $\sum_{\alpha}$ is the summation over all occupied orbitals. And

$$r_{\gtrless} = \max \text{ or } \min\ (r,r') \tag{48}$$

$$r_{a\gtrless} = \max \text{ or } \min\ (r,aR)$$

$$r_{b\lesssim} = \max \text{ or } \min\ (r,bR)$$

with

$$a = M_A/(M_A+M_B)\ ,\ b = M_B/(M_A+M_B) \tag{49}$$

It is convenient to express the LCAO molecular orbital wave function in terms of the single center expansion such as

$$\phi_\alpha(r',\Theta',\phi',R) = \sum_\ell \phi_{\alpha\ell}(r',R) Y_{\ell m_\alpha}(\Theta',\phi') \qquad (50)$$

in order to evaluate the static potential. Then

$$\rho_\lambda(r',R) = \frac{1}{4\pi} \sum_{\alpha\ell\ell'} (-1)^{m_\alpha} [(2\ell+1)(2\ell'+1)]^{1/2} \langle \ell o \ell' o | \lambda o \rangle \langle \ell m_\alpha \ell' - m_\alpha | \lambda o \rangle$$
$$\times \phi_{\alpha\ell}(r',R) \phi_{\alpha\ell'}(r',R) \qquad (51)$$

Harris and Michael (Ref. 28) have developed recurrence relations for the purpose of evaluating the coefficient of expansion $\phi_{\alpha\ell}(r',R)$ from Slater type orbitals which have different centers. Faisal (Ref. 29) has made a computer program for computing the static potential using the above recurrence relations. It was found that this program contains an error which was corrected later by Chandra (Ref. 30). For the present e-CO project, we have made our own (efficient) computer program to evaluate the static potential.

For the molecular wave function of CO in the ground electronic state, Eq. (44), those obtained by McLean and Yoshimine (Ref. 31) were used for the computation of static potential. They performed the self-consistent field calculation with an extended basis set with 17 Slater type atomic orbitals centered each on carbon and oxygen nuclei. The vibrational close-coupling calculation requires the numerical values of this potential at each internuclear separation R. We have evaluated the potential for R = 1.8, 1.898, 2.015, 2.132, 2.249, 2.366, 2.483 a_o for which the molecular wave functions were given in Ref. 27. The contributions of some harmonic components of the static potential are shown in Figure 2 at the equilibrium internuclear separation $R_o = 2.132\ a_o$. The sharp kinks in that figure corresponds to the centers of carbon and oxygen nuclei. In Figure 3, the variation of these harmonic components are illustrated as functions of the internuclear separation R. As this separation decreases, that is, as the carbon and oxygen

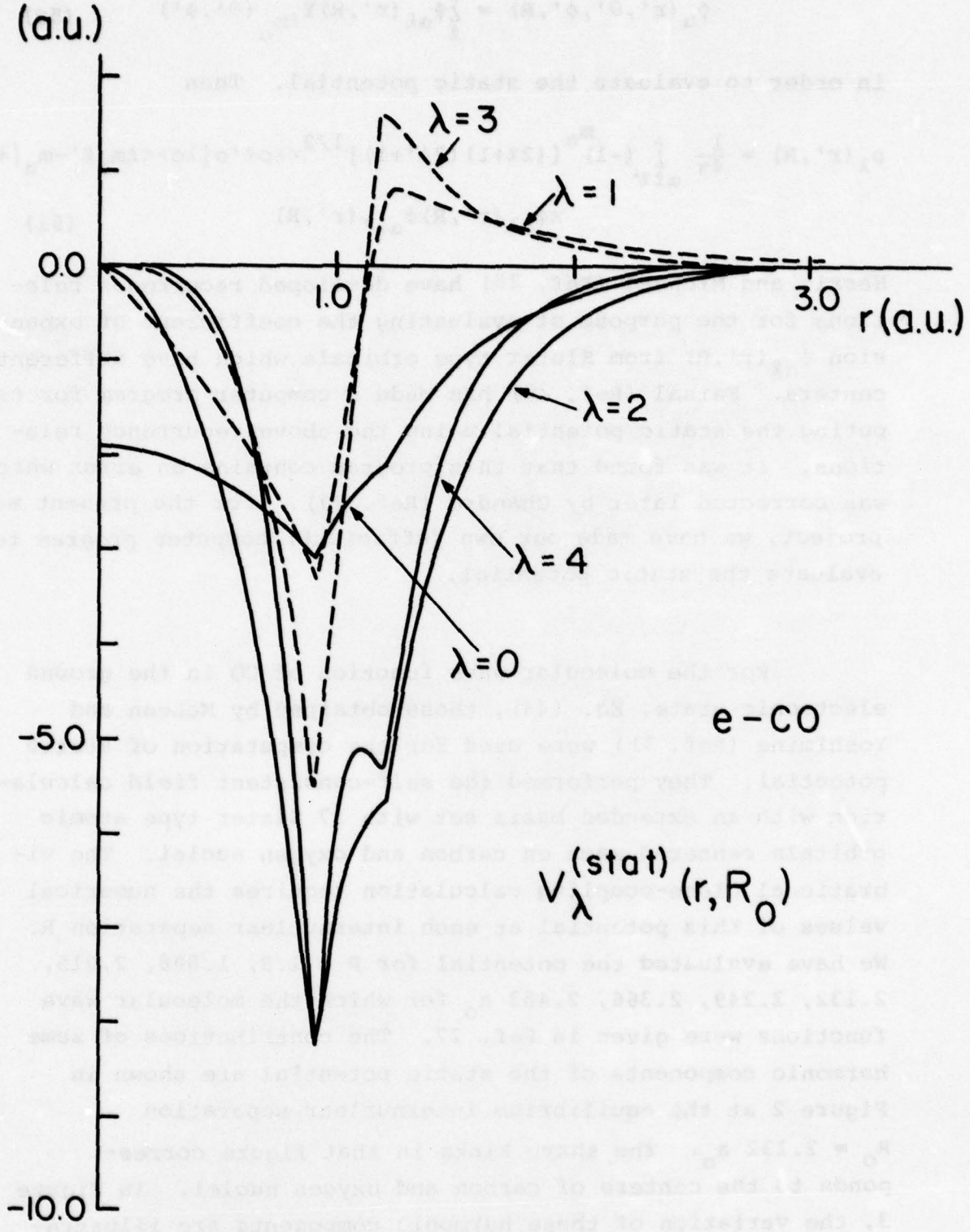

Figure 2. The Harmonic Components of Static Potential at the Equilibrium Distance of CO.

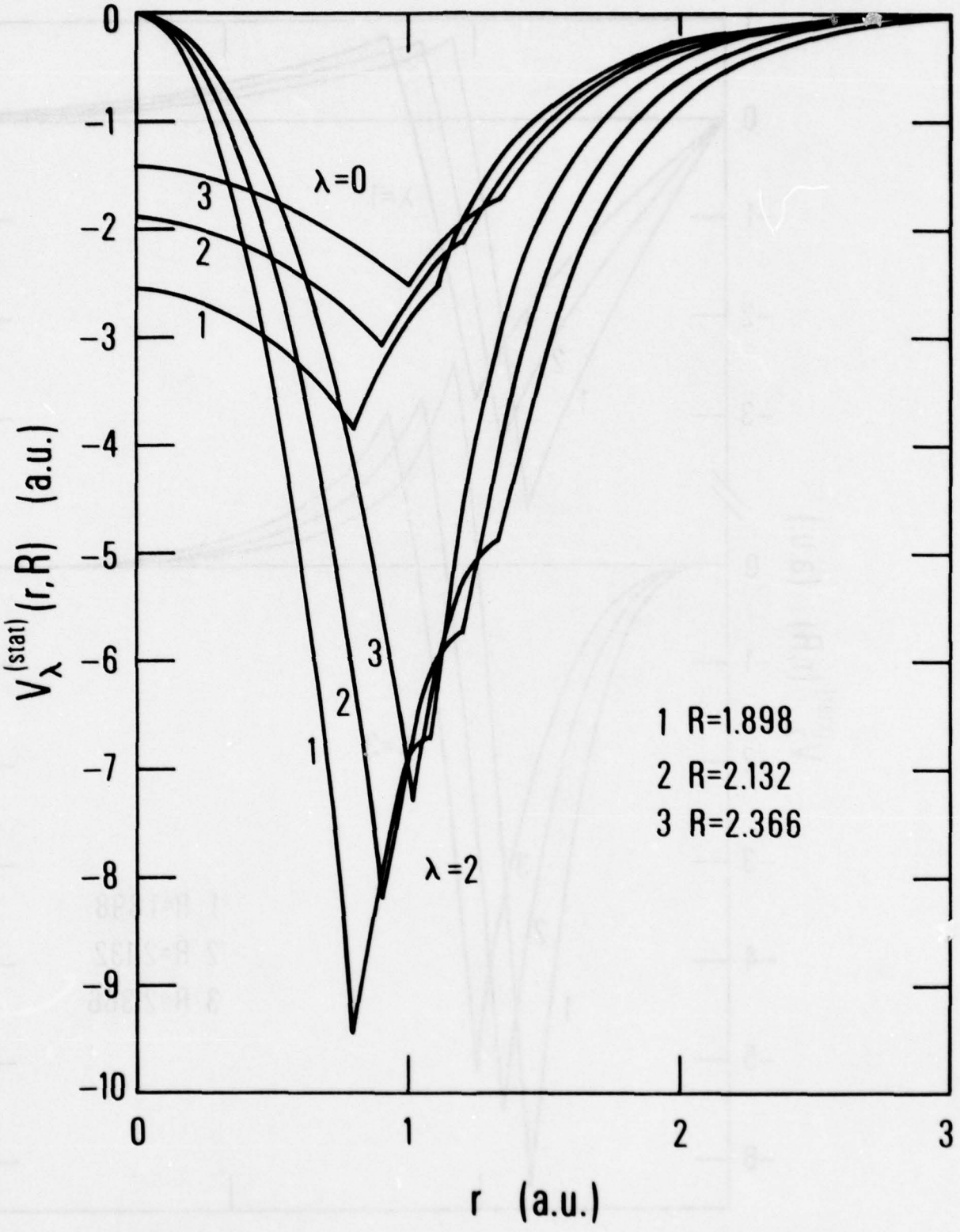

Figure 3. Variation of Static Potential as Functions of the Internuclear Separations.
(a) Even Harmonic Components

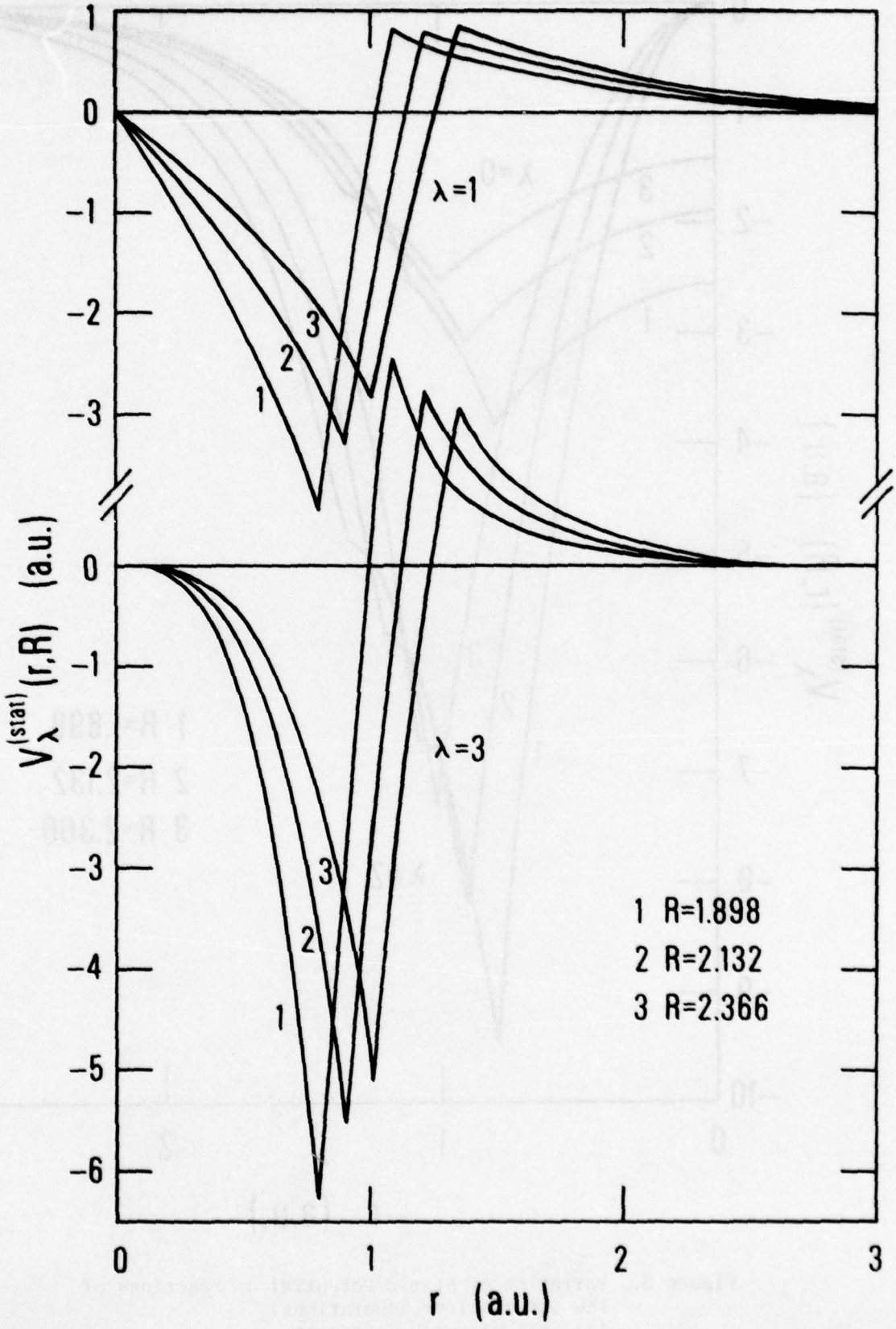

Figure 3 - Concluded -- (b) Odd Harmonic Components

nuclei are closer to each other, the depth or the height of the kinks increases. In particular, the even components of the static potential become more attractive in this case.

The dominant contributions of the long range part of the static potential mainly come from the permanent dipole and quadrupole moments of CO as follows

$$V_1(r,R) \underset{r\to\infty}{\sim} \frac{D(R)}{r^2}$$
$$V_2(r,R) \underset{r\to\infty}{\sim} \frac{Q(R)}{r^3} \qquad (52)$$

We obtained $D(R_o) = 0.116$, $Q(R_o) = 1.60$ in a.u. from the above wave functions. The experimentally measured values of these moments are 0.044, 1.859 a.u. respectively. Therefore, a discrepancy exists between the experimental and the theoretical dipole moments. The effect of this discrepancy will be discussed in Section VI, when the elastic momentum transfer cross sections are presented. The vibrational matrix elements of the static potential $V^{\lambda(stat)}_{v,v'}(r)$ (See Eq. (6)) were obtained using the vibrational wave function $\phi_v(R)$ generated from Levin's C-O potential (Ref. 32). To obtain the numerical values of $V^{(stat)}_{\lambda}(r,R)$ at much finer mesh points of R, interpolation or extrapolation procedures were necessary.

b. Polarization Potential

The polarization potential due to the induced polarizabilities of target in the presence of incident electron is of the form

$$V^{(pol)}(r,R,\gamma) = -\frac{1}{2r^4}\left[\alpha_o(R)+\alpha_2(R)P_2(\cos\gamma)\right] \qquad (53)$$
$$\times \left\{1-\exp\left[-\left(\frac{r}{r_c}\right)^6\right]\right\}$$

Here, $\alpha_o(R)$ and $\alpha_2(R)$ are the spherical and nonspherical polarizabilities, and r_c is the cutoff radius. The empirical method of determining this radius will be discussed later. We have made a linear approximation for the polarizabilities to estimate them for each internuclear separation R as follows

$$\alpha_o(R) \simeq \alpha_o(R_o) + \alpha_o'(R_o)(R-R_o)$$
$$\alpha_2(R) \simeq \alpha_2(R_o) + \alpha_2'(R_o)(R-R_o) \tag{54}$$

Here, the prime denotes the derivative with respect to R. The quantities $\alpha_o(R_o)$, $\alpha_o'(R_o)$ and $\alpha_2(R_o)$ of CO were experimentally measured (Ref. 33 and 34) and they are

$$\alpha_o(R_o) = 13.294 \quad , \quad \alpha_o'(R_o) = 5.156 \tag{55}$$
$$\alpha_2(R_o) = 2.384$$

in atomic units. However, measurements on $\alpha_2'(R_o)$ are not available. Thus, we have determined $\alpha_2'(R_o)$ from the molecular wave function using a method described below. It is known that (Ref. 35)

$$\alpha_o(R) = \frac{1}{3}(\alpha^{\parallel}(R)+2\alpha^{\perp}(R))$$
$$\alpha_2(R) = \frac{2}{3}(\alpha^{\parallel}(R) - \alpha^{\perp}(R)) \tag{56}$$

with

$$\alpha^{\parallel}(R) = \alpha_{zz}(R)$$
$$\alpha^{\perp}(R) = \alpha_{xx}(R) = \alpha_{yy}(R) \tag{57}$$

The molecular axis was chosen to be z-axis in the above expression. In terms of the molecular wave function Ψ, the perpendicular component of target polarizability is given approximately as

$$\alpha_{xx}(R) \cong 4n\langle x_i^2\rangle^2 \qquad \text{(in a.u.)} \tag{58}$$

Here, n is the number of electrons in the target CO and

$$\langle x_i^2\rangle = \int d\tau\ \Psi^*\ x_i^2\ \Psi \tag{59}$$

The x_i is the x-coordinate of ith electron. Since Ψ is antisymmetric for all electronic coordinates, the above expectation value is independent of i. It can be shown that

$$\langle x_i^2\rangle = \frac{4\pi}{3n} \int r'^4\ dr'(\rho_o(r',R) - \frac{1}{5}\ \rho_2(r',R)) \tag{60}$$

in terms of the harmonic components of the electronic density. From Eqs. (56)-(58), we have

$$\begin{aligned}\alpha_2(R_o) &= 2\{\alpha_o(R_o) - \alpha_{xx}(R_o)\} \\ &= 2\{\alpha_o(R_o) - 4n\langle x_i^2\rangle^2_{R=R_o}\}\end{aligned} \tag{61}$$

$$\begin{aligned}\alpha_2'(R_o) &= 2\{\alpha_o'(R_o) - \alpha_{xx}'\ (R_o)\} \\ &= 2\{\alpha_o'(R_o) - 4n\ \frac{d}{dR}\langle x_i^2\rangle^2_{R=R_o}\}\end{aligned} \tag{62}$$

We have computed $\langle x_i^2\rangle^2$ from the molecular wave function of

McLean and Yoshimine. The results are shown in Table 1 in atomic units.

TABLE 1

THE SQUARE OF THE MEAN SQUARE DEVIATION FOR X-COORDINATE OF TARGET ELECTRON AS FUNCTION OF THE INTERNUCLEAR SEPARATION

R	1.898	2.015	2.132	2.249	2.366
$\langle x_i^2 \rangle^2$	0.2714	0.2810	0.2902	0.2991	0.3077

When the above value of R = 2.132 is substituted into Eq. (61), it is seen that the ab initio result for $\alpha^{\perp}(R_o)$ is somewhat bigger than the experiment. Therefore, we normalized the above table by multiplying 0.745 to satisfy Eq. (61) and found $\frac{d}{dR}\langle x_i^2 \rangle^2_{R=R_o}$ from 5-strip derivative formula (Ref. 36). The $\alpha_2'(R_o)$ is then obtained from Eq. (62). Our final result is

$$\alpha_2'(R_o) = 1.653 \text{ in a.u.} \qquad (63)$$

c. Exchange Potential

The number of channels of the vibrational close-coupling differential equation is very large. The treatment of full non-local exchange for the present project is an unmanageably complex task. Therefore, it is desirable to employ an approximation scheme for the exchange effect. There exist two approximation schemes, the orthogaonlization method (Refs. 16 and 22) and the local exchange potential (Refs. 37, 38, and 39). It was found that the inclusion of the local exchange potential in the vibrational close-coupling calculation is more tractable and yields better results for the vibrational transition cross sections than that of the orthogonalization method as

discussed in subsection 2 of this section. Therefore, we describe below the procedures of computation for the local exchange potential. In the present work, we have adopted a procedure which was first derived by Slater (Ref. 37) in addressing the bound state problem, and used by Hara and others (Refs. 38 and 39) for the electron-molecule fixed-nuclei elastic scattering calculation. It is given by

$$V^{(ex)}(r,R,\gamma) = -\frac{2}{\pi} k_F(r,R,\gamma) F(\eta) \tag{64}$$

with

$$F(\eta) = \frac{1}{2} + \frac{1-\eta^2}{4\eta} \log \left|\frac{1+\eta}{1-\eta}\right| \tag{65}$$

Here, $k_F(r,R,\gamma)$ is the Fermi momentum, which is obtained from

$$k_F(r,R,\gamma) = (3\pi^2 \rho(r,R,\gamma))^{1/3} \tag{66}$$

$\rho(r,R,\gamma)$ is the electronic density of target molecule and

$$\begin{aligned} \eta &= \eta(r,R,\gamma) \\ &= k(r,R,\gamma)/k_F(r,R,\gamma) \end{aligned} \tag{67}$$

The $k(r,R,\gamma)$ is the local wave number of the incident or scattered electron. It is approximately given as

$$k(r,R,\gamma) = [2(E+I(R)) + k_F^2(r,R,\gamma)]^{1/2} \tag{68}$$

E is the incident (kinetic) energy and I(R) is the ionization potential of target molecule as a function of the internuclear separation R. Therefore, the present local exchange potential is energy dependent. However, it is a slowly varying function of E and the vibrational energy spacings

(0.2 ∿ 0.3 eV) are small compared to I(R). Thus, the small difference between the incident and the scattered energies was neglected in the present calculation. For the ionization potential I(R). we used the values in Table 2.

TABLE 2

THE IONIZATION POTENTIAL OF CO AS FUNCTION OF THE INTERNUCLEAR SEPARATION

R	1.8	1.898	2.015	2.132	2.249	2.366	2.483
I	.52845	.53698	.54634	.55437	.56053	.56427	.56514

The entries of the above table are in atomic units and were presented again by McLean and Yoshimine (Ref. 31). The local exchange potential was represented by the following harmonic expansion

$$V^{(ex)}(r,R,\gamma) = \sum_{\lambda} V_{\lambda}^{(ex)}(r,R) P_{\lambda}(\cos\gamma) \qquad (69)$$

It should be noted that the use of the harmonic expansion for the density as in Eq. (51) is not convenient in this case. The computation of harmonic coefficient $V_{\lambda}^{(ex)}(r,R)$ was mainly obtained on the direct numerical integration, because the local exchange potential was expressed in terms of the density with non-integer power.

In Figure 4, we illustrate the contribution of local exchange potential at $R = R_o$ and E = 1.7 eV. It mainly affects the spherical part (λ=0 component) of the potential and makes this potential more attractive. The λ=2 component of the potential also becomes slightly deeper due to the local exchange potential.

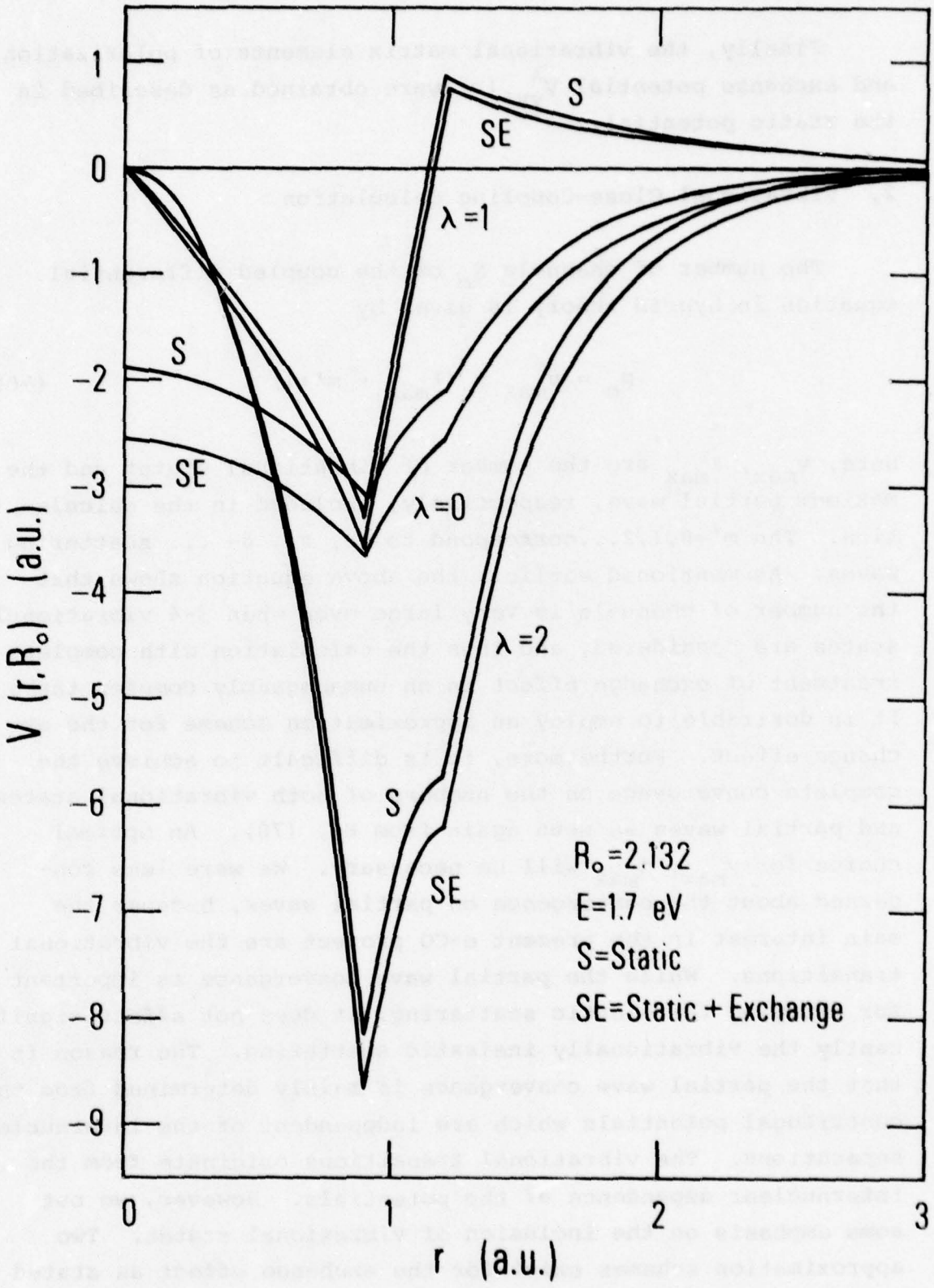

Figure 4. Effect of the Local Exchange Potential at the Equilibrium Distance of CO and at E=1.7 eV.

Finally, the vibrational matrix elements of polarization and exchange potential $V^{\lambda}_{vv'}(r)$ were obtained as described in the static potential.

2. Vibrational Close-Coupling Calculation

The number of channels N_c of the coupled differential equation in hybrid theory is given by

$$N_c = v_{max} \times (\ell_{max} - m' + 1) \tag{70}$$

Here, v_{max}, ℓ_{max} are the number of vibrational states and the maximum partial wave, respectively, included in the calculation. The $m'=0,1,2...$correspond to σ-, π-, δ- ... scattering waves. As mentioned earlier, the above equation shows that the number of channels is very large even when 3-4 vibrational states are considered, and thus the calculation with complete treatment of exchange effect is an unmanageably complex task. It is desirable to employ an approximation scheme for the exchange effect. Furthermore, it is difficult to achieve the complete convergence on the numbers of both vibrational states and partial waves as seen again from Eq. (70). An optimal choice for v_{max}, ℓ_{max} will be necessary. We were less concerned about the convergence on partial waves, because the main interest in the present e-CO project are the vibrational transitions. While the partial wave convergence is important for studying the elastic scattering, it does not affect significantly the vibrationally inelastic scattering. The reason is that the partial wave convergence is mainly determined from the centrifugal potentials which are independent of the internuclear separations. The vibrational transitions originate from the internuclear dependence of the potentials. However, we put some emphasis on the inclusion of vibrational states. Two approximation schemes exist for the exchange effect as stated

in subsection 1.c. They are the orthogonalization approach and the inclusion of local exchange potential. These approaches have been used in the fixed-nuclei calculation for vibrationally elastic scattering.

a. The Orthogonalization Approach

In the orthogonalization approach for the exchange effect, the scattering waves are made to be orthogonal to all electronic orbitals of target molecule. This approach was implicitly employed by Chandra and Temkin (Ref. 22) in their study of e-N_2 vibrationally inelastic scattering. They performed vibrational close-coupling calculations only for resonant π_g-wave which gives the dominant contribution to the cross sections and for which the orthogonalization procedures are not necessary because π_g orbitals are not occupied in target molecule. That is, the incident π_g-wave is already orthogonal to all orbitals in the target. For all other non-resonant partial waves, the orthogonalization procedures were included with fixed-nuclei close-coupling calculation and the adiabatic-nuclei approximation was applied to the vibrational transitions (See subsection II.11). They produced reasonably results when compared with experimental data.

To apply the above orthogonalization approach to our situation is more complex. We have to study the vibrational transitions of e-CO scattering in 0-10 eV of low energy region, in particular, around 1.7 eV $^2\Pi$-shape resonance of e-CO scattering. The π-orbitals are occupied in CO and the numerical procedure in which the incident π-wave is made to be orthogonal to the orbitals of target electron for all values of internuclear separation, R, in the vibrational close-coupling approximation is very tedious. Therefore, we performed calculations in a similar manner to the above e-N_2 scattering, that is, the

vibrational close-coupling calculation was carried out without the orthogonalization procedure for the resonant π-wave; and a fixed-nuclei close-coupling calculation was made for non-resonant σ, δ, ... waves with the orthogonalization procedures. The static + polarization potentials described in the subsections 1.a. and 1.b. were used. The cutoff radius r_c in the polarization potential is roughly given by the boundary of electronic cloud of the target molecule, because this potential is effective when the incident electron is outside of the electronic density of target. However, there are no strict theoretical criteria for the precise value of cutoff radius r_c. Therefore, it was determined in an empirical manner as follows. We first put v_{max}=1 and carried out the π-wave close-coupling calculation for each value of r_c. This is quantitatively very close to the fixed-nuclei close-coupling calculation for elastic scattering of $R=R_o$. We chose the value of r_c for which π-wave resonance peak occurs around experimentally observed resonance energy E=1.75 eV. As one can see in Figure 5, the positions of the resonance peak are sensitive to the choice of r_c. For r_c=1.50 a_o, the resonance energy is around E=1.5 eV, but for r_c = 1.51 a_o, it is around E=1.7 eV. It was further found that non π-waves (σ,δ...) do not give any vibrationally elastic resonance peak in this energy region for reasonable value of r_c. The contribution of these waves to the cross sections are mainly the background of the π-resonance.

The coupled differential equation was integrated out from the origin up to 20 a_o where the static dipole potential has already become very small. We truncated that potential beyond this region. The five partial waves (ℓ values) were coupled. After the cutoff radius r_c was determined, the π-wave vibrational close-coupling calculations were performed with 7-10 vibrational states included and with the same number of partial waves as above. The contributions of σ,δ... waves to the

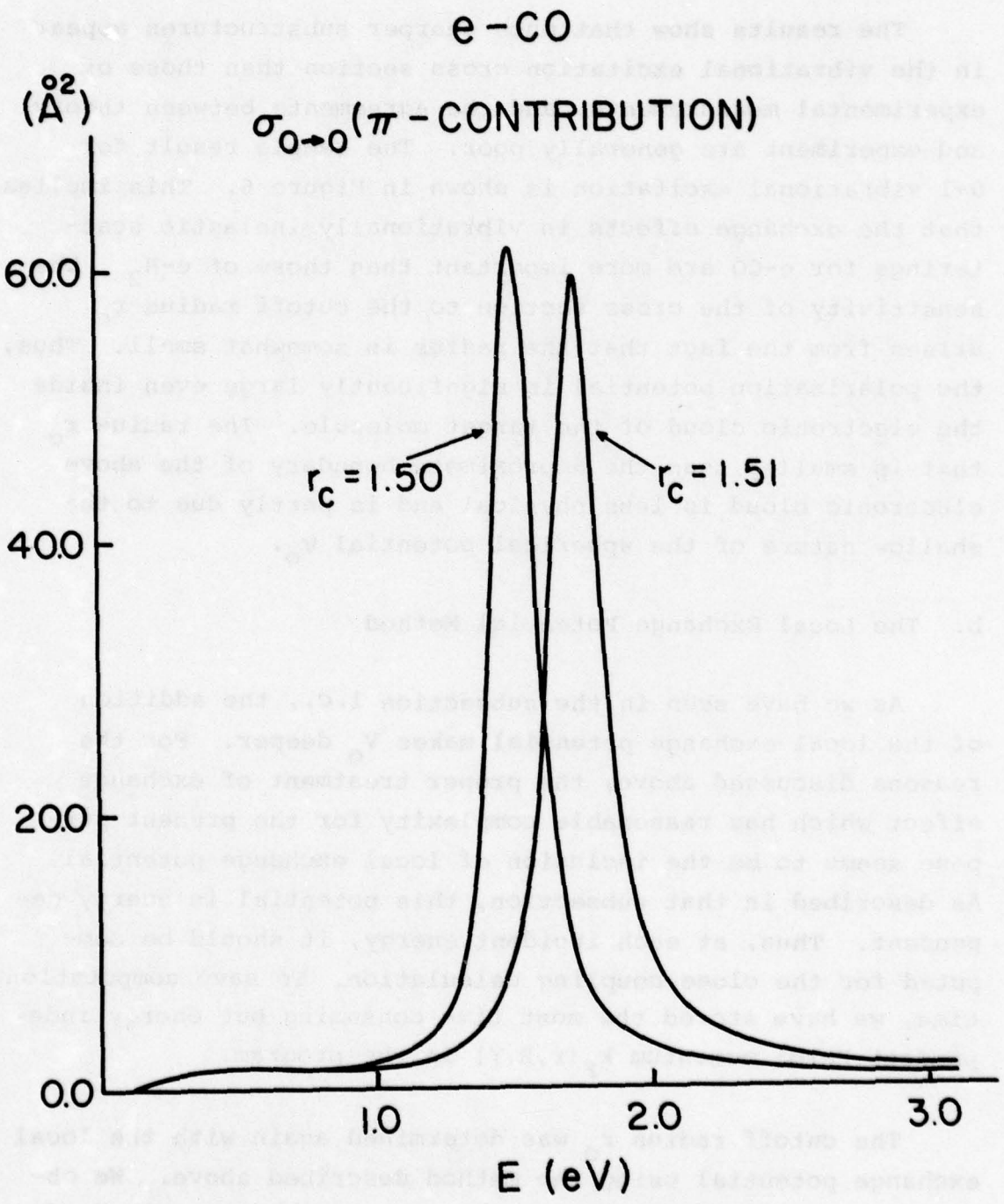

Figure 5. The Sensitivity of the π-Resonance Peak to the Cut-off Radius Without the Local Exchange Potential.

vibrational transition cross section were again found to be small in this energy region.

The results show that much sharper substructures appear in the vibrational excitation cross section than those of experimental measurements, and the agreements between theory and experiment are generally poor. The sample result for 0→1 vibrational excitation is shown in Figure 6. This implies that the exchange effects in vibrationally inelastic scatterings for e-CO are more important than those of e-N_2. The sensitivity of the cross section to the cutoff radius r_c arises from the fact that the radius is somewhat small. Thus, the polarization potential is signficantly large even inside the electronic cloud of the target molecule. The radius r_c that is smaller than the approximate boundary of the above electronic cloud is less physical and is partly due to the shallow nature of the spherical potential V_o.

b. The Local Exchange Potential Method

As we have seen in the subsection 1.c., the addition of the local exchange potential makes V_o deeper. For the reasons discussed above, the proper treatment of exchange effect which has reasonable complexity for the present purpose seems to be the inclusion of local exchange potential. As described in that subsection, this potential is energy dependent. Thus, at each incident energy, it should be computed for the close-coupling calculation. To save computation time, we have stored the most time consuming but energy independent Fermi momentum $k_F(r,R,\gamma)$ in the program.

The cutoff radius r_c was determined again with the local exchange potential using the method described above. We obtained r_c=1.945 which is outside of the electronic cloud of

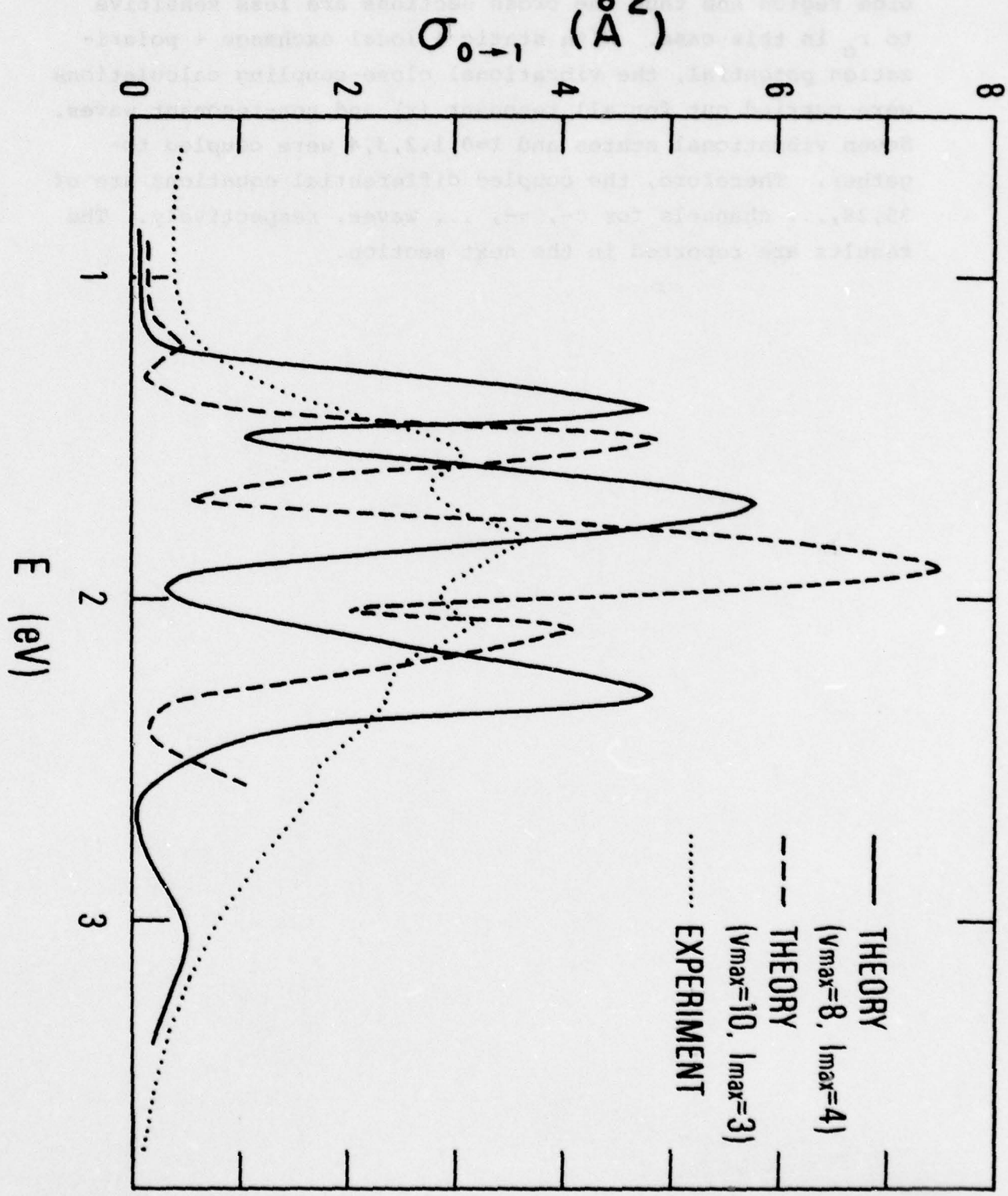

Figure 6. The 0 → 1 Vibrational Excitation Cross Section Without the Local Exchange Potential

target molecule. The polarization potential becomes small inside region and thus the cross sections are less sensitive to r_c in this case. With static + local exchange + polarization potential, the vibrational close-coupling calculations were carried out for all resonant (π) and non-resonant waves. Seven vibrational states and ℓ=0,1,2,3,4 were coupled together. Therefore, the coupled differential equations are of 35,28,... channels for σ-, π-, ... waves, respectively. The results are reported in the next section.

SECTION V

RESULTS OF CALCULATION AND COMPARISON WITH EXPERIMENTAL DATA

We have computed the integral, differential and momentum transfer cross section for the vibrationally elastic and inelastic scattering of CO in 0.1 ~ 10 eV of the energy range.

In Table 3, all integral cross sections in the above energy range are tabulated. The total energy E and the incident (kinetic) energy E_{inc} are in units of eV. The cross sections are in units of a.u. (a_o^2). Note that the relation $E=E_{inc}+\varepsilon_{v_i}$ is satisfied. Here, ε_{v_i} is the initial vibrational energy level of CO and ε_o is set to zero. In the table, a±n should read as $ax10^{\pm n}$. The v_i and v_f are the initial and the final vibrational quantum number, respectively. The diagonal entries of the table are the vibrationally elastic cross sections, that is, $v_i=v_f$ and the upper diagonal entries are the vibrational excitation cross sections. The (vibrational) de-excitation cross sections are tabulated under diagonal entries. It can be seen from the table above that detailed balancing

$$k_v^2 \, \sigma_{v\to v'} = k_{v'}^2 \sigma_{v'\to v}$$

is satisfied. The above results are the sum of σ-, π-, and δ-wave partial cross sections. The contributions of the higher scattering waves to the cross sections are found to be small. Furthermore, the major contribution to the vibrational transition cross sections and the sharp resonance peak of elastic scattering arise from the π-wave. The σ-, δ- ... waves contribute only to the background of the vibrationally elastic scattering cross section.

TABLE 3

THE ELASTIC AND VIBRATIONAL TRANSITION CROSS SECTIONS OF ELECTRON-CARBON MONOXIDE SCATTERING

E = 0.1

E_{inc}	v_i \ v_f	0
0.1	0	9.3751+1

E = 0.2

E_{inc}	v_i \ v_f	0
0.2	0	9.8996+1

E = 0.3

E_{inc}	v_i \ v_f	0	1
0.3	0	1.0181+2	4.3740-1
0.0343	1	3.8280+0	9.0932+1

E = 0.4

E_{inc}	v_i \ v_f	0	1
0.4	0	1.0353+2	7.1855-1
0.1343	1	2.1404+0	9.8068+1

TABLE 3 (continued)

E = 0.5

E_{inc}	v_i \ v_f	0	1
0.5	0	1.0419+2	7.8265-1
0.2343	1	1.6703+0	1.0267+2

E = 0.6

E_{inc}	v_i \ v_f	0	1	2
0.6	0	1.0416+2	7.8012-1	1.3966-3
0.3343	1	1.4002+0	1.0409+2	1.2118+0
0.0719	2	1.1662-2	5.6375+0	9.4739+1

E = 0.7

E_{inc}	v_i \ v_f	0	1	2
0.7	0	1.0381+2	7.5167-1	1.9294-3
0.4343	1	1.2116+0	1.0546+2	1.5419+0
0.1719	2	7.8588-3	3.8963+0	1.0121+2

TABLE 3 (continued)

E = 0.8

E_{inc}	v_i \ v_f	0	1	2	3
0.8	0	1.0335+2	7.2327-1	1.9526-3	8.5472-4
0.5343	1	1.0829+0	1.0587+2	1.6186+0	1.8485-3
0.2719	2	5.7460-3	3.1811+0	1.0375+2	8.5229-1
0.0127	3	5.3705-2	7.7570-2	1.8198+1	8.9521+1

E = 0.9

E_{inc}	v_i \ v_f	0	1	2	3
0.9	0	1.0299+2	7.0249-1	2.0096-3	2.4258-3
0.6343	1	9.9679-1	1.0580+2	1.5845+0	4.3656-3
0.3719	2	4.8638-3	2.7027+0	1.0596+2	2.1398+0
0.1127	3	1.9366-2	2.4562-2	7.0584+0	9.9051+1

TABLE 3 (continued)

E = 1.0

E_{inc}	v_i \ v_f	0	1	2	3
1.0	0	1.0300+2	7.0089-1	2.0768-3	3.2217-3
0.7343	1	9.5453-1	1.0552+2	1.5414+0	4.7369-3
0.4719	2	4.4013-3	2.3987+0	1.0712+2	2.4224+0
0.2127	3	1.5144-2	1.6350-2	5.3732+0	1.0465+2

E = 1.1

E_{inc}	v_i \ v_f	0	1	2	3	4
1.1	0	1.0372+2	7.3687-1	2.5617-3	3.5215-3	2.9109-5
0.8343	1	9.7156-1	1.0534+2	1.5417+0	5.4547-3	2.4641-4
0.5719	2	4.9276-3	2.2492+0	1.0748+2	2.5015+0	8.5274-3
0.3127	3	1.2386-2	1.4551-2	4.5743+0	1.0610+2	2.2516+0
0.0569	4	5.6269-4	3.6126-3	8.5694-2	1.2374+1	9.5435+1

TABLE 3 (continued)

E = 1.2

E_{inc}	v_i \ v_f	0	1	2	3	4
1.2	0	1.0577+2	8.5571-1	5.6754-3	5.0226-3	7.4551-5
0.9343	1	1.0990+0	1.0571+2	1.6442+0	8.8695-3	4.4761-4
0.6719	2	1.0136-2	2.2864+0	1.0774+2	2.5050+0	1.1145-2
0.4127	3	1.4603-2	2.0077-2	4.0777+0	1.0805+2	3.1005+0
0.1569	4	5.7015-4	2.6653-3	4.7723-2	8.1559+0	1.0342+2

E = 1.3

E_{inc}	v_i \ v_f	0	1	2	3	4	5
1.3	0	1.1040+2	1.1953+0	2.3270-2	9.7490-3	2.2487-4	4.3297-4
1.0343	1	1.5024+0	1.0745+2	2.0378+0	3.2490-2	1.7043-3	2.4608-5
0.7719	2	3.9193-2	2.7306+0	1.0852+2	2.6577+0	1.5637-2	1.6964-4
0.5127	3	2.4718-2	6.5539-2	4.0008+0	1.0913+2	3.4098+0	4.8784-3
0.2569	4	1.1379-3	6.8614-3	4.6981-2	6.8054+0	1.0568+2	8.6102-1
0.0044	5	1.2858-1	5.8142-3	2.9913-2	5.7141-1	5.0532+1	8.8574+1

TABLE 3 (continued)

E = 1.4

E_{inc}	v_i \ v_f	0	1	2	3	4	5
1.4	0	1.2033+2	2.2870+0	1.4561-1	3.7753-2	1.4317-3	2.1449-3
1.1343	1	2.8228+0	1.1272+2	3.4442+0	1.8505-1	1.2791-2	2.7654-4
0.8719	2	2.3381-1	4.4809+0	1.1148+2	3.3354+0	4.8583-2	1.0962-3
0.6127	3	8.6260-2	3.4256-1	4.7459+0	1.1046+2	3.5422+0	1.8416-2
0.3569	4	5.6160-3	4.0653-2	1.1868-1	6.0812+0	1.0847+2	3.5932+0
0.1044	5	2.8769-2	3.0051-3	9.1569-3	1.0810-1	1.2286+1	1.0090+2

E = 1.5

E_{inc}	v_i \ v_f	0	1	2	3	4	5
1.5	0	1.4097+2	6.6454+0	1.3242+0	3.3706-1	2.8630-2	3.3618-3
1.2343	1	8.0760+0	1.2878+2	1.0189+1	1.5747+0	1.6065-1	4.0578-3
0.9719	2	2.0439+0	1.2940+1	1.2346+2	6.7315+0	3.6655-1	9.7742-3
0.7127	3	7.0938-1	2.7270+0	9.1789+0	1.1423+2	4.1130+0	2.9074-2
0.4569	4	9.3991-2	4.3399-1	7.7968-1	6.4160+0	1.1068+2	4.2033+0
0.2044	5	2.4673-2	2.4506-2	4.6478-2	1.0139-1	9.3970+0	1.0744+2

TABLE 3 (continued)

E = 1.6

E_{inc}	v_i	v_f 0	1	2	3	4	5	6
1.6	0	1.5422+2	1.1560+1	9.1727+0	3.5444+0	7.4985-1	8.9834-2	7.3633-4
1.3343	1	1.3862+1	1.3046+2	3.1070+1	1.2911+1	2.4085+0	1.7702-1	7.7638-4
1.0719	2	1.3692+1	3.8677+1	1.4200+2	1.9670+1	3.6074+0	2.8512-1	1.4919-3
0.8127	3	6.9779+0	2.1196+1	2.5942+1	1.1936+2	5.9894+0	2.5583-1	1.2566-3
0.5569	4	2.1543+0	5.7706+0	6.9431+0	8.7408+0	1.1221+2	4.6700+0	2.6314-2
0.3044	5	4.7222-1	7.7603-1	1.0040+0	6.8311-1	8.5445+0	1.0854+2	3.4371+0
0.0551	6	2.1363-2	1.8784-2	2.8998-2	1.8519-2	2.6573-1	1.8970+1	9.7284+1

E = 1.7

E_{inc}	v_i	v_f 0	1	2	3	4	5	6
1.7	0	2.1304+2	7.0688+0	4.6733+0	5.1492+0	2.4080+0	5.2821-1	1.6897-2
1.4343	1	8.3784+0	1.0262+2	8.4605+0	1.1116+1	3.7942+0	4.9302-1	1.0584-2
1.1719	2	6.7795+0	1.0355+1	1.0389+2	1.0876+1	4.2446+0	5.7969-1	1.2635-2
0.9127	3	9.5907+0	1.7468+1	1.3963+1	1.0722+2	4.6565+0	4.6085-1	1.0029-2
0.6569	4	6.2318+0	8.2842+0	7.5719+0	6.4700+0	1.1082+2	4.6090+0	4.2616-2
0.4044	5	2.2206+0	1.7486+0	1.6799+0	1.0402+0	7.4874+0	1.1083+2	4.8212+0
0.1551	6	1.8515-1	9.7848-2	9.5438-2	5.9000-2	1.8044-1	1.2566+1	1.0665+2

TABLE 3 (continued)

E = 1.8

E_{inc}	v_i \ v_f	0	1	2	3	4	5	6
1.8	0	1.8650+2	2.5811+1	6.5384-1	4.4459+0	4.4587+0	1.2601+0	6.6006-2
1.5343	1	3.0281+1	1.1941+2	1.6172+0	6.4523+0	4.6640+0	9.9387-1	4.3455-2
1.2719	2	9.2535-1	1.9509+0	9.6384+1	6.2681+0	5.3864+0	1.1735+0	4.9053-2
1.0127	3	7.9021+0	9.7752+0	7.8720+0	1.0239+2	4.6700+0	9.4898-1	4.1611-2
0.7569	4	1.0603+1	9.4541+0	9.0510+0	6.2484+0	1.0984+2	4.6157+0	7.8369-2
0.5044	5	4.4971+0	3.0232+0	2.9591+0	1.9054+0	6.9267+0	1.1181+2	5.1326+0
0.2551	6	4.6566-1	2.6130-1	2.4452-1	1.6516-1	2.3248-1	1.0146+1	1.1167+2

E = 1.9

E_{inc}	v_i \ v_f	0	1	2	3	4	5	6
1.9	0	1.4935+2	2.7424+1	5.8317+0	2.1526+0	5.5000+0	1.7993+0	1.1589-1
1.6343	1	3.1883+1	1.2310+2	7.8969+0	2.8738+0	6.1506+0	2.1334+0	1.4365-1
1.3719	2	8.0768+0	9.4075+0	1.0182+2	2.8372+0	6.4833+0	2.1861+0	1.3766-1
1.1127	3	3.6757+0	4.2209+0	3.4979+0	9.9145+1	4.8850+0	1.8021+0	1.2182-1
0.8569	4	1.2195+1	1.1730+1	1.0379+1	6.3434+0	1.0856+2	4.9184+0	1.7594-1
0.6044	5	5.6568+0	5.7691+0	4.9622+0	3.3180+0	6.9734+0	1.1183+2	5.0766+0
0.3551	6	6.2001-1	6.6107-1	5.3175-1	3.8169-1	4.2451-1	8.6392+0	1.1411+2

TABLE 3 (continued)

E = 2.0

E_{inc}	v_i \ v_f	0	1	2	3	4	5	6
2.0	0	1.7640+2	9.4743+0	9.7977+0	2.7138-1	3.6587+0	1.4649+0	1.0775-1
1.7343	1	1.0925+1	1.0417+2	1.7683+1	1.0019+0	5.7889+0	3.8371+0	3.7819-1
1.4719	2	1.3313+1	2.0836+1	1.0497+2	1.1963+0	4.4643+0	2.5640+0	2.3054-1
1.2127	3	4.4755-1	1.4327+0	1.4520+0	9.8163+1	4.5577+0	3.0818+0	3.0193-1
0.9569	4	7.6471+0	1.0491+1	6.8668+0	5.7762+0	1.0442+2	4.7769+0	3.3575-1
0.7044	5	4.1596+0	9.4475+0	5.3578+0	5.3061+0	6.4895+0	1.1014+2	4.7804+0
0.4551	6	4.7350-1	1.4410+0	7.4554-1	8.0449-1	7.0589-1	7.3981+0	1.1477+2

E = 2.1

E_{inc}	v_i \ v_f	0	1	2	3	4	5	6
2.1	0	1.5139+2	4.0867+0	6.4977+0	3.9027-1	1.4704+0	9.0861-1	8.7533-2
1.8343	1	4.6787+0	1.0440+2	1.7735+1	5.3208+0	3.4325+0	5.4904+0	7.7815-1
1.5719	2	8.6810+0	2.0696+1	1.0092+2	2.5036+0	2.1787+0	2.6797+0	3.4633-1
1.3127	3	6.2433-1	7.4347+0	2.9978+0	1.0114+2	3.5111+0	4.5865+0	6.4324-1
1.0569	4	2.9217+0	5.9572+0	3.2402+0	4.3610+0	1.0084+2	4.4257+0	4.7472-1
0.8044	5	2.3721+0	1.2520+1	5.2365+0	7.4852+0	5.8152+0	1.0938+2	4.6693+0
0.5551	6	3.3111-1	2.5711+0	9.8063-1	1.5210+0	9.0380-1	6.7656+0	1.1452+2

TABLE 3 (continued)

E = 2.2

E_{inc}	v_i \ v_f	0	1	2	3	4	5	6
2.2	0	1.3077+2	7.1473+0	2.9905+0	1.3971+0	4.6490-1	6.6429-1	1.1682-1
1.9343	1	8.1292+0	1.3758+2	1.1233+1	1.5011+1	1.3064+0	7.5526+0	1.5037+0
1.6719	2	3.9352+0	1.2996+1	9.6962+1	6.3707+0	1.0647+0	3.8981+0	7.1470-1
1.4127	3	2.1756+0	2.0553+1	7.5393+0	1.0618+2	2.3837+0	6.1387+0	1.2124+0
1.1569	4	8.8406-1	2.1842+0	1.5386+0	2.9108+0	9.8664+1	4.7961+0	8.0977-1
0.9044	5	1.6159+0	1.6153+1	7.2062+0	9.5894+0	6.1354+0	1.0851+2	4.6316+0
0.6551	6	3.9228-1	4.4398+0	1.8238+0	2.6143+0	1.4299+0	6.3936+0	1.1324+2

E = 2.3

E_{inc}	v_i \ v_f	0	1	2	3	4	5	6
2.3	0	1.2289+2	5.3760+0	1.1765+0	1.4452+0	1.8309-1	3.7534-1	1.3138-1
2.0343	1	6.0782+0	1.3816+2	3.3030+0	1.5328+1	1.5374-1	5.6651+0	1.5604+0
1.7719	2	1.5272+0	3.7922+0	9.1511+1	8.5161+0	2.2438-1	3.8197+0	9.6885-1
1.5127	3	2.1973+0	2.0612+1	9.9749+0	1.0251+2	1.5992+0	4.1164+0	1.1343+0
1.2569	4	3.3504-1	2.4883-1	3.1631-1	1.9247+0	9.7174+1	4.6412+0	1.1028+0
1.0044	5	8.5953-1	1.1474+1	6.7385+0	6.2000+0	5.8081+0	1.0443+2	4.0246+0
0.7551	6	4.0016-1	4.2037+0	2.2733+0	2.2722+0	1.8356+0	5.3529+0	1.1113+2

TABLE 3 (continued)

E = 2.4

E_{inc}	v_i \ v_f	0	1	2	3	4	5	6
2.4	0	1.1430+2	2.5077+0	1.1451+0	9.6118-1	2.2752-1	2.3483-1	1.3479-1
2.143	1	2.8199+0	1.1565+2	2.7642+0	1.0369+1	3.6058-1	3.4639+0	1.3133+0
1.8719	2	1.4682+0	3.1517+0	8.9486+1	8.0899+0	1.9646-1	3.1328+0	1.0963+0
1.6127	3	1.4304+0	1.3722+1	9.3897+0	9.6831+1	1.5612+0	2.1676+0	8.3175-1
1.3569	4	4.0242-1	5.6715-1	2.7102-1	1.8555+0	9.6368+1	4.2747+0	1.3433+0
1.1044	5	5.1032-1	6.6943+0	5.3099+0	3.1654+0	5.2522+0	1.0131+2	3.5477+0
0.8551	6	3.7829-1	3.2779+0	2.3998+0	1.5686+0	2.1315+0	4.5817+0	1.0972+2

E = 2.5

E_{inc}	v_i \ v_f	0	1	2	3	4	5	6
2.5	0	1.0683+2	1.3472+0	1.4489+0	6.8334-1	3.1689-1	2.0667-1	1.6501-1
2.2343	1	1.5074+0	1.0143+2	5.0452+0	7.4373+0	9.4532-1	2.5663+0	1.3451+0
1.9719	2	1.8370+0	5.7166+0	9.0807+1	7.9369+0	8.0848-1	3.0112+0	1.4729+0
1.7127	3	9.9744-1	9.7021+0	9.1377+0	9.3670+1	1.7454+0	1.4579+0	7.8140-1
1.4569	4	5.4378-1	1.4497+0	1.0942+0	2.0519+0	9.6125+1	4.2542+0	1.8478+0
1.2044	5	4.2899-1	4.7609+0	4.9301+0	2.0733+0	5.1462+0	9.9448+1	3.3868+0
0.9551	6	4.3191-1	3.1465+0	3.0408+0	1.4011+0	2.8185+0	4.2706+0	1.0886+2

TABLE 3 (continued)

E = 2.6

E_{inc}	v_i \ v_f	0	1	2	3	4	5	6
2.6	0	1.0126+2	1.1785+0	1.8275+0	5.2810-1	4.4345-1	2.2606-1	2.3267-1
2.3343	1	1.3127+0	9.5083+1	8.6151+0	5.7159+0	1.8743+0	2.2658+0	1.6640+0
2.0719	2	2.2934+0	9.7063+0	9.5874+1	8.0399+0	2.3702+0	3.3143+0	2.3165+0
1.8127	3	7.5745-1	7.3604+0	9.1892+0	9.1896+1	2.2279+0	1.3722+0	1.0384+0
1.5569	4	7.4056-1	2.8102+0	3.1541+0	2.5940+0	9.6732+1	4.4897+0	2.7873+0
1.3044	5	4.5061-1	4.0548+0	5.2645+0	1.9070+0	5.3589+0	9.8113+1	3.5515+0
1.0551	6	5.7333-1	3.6814+0	4.5487+0	1.7841+0	4.1128+0	4.3904+0	1.0844+2

E = 2.7

E_{inc}	v_i \ v_f	0	1	2	3	4	5	6
2.7	0	9.7650+1	1.6170+0	2.0553+0	3.7880-1	5.7744-1	2.5107-1	3.2473-1
2.4343	1	1.7935+0	9.6098+1	1.2295+1	4.0514+0	3.1179+0	2.0285+0	2.1367+0
2.1719	2	2.5551+0	1.3781+1	1.0456+2	7.3504+0	5.3460+0	3.5744+0	3.6801+0
1.9127	3	5.3471-1	5.1561+0	8.3462+0	9.0535+1	3.4152+0	1.5850+0	1.7400+0
1.6569	4	9.4097-1	4.5808+0	7.0075+0	3.9426+0	9.8072+1	4.6175+0	4.0343+0
1.4044	5	4.8271-1	3.5162+0	5.5279+0	2.1588+0	5.4478+0	9.6966+1	4.1959+0
1.1551	6	7.5902-1	4.5028+0	6.9192+0	2.8812+0	5.7867+0	5.1012+0	1.0798+2

TABLE 3 (continued)

E = 2.8

E_{inc}	v_i \ v_f	0	1	2	3	4	5	6
2.8	0	9.5827+1	2.0536+0	1.6975+0	1.9733-1	5.7997-1	2.2034-1	3.5817-1
2.5343	1	2.2689+0	1.0144+2	1.2448+1	2.1735+0	3.8013+0	1.4454+0	2.2608+0
2.2719	2	2.0922+0	1.3886+1	1.0960+2	5.1243+0	8.3510+0	2.9837+0	4.7128+0
2.0127	3	2.7451-1	2.7367+0	5.7841+0	8.8808+1	5.2827+0	1.6324+0	2.7161+0
1.7569	4	9.2430-1	5.4832+0	1.0798+1	6.0520+0	9.8264+1	4.0193+0	4.5841+0
1.5044	5	4.1012-1	2.4350+0	4.5059+0	2.1840+0	4.6940+0	9.5518+1	5.1066+0
1.2551	6	7.9901-1	4.5648+0	8.5304+0	4.3555+0	6.4167+0	6.1207+0	1.0624+2

E = 2.9

E_{inc}	v_i \ v_f	0	1	2	3	4	5	6
2.9	0	9.4341+1	1.9149+0	9.9976-1	7.5669-2	4.3577-1	1.4364-1	2.9782-1
2.6343	1	2.1081+0	1.0299+2	8.8449+0	1.0599+0	3.3612+0	7.6730-1	1.8693+0
2.3719	2	1.2223+0	9.8235+0	1.0524+2	3.2837+0	9.0909+0	1.8128+0	4.6347+0
2.1127	3	1.0386-1	1.3215+0	3.6865+0	8.7209+1	6.8591+0	1.2842+0	3.4286+0
1.8569	4	6.8056-1	4.7684+0	1.1611+1	7.8041+0	9.6321+1	2.9898+0	4.0520+0
1.6044	5	2.5965-1	1.2598+0	2.6799+0	1.6912+0	3.4604+0	9.3712+1	5.6137+0
1.3551	6	6.3734-1	3.6338+0	8.1119+0	5.3454+0	5.5523+0	6.6462+0	1.0357+2

TABLE 3 (continued)

E = 3.0

E_{inc}	v_i \ v_f	0	1	2	3	4	5	6
3.0	0	9.2470+1	1.5191+0	5.1429-1	4.0487-2	2.9538-1	8.2667-2	2.2364-1
2.7343	1	1.6667+0	1.0028+2	5.4704+0	8.6636-1	2.6247+0	3.5738-1	1.4395+0
2.4719	2	6.2417-1	6.0512+0	9.8031+1	3.1743+0	8.4813+0	9.4693-1	4.1856+0
2.2127	3	5.4892-2	1.0705+0	3.5460+0	8.6743+1	8.0148+0	8.6707-1	3.9761+0
1.9569	4	4.5283-1	3.6674+0	1.0713+1	9.0625+0	9.4189+1	2.2425+0	3.5218+0
1.7044	5	1.4550-1	5.7334-1	1.3733+0	1.1256+0	2.5747+0	9.2001+1	5.7923+0
1.4551	6	4.6108-1	2.7050+0	7.1101+0	6.0461+0	4.7362+0	6.7843+0	1.0160+2

E = 3.1

E_{inc}	v_i \ v_f	0	1	2	3	4	5	6
3.1	0	9.0509+1	1.1793+0	2.7773-1	4.8210-2	2.0472-1	4.7756-2	1.7158-1
2.8343	1	1.2899+0	9.6589+1	3.5476+0	1.0954+0	2.0627+0	1.6584-1	1.1631+0
2.5719	2	3.3474-1	3.9096+0	9.2630+1	4.3610+0	7.7785+0	4.8484-1	3.9205+0
2.3127	3	6.4621-2	1.3424+0	4.8497+0	8.7819+1	9.1885+0	5.6159-1	4.6939+0
2.0569	4	3.0854-1	2.8423+0	9.7259+0	1.0331+1	9.2968+1	1.8170+0	3.5739+0
1.8044	5	8.2047-2	2.6051-1	6.9107-1	7.1981-1	2.0714+0	9.0528+1	5.9909+0
1.5551	6	3.4202-1	2.1198+0	6.4836+0	6.9806+0	4.7271+0	6.9511+0	1.0074+2

TABLE 3 (continued)

E = 3.2

E_{inc}	v_i	v_f 0	1	2	3	4	5	6
3.2	0	8.8675+1	9.4705-1	1.8285-1	7.2120-2	1.4702-1	2.9289-2	1.3636-1
2.9343	1	1.0328+0	9.3330+1	2.7323+0	1.4614+0	1.6588+0	8.5732-2	9.9618-1
2.6719	2	2.1900-1	3.0007+0	8.9870+1	6.3574+0	7.1641+0	2.7769-1	3.8553+0
2.4127	3	9.5652-2	1.7773+0	7.0402+0	9.0720+1	1.0436+1	3.9533-1	5.6854+0
2.1569	4	2.1813-1	2.2567+0	8.8745+0	1.1674+1	9.2702+1	1.5775+0	4.3133+0
1.9044	5	4.9216-2	1.3209-1	3.8960-1	5.0087-1	1.7867+0	8.9267+1	6.3267+0
1.6551	6	2.6363-1	1.7660+0	6.2235+0	8.2878+0	5.6209+0	7.2793+0	1.0079+2

E = 3.3

E_{inc}	v_i	v_f 0	1	2	3	4	5	6
3.3	0	8.7032+1	8.0382-1	1.5969-1	9.8273-2	1.0448-1	2.0507-2	1.0738-1
3.0343	1	8.7422-1	9.0897+1	2.6248+0	1.7867+0	1.3067+0	6.3004-2	8.6251-1
2.7719	2	1.9011-1	2.8733+0	8.9716+1	8.5985+0	6.3646+0	2.3719-1	3.8013+0
2.5127	3	1.2906-1	2.1576+0	9.4852+0	9.5240+1	1.1291+1	4.0527-1	6.7544+0
2.2569	4	1.5276-1	1.7568+0	7.8168+0	1.2571+1	9.2981+1	1.4821+0	5.6761+0
2.0044	5	3.3763-2	9.5377-2	3.2801-1	5.0806-1	1.6688+0	8.8201+1	6.7466+0
1.7551	6	2.0191-1	1.4911+0	6.0033+0	9.6699+0	7.2987+0	7.7047+0	1.0130+2

TABLE 3 (continued)

E = 3.4

E_{inc}	v_i \ v_f	0	1	2	3	4	5	6
3.4	0	8.5585+1	7.2260-1	1.6325-1	1.1312-1	6.8775-2	1.7702-2	7.8592-2
3.1343	1	7.8386-1	8.9307+1	2.8364+0	1.8840+0	9.4572-1	6.9914-2	7.0621-1
2.8719	2	1.9328-1	3.0956+0	9.1384+1	1.0084+1	5.1298+0	3.0866-1	3.5189+0
2.6127	3	1.4721-1	2.2601+0	1.1084+1	9.9711+1	1.0986+1	6.2711-1	7.3887+0
2.3569	4	9.9212-2	1.2576+0	6.2506+0	1.2178+1	9.2924+1	1.5841+0	7.2540+0
2.1044	5	2.8601-2	1.0413-1	4.2124-1	7.7860-1	1.7742+0	8.7326+1	7.1088+0
1.8551	6	1.4403-1	1.1931+0	5.4475+0	1.0406+1	9.2160+0	8.0639+0	1.0137+2

E = 3.5

E_{inc}	v_i \ v_f	0	1	2	3	4	5	6
3.5	0	8.4306+1	6.7197-1	1.6162-1	1.0874-1	4.0448-2	1.7723-2	5.1584-2
3.2343	1	7.2718-1	8.8232+1	2.9686+0	1.6806+0	6.0766-1	8.4268-2	5.2672-1
2.9719	2	1.9034-1	3.2307+0	9.3074+1	1.0018+1	3.6345+0	4.1957-1	2.9482+0
2.7127	3	1.4030-1	2.0038+0	1.0975+1	1.0168+2	9.3528+0	1.0010+0	7.1936+0
2.4569	4	5.7620-2	7.9993-1	4.3963+0	1.0326+1	9.1745+1	1.9374+0	8.3927+0
2.2044	5	2.8140-2	1.2364-1	5.6565-1	1.2318+0	2.1593+0	8.6639+1	7.3573+0
1.9551	6	9.2344-2	8.7132-1	4.4814+0	9.9810+0	1.0546+1	8.2951+0	1.0028+2

TABLE 3 (continued)

E = 3.6

E_{inc}	v_i	v_f 0	1	2	3	4	5	6
3.6	0	8.3147+1	6.2784-1	1.4535-1	9.1159-2	2.1793-2	1.8050-2	3.1051-2
3.3343	1	6.7787-1	8.7241+1	2.8515+0	1.3159+0	3.5637-1	9.2263-2	3.6552-1
3.0719	2	1.7034-1	3.0951+0	9.3416+1	8.7312+0	2.3341+0	5.0633-1	2.2848+0
2.8127	3	1.1667-1	1.5600+0	9.5356+0	1.0056+2	7.2032+0	1.3970+0	6.3861+0
2.5569	4	3.0683-2	4.6472-1	2.8042+0	7.9239+0	8.9620+1	2.5087+0	8.8397+0
2.3044	5	2.8199-2	1.3349-1	6.7497-1	1.7052+0	2.7836+0	8.6152+1	7.6367+0
2.0551	6	5.4392-2	5.9302-1	3.4151+0	8.7402+0	1.0997+1	8.5629+0	9.8321+1

E = 3.7

E_{inc}	v_i	v_f 0	1	2	3	4	5	6
3.7	0	8.2075+1	5.8359-1	1.2185-1	7.1175-2	1.1411-2	1.7771-2	1.8005-2
3.4343	1	6.2874-1	8.6151+1	2.5717+0	9.6284-1	2.0323-1	9.2420-2	2.4793-1
3.1719	2	1.4214-1	2.7844+0	9.2464+1	7.1013+0	1.4535+0	5.5399-1	1.7212+0
2.9127	3	9.0413-2	1.1352+0	7.7330+0	9.7697+1	5.3666+0	1.7435+0	5.4444+0
2.6569	4	1.5892-2	2.6269-1	1.7352+0	5.8834+0	8.7295+1	3.2416+0	8.8569+0
2.4044	5	2.7347-2	1.3200-1	7.3082-1	2.1121+0	3.5821+0	8.5940+1	8.1396+0
2.1551	6	3.0912-2	3.9509-1	2.5333+0	7.3583+0	1.0918+1	9.0809+0	9.6324+1

TABLE 3 (continued)

E = 3.8

E_{inc}	v_i	v_f 0	1	2	3	4	5	6
3.8	0	8.1074+1	5.4113-1	9.8992-2	5.4458-2	6.1523-3	1.7001-2	1.0415-2
3.5343	1	5.8181-1	8.4991+1	2.2544+0	6.9176-1	1.2018-1	8.8255-2	1.7053-1
3.2719	2	1.1497-1	2.4352+0	9.0852+1	5.6620+0	9.4098-1	5.7553-1	1.3082+0
3.0127	3	6.8689-2	8.1151-1	6.1490+0	9.4439+1	4.1180+0	2.0421+0	4.6341+0
2.7569	4	8.4801-3	1.5407-1	1.1167+0	4.5001+0	8.5309+1	4.1211+0	8.7535+0
2.5044	5	2.5796-2	1.2454-1	7.5190-1	2.4567+0	4.5367+0	8.6120+1	8.9651+0
2.2551	6	1.7551-2	2.6725-1	1.8979+0	6.1909+0	1.0701+1	9.9559+0	9.4864+1

E = 3.9

E_{inc}	v_i	v_f 0	1	2	3	4	5	6
3.9	0	8.0136+1	5.0265-1	7.9899-2	4.1998-2	3.5920-3	1.6003-2	6.0731-3
3.6343	1	5.3940-1	8.3829+1	1.9644+0	5.0244-1	7.8095-2	8.2393-2	1.2058-1
3.3719	2	9.2414-2	2.1173+0	8.9062+1	4.5543+0	6.7337-1	5.8329-1	1.0173+0
3.1127	3	5.2620-2	5.8663-1	4.9334+0	9.1462+1	3.4098+0	2.3104+0	4.0000+0
2.8569	4	4.9035-3	9.9345-2	7.9475-1	3.7152+0	8.3900+1	5.1564+0	8.6667+0
2.6044	5	2.3965-2	1.1497-1	7.5518-1	2.7614+0	5.6564+0	8.6824+1	1.0123+1
2.3551	6	1.0056-2	1.8608-1	1.4565+0	5.2866+0	1.0513+1	1.1194+1	9.4181+1

TABLE 3 (continued)

E = 4.0

E_{inc}	v_i \ v_f	0	1	2	3	4	5	6
4.0	0	7.9256+1	4.6888-1	6.4898-2	3.3089-2	2.3713-3	1.4912-2	3.5430-3
3.7343	1	5.0224-1	8.2709+1	1.7210+0	3.7509-1	5.8181-2	7.5716-2	8.7383-2
3.4719	2	7.4771-2	1.8511+0	8.7330+1	3.7537+0	5.5379-1	5.8108-1	8.0706-1
3.2127	3	4.1197-2	4.3598-1	4.0565+0	8.8995+1	3.1248+0	2.5475+0	3.4948+0
2.9569	4	3.2078-3	7.3477-2	6.5023-1	3.3951+0	8.3174+1	6.3326+0	8.5867+0
2.7044	5	2.2057-2	1.0455-1	7.4599-1	3.0264+0	6.9239+0	8.8154+1	1.1544+1
2.4551	6	5.7723-3	1.3290-1	1.1412+0	4.5732+0	1.0341+1	1.2716+1	9.4344+1

E = 4.2

E_{inc}	v_i \ v_f	0	1	2	3	4	5	6
4.2	0	7.7650+1	4.1431-1	4.4562-2	2.2390-2	1.5166-3	1.2484-2	1.1631-3
3.9343	1	4.4229-1	8.0662+1	1.3662+0	2.3557-1	4.6494-2	5.9112-2	4.6501-2
3.6719	2	5.0972-2	1.4638+0	8.4357+1	2.8273+0	5.2153-1	5.3126-1	5.0763-1
3.4127	3	2.7555-2	2.7157-1	3.0420+0	8.5714+1	3.3612+0	2.7930+0	2.6153+0
3.1569	4	2.0177-3	5.7944-2	6.0660-1	3.6336+0	8.3802+1	8.6526+0	8.0194+0
2.9044	5	1.8053-2	8.0073-2	6.7164-1	3.2819+0	9.4049+0	9.2370+1	1.4302+1
2.6551	6	1.8398-3	6.8903-2	7.0201-1	3.3615+0	9.5349+0	1.5645+1	9.6730+1

TABLE 3 (continued)

E = 4.4

E_{inc}	v_i	v_f 0	1	2	3	4	5	6
4.4	0	7.6220+1	3.7325-1	3.2534-2	1.6967-2	1.1798-3	9.8071-3	5.0587-4
4.1343	1	3.9724-1	7.8880+1	1.1384+0	1.7197-1	4.1614-2	3.8359-2	2.2586-2
3.8719	2	3.6971-2	1.2155+0	8.2072+1	2.4023+0	5.1992-1	4.0147-1	2.8487-1
3.6127	3	2.0664-2	1.9680-1	2.5746+0	8.4080+1	3.8031+0	2.4733+0	1.7098+0
3.3569	4	1.5464-3	5.1250-2	5.9967-1	4.0930+0	8.5750+1	9.5156+0	6.3333+0
3.1044	5	1.3900-2	5.1085-2	5.0072-1	2.8783+0	1.0289+1	9.5810+1	1.4785+1
2.8551	6	7.7959-4	3.2705-2	3.8632-1	2.1635+0	7.4463+0	1.6076+1	9.9030+1

E = 4.6

E_{inc}	v_i	v_f 0	1	2	3	4	5	6
4.6	0	7.4935+1	3.4156-1	2.4933-2	1.3760-2	8.4277-4	7.5744-3	5.2530-4
4.3343	1	3.6250-1	7.7318+1	9.8056-1	1.3248-1	3.2287-2	2.0720-2	9.9011-3
4.0719	2	2.8167-2	1.0437+0	8.0214+1	2.1102+0	4.3682-1	2.5017-1	1.3892-1
3.8127	3	1.6601-2	1.5060-1	2.2536+0	8.2807+1	3.7164+0	1.7733+0	9.5517-1
3.5569	4	1.0899-3	3.9344-2	5.0006-1	3.9837+0	8.6306+1	8.4030+0	4.1665+0
3.3044	5	1.0544-2	2.7178-2	3.0828-1	2.0461+0	9.0452+0	9.5352+1	1.2506+1
3.0551	6	7.9092-4	1.4046-2	1.8515-1	1.1920+0	4.8508+0	1.3526+1	9.8103+1

TABLE 3 (continued)

E = 4.8

E_{inc}	v_i	v_f 0	1	2	3	4	5	6
4.8	0	7.3773+1	3.1626-1	1.9720-2	1.1498-2	5.6285-4	6.1594-3	6.5549-4
4.5343	1	3.3479-1	7.5928+1	8.6005-1	1.0187-1	2.2538-2	1.0454-2	4.4336-3
4.2719	2	2.2159-2	9.1288-1	7.8563+1	1.8339+0	3.2557-1	1.4324-1	6.4672-2
4.0127	3	1.3754-2	1.1511-1	1.9523+0	8.1278+1	3.2488+0	1.1509+0	5.0211-1
3.7569	4	7.1912-4	2.7202-2	3.7020-1	3.4700+0	8.5076+1	6.6442+0	2.5287+0
3.5044	5	8.4366-3	1.3526-2	1.7461-1	1.3178+0	7.1229+0	9.2251+1	9.5811+0
3.2551	6	9.6659-4	6.1759-3	8.4871-2	6.1897-1	2.9184+0	1.0314+1	9.4857+1

E = 5.0

E_{inc}	v_i	v_f 0	1	2	3	4	5	6
5.0	0	7.2714+1	2.9558-1	1.5981-2	9.8172-3	3.8104-4	5.3280-3	7.3481-4
4.7343	1	3.1217-1	7.4674+1	7.6480-1	7.8626-2	1.5386-2	5.4520-3	2.2842-3
4.4719	2	1.7868-2	8.0969-1	7.7061+1	1.5894+0	2.3489-1	8.2557-2	3.1218-2
4.2127	3	1.1651-2	8.8361-2	1.6871+0	7.9626+1	2.7403+0	7.4267-1	2.7015-1
3.9569	4	4.8149-4	1.8409-2	2.6546-1	2.9175+0	8.3117+1	5.1580+0	1.5463+0
3.7044	5	7.1915-3	6.9679-3	9.9661-2	8.4459-1	5.5097+0	8.8679+1	7.2640+0
3.4551	6	1.0633-3	3.1298-3	4.0404-2	3.2938-1	1.7709+0	7.7879+0	9.1206+1

TABLE 3 (continued)

E = 5.4

E_{inc}	v_i \ v_f	0	1	2	3	4	5	6
5.4	0	7.0856+1	2.6390-1	1.1163-2	7.5994-3	2.0798-4	4.4470-3	7.6829-4
5.1343	1	2.7756-1	7.2501+1	6.2734-1	4.9229-2	7.7130-3	1.9289-3	1.0487-3
4.8719	2	1.2373-2	6.6113-1	7.4463+1	1.2285+0	1.2803-1	3.1506-2	8.9752-3
4.6127	3	8.8964-3	5.4795-2	1.2976+0	7.6570+1	1.9890+0	3.4474-1	9.2836-2
4.3569	4	2.5777-4	9.0892-3	1.4316-1	2.1057+0	7.9250+1	3.3312+0	6.6257-1
4.1044	5	5.8509-3	2.4130-3	3.7398-2	3.8744-1	3.5361+0	8.2823+1	4.5437+0
3.8551	6	1.0761-3	1.3967-3	1.1342-2	1.1108-1	7.4880-1	4.8374+0	8.5154+1

E = 5.8

E_{inc}	v_i \ v_f	0	1	2	3	4	5	6
5.8	0	6.9274+1	2.4072-1	8.3403-3	6.2721-3	1.4371-4	3.9565-3	7.4311-4
5.5343	1	2.5228-1	7.0678+1	5.3558-1	3.3284-2	4.4284-3	1.0083-3	7.8140-4
5.2719	2	9.1759-3	5.6224-1	7.2321+1	9.9736-1	7.7413-2	1.4543-2	3.3935-3
5.0127	3	7.2572-3	3.6748-2	1.0489+0	7.4043+1	1.5401+0	1.8741-1	3.9629-2
4.7569	4	1.7522-4	5.1521-3	8.5793-2	1.6229+0	7.6137+1	2.3970+0	3.4073-1
4.5044	5	5.0945-3	1.2388-3	1.7021-2	2.0856-1	2.5314+0	7.8695+1	3.2045+0
4.2551	6	1.0129-3	1.0162-3	4.2043-3	4.6685-2	3.8091-1	3.3922+0	8.0804+1

TABLE 3 (continued)

E = 6.2

E_{inc}	v_i \ v_f	0	1	2	3	4	5	6
6.2	0	6.7908+1	2.2286-1	6.5626-3	5.4104-3	1.1613-4	3.6154-3	7.0774-4
5.9343	1	2.3284-1	6.9125+1	4.7106-1	2.4020-2	2.8583-3	7.1006-4	6.9466-4
5.6719	2	7.1737-3	4.9285-1	7.0526+1	8.4334-1	5.1213-2	7.7832-3	1.6140-3
5.4127	3	6.1974-3	2.6334-2	8.8372-1	7.1964+1	1.2603+0	1.1511-1	1.9906-2
5.1569	4	1.3962-4	3.2891-3	5.6327-2	1.3228+0	7.3662+1	1.8681+0	2.0122-1
4.9044	5	4.5705-3	8.5917-4	9.0012-3	1.2705-1	1.9643+0	7.5637+1	2.4628+0
4.6551	6	9.4262-4	8.8554-4	1.9665-3	2.3145-2	2.2290-1	2.5946+0	7.7545+1

E = 6.6

E_{inc}	v_i \ v_f	0	1	2	3	4	5	6
6.6	0	6.6713+1	2.0848-1	5.3750-3	4.8088-3	1.0231-4	3.3520-3	6.7371-4
6.3343	1	2.1723-1	6.7780+1	4.2344-1	1.8253-2	2.0208-3	5.9232-4	6.5183-4
6.0719	2	5.8425-3	4.4174-1	6.8999+1	7.3538-1	3.6330-2	4.6545-3	9.2886-4
5.8127	3	5.4600-3	1.9891-2	7.6816-1	7.0224+1	1.0742+0	7.7362-2	1.1265-2
5.5569	4	1.2151-4	2.3035-3	3.9697-2	1.1237+0	7.1644+1	1.5387+0	1.3149-1
5.3044	5	4.1708-3	7.0733-4	5.3280-3	8.4776-2	1.6119+0	7.3243+1	2.0072+0
5.0551	6	8.7960-4	8.1677-4	1.1156-3	1.2953-2	1.4454-1	2.1061+0	7.4979+1

TABLE 3 (continued)

E = 7.0

E_{inc}	v_i \ v_f	0	1	2	3	4	5	6
7.0	0	6.5651+1	1.9640-1	4.5408-3	4.3627-3	9.4278-5	3.1371-3	6.4331-4
6.7343	1	2.0415-1	6.6600+1	3.8650-1	1.4449-2	1.5319-3	5.3648-4	6.2252-4
6.4719	2	4.9114-3	4.0217-1	6.7677+1	6.5562-1	2.7206-2	3.0320-3	6.2374-4
6.2127	3	4.9156-3	1.5662-2	6.8296-1	6.8743+1	9.4273-1	5.5623-2	6.9753-3
5.9569	4	1.1078-4	1.7318-3	2.9558-2	9.8322-1	6.9958+1	1.3174+0	9.2704-2
5.7044	5	3.8496-3	6.3334-4	3.4399-3	6.0580-2	1.3757+0	7.1294+1	1.7049+0
5.4551	6	8.2549-4	7.6849-4	7.4000-4	7.9440-3	1.0123-1	1.7828+0	7.2887+1

E = 7.4

E_{inc}	v_i \ v_f	0	1	2	3	4	5	6
7.4	0	6.4695+1	1.8605-1	3.9301-3	4.0159-3	8.8932-5	2.9557-3	6.1652-4
7.1343	1	1.9298-1	6.5549+1	3.5687-1	1.1819-2	1.2246-3	5.0495-4	5.9843-4
6.8719	2	4.2321-3	3.7049-1	6.6515+1	5.9423-1	2.1262-2	2.1131-3	4.7116-4
6.6127	3	4.4941-3	1.2751-2	6.1751-1	6.7460+1	8.4503-1	4.2135-2	4.6326-3
6.3569	4	1.0352-4	1.3744-3	2.2984-2	8.7903-1	6.8521+1	1.1597+0	6.9301-2
6.1044	5	3.5830-3	5.9015-4	2.3788-3	4.5643-2	1.2077+0	6.9666+1	1.4923+0
5.8551	6	7.7918-4	7.2917-4	5.5297-4	5.2321-3	7.5240-2	1.5558+0	7.1138+1

TABLE 3 (continued)

E = 8.0

E_{inc}	v_i \ v_f	0	1	2	3	4	5	6
8.0	0	6.3417+1	1.7302-1	3.2745-3	3.6145-3	8.3248-5	2.7281-3	5.8191-4
7.7343	1	1.7897-1	6.4158+1	3.2173-1	9.1688-3	9.4096-4	4.7584-4	5.6677-4
7.4719	2	3.5060-3	3.3303-1	6.4999+1	5.2414-1	1.5619-2	1.3570-3	3.5897-4
7.2127	3	4.0091-3	9.8318-3	5.4297-1	6.5811+1	7.3685-1	2.9910-2	2.7764-3
6.9569	4	9.5730-5	1.0461-3	1.6775-2	7.6395-1	6.6708+1	9.9215-1	4.8664-2
6.7044	5	3.2553-3	5.4894-4	1.5124-3	3.2178-2	1.0295+0	6.7650+1	1.2698+0
6.4551	6	7.2117-4	6.7908-4	4.1550-4	3.1023-3	5.2447-2	1.3188+0	6.8980+1

E = 9.0

E_{inc}	v_i \ v_f	0	1	2	3	4	5	6
9.0	0	6.1578+1	1.5652-1	2.5783-3	3.1318-3	7.6321-5	2.4290-3	5.3490-4
8.7343	1	1.6128-1	6.2191+1	2.8023-1	6.5878-3	6.8566-4	4.4499-4	5.2015-4
8.4719	2	2.7390-3	2.8891-1	6.2893+1	4.4422-1	1.0513-2	7.8374-4	2.8222-4
8.2127	3	3.4320-3	7.0061-3	4.5824-1	6.3567+1	6.1649-1	1.9413-2	1.4418-3
7.9569	4	8.6326-5	7.5265-4	1.1193-2	6.3631-1	6.4292+1	8.1270-1	3.1497-2
7.7044	5	2.8375-3	5.0448-4	8.6181-4	2.0694-2	8.3934-1	6.5029+1	1.0344+0
7.4551	6	6.4575-4	6.0940-4	3.2071-4	1.5883-3	3.3617-2	1.0690+0	6.6201+1

TABLE 3 (continued)

E = 10.0

E_{inc}	v_i	v_f 0	1	2	3	4	5	6
10.0	0	5.9961+1	1.4446-1	2.1478-3	2.7787-3	7.0559-5	2.1955-3	4.9674-4
9.7343	1	1.4841-1	6.0496+1	2.5262-1	5.1361-3	5.4377-4	4.2293-4	4.7891-4
9.4719	2	2.2675-3	2.5961-1	6.1116+1	3.9281-1	7.8486-3	5.2930-4	2.4935-4
9.2127	3	3.0161-3	5.4268-3	4.0386-1	6.1712+1	5.4014-1	1.4179-2	8.9032-4
8.9569	4	7.8776-5	5.9097-4	8.2998-3	5.5557-1	6.2338+1	7.0152-1	2.3178-2
8.7044	5	2.5223-3	4.7297-4	5.7597-4	1.5007-2	7.2187-1	6.2959+1	8.8827-1
8.4551	6	5.8750-4	5.5137-4	2.7933-4	9.7009-4	2.4553-2	9.1445-1	6.4042+1

The vibrational excitation cross sections $\sigma_{0\to v}$ for v=1,2,3,4,5 are shown in Figure 7. The substructures appear in those cross sections, but they are less pronounced than those found in e-N_2 scattering (Ref. 22). The 0→1 transition cross section gives the dominant contribution to the cross sections and the cross section, in general, decrease as $\Delta v=v_f-v_i$ increases.

In Figure 8, the vibrational excitation cross sections from the initially first excited state $\sigma_{1\to v}$ with v=2,3,4,5 are shown. Again, 1→2 transition cross section is the largest one among these cross sections and the trend of the contribution in terms of Δv is similar to the 0→v case. However, the energy separations between the resonance peaks become larger and the energy regions, for which the excitation cross sections is appreciable, is widened compared with those of 0→v excitation. In Figure 9, where the excitation cross section from initially second excited state $\sigma_{2\to v}$ with v=3,4,5 are shown, these features are more enhanced and the cross sections as functions of the incident energy become smoother except the first peak in 2→3 transition. The cross section $\sigma_{3\to v}$ with v=4,5 are shown in Figure 10. All peaks in that figure are very broad.

The possible explanation for the above broadened resonance peak when the initial vibrational states are in the excited states can be understood by the fact that the overlap between initially excited state and compound state of CO^- becomes larger than that for the initially ground state. Thus the escape probability from the compound state or the width of the resonance become bigger.

Sharp resonances for the elastic scattering appear only in the ground vibrational state. For the first excited state,

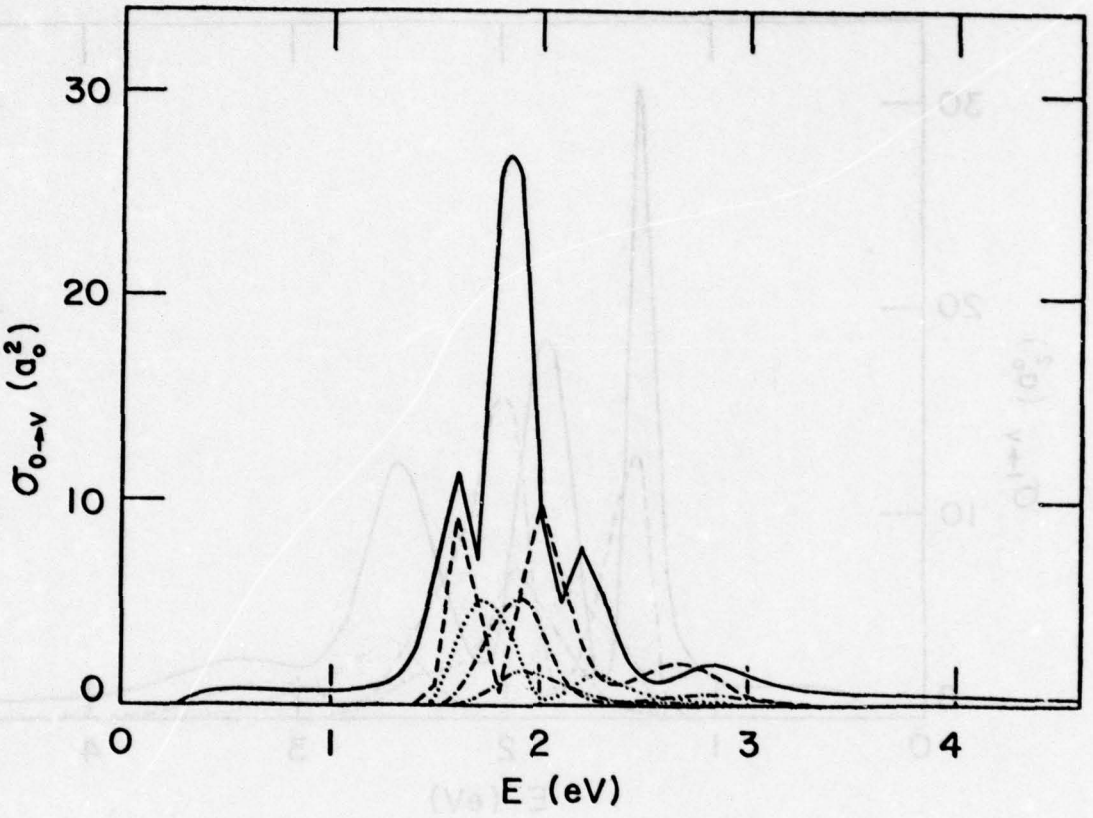

Figure 7. The Vibrational Excitation Cross Sections $\sigma_{0\to v}$ for v = 1,2,3,4,5; ——— v = 1; -----v = 2; ..... v = 3; -·-·- v = 4; -··-··- v = 5.

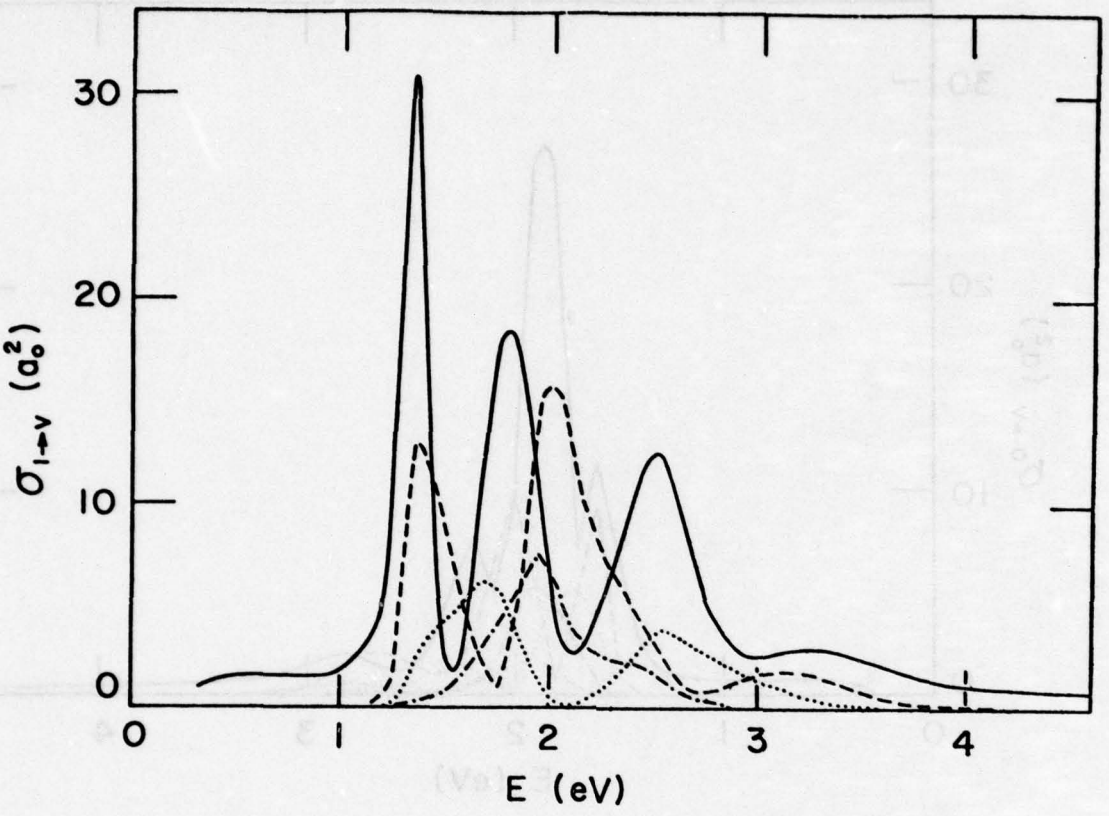

Figure 8. The Vibrational Excitation Cross Sections $\sigma_{1\to v}$ for v = 2,3,4,5; ——— v = 2; ----- v = 3; ····· v = 4; -·-·- v = 5.

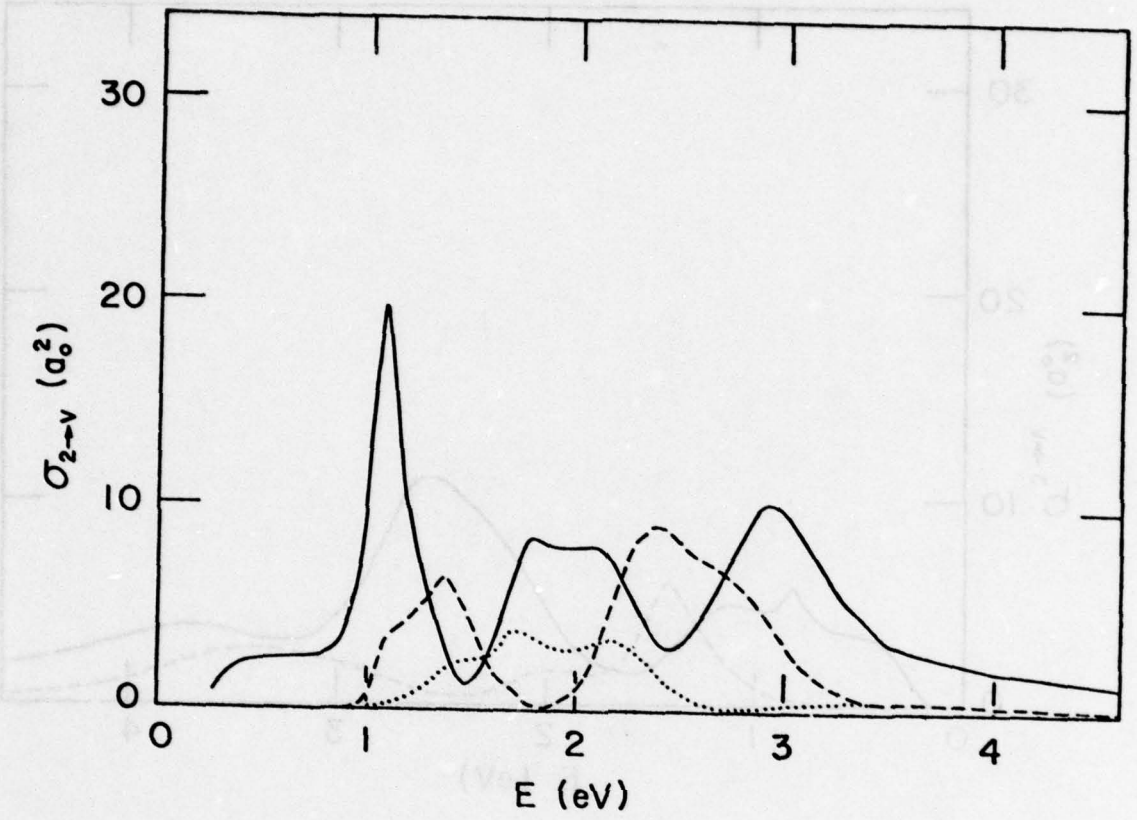

Figure 9. The Vibrational Excitation Cross Sections $\sigma_{2\to v}$ for v = 3,4,5; ——— v = 3; ----- v = 4; ····· v = 5.

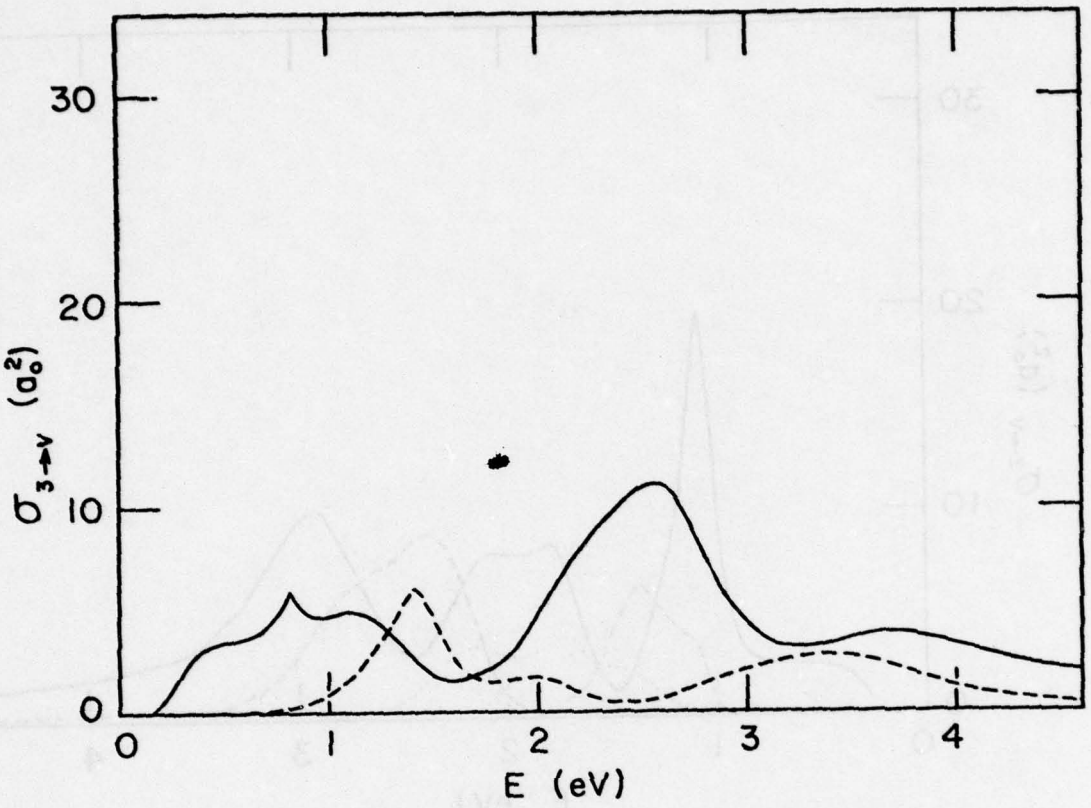

Figure 10. The Vibrational Excitation Cross Sections $\sigma_{3\to v}$ for v = 4,5; ——— v = 4; ----- v = 5.

the broad substructures are present but there is no sign of the resonance of the elastic scattering in the second excited state. (See Figure 11).

Comparison between the experimental measurements and the results of the present calculation are made in Figures 12-15 for the vibrational excitation cross sections $\sigma_{0\to v}$ with v=1,2,3,4, respectively. The experimental data were taken from the work of Ehrhardt, Laughans, Linder and Taylor (Ref. 40). The present results somewhat overestimate the experimental measurements. However, the theoretical ratios between the excitation cross sections are consistent with those of experiment. Furthermore, the present theory accounts for all major features in the substructures of these cross sections.

After we finished a preliminary draft of the present report, Phillips, Michejda and Wong (Ref.41) reported experimental measurement for 1-2 vibrational excitation cross sections. They observed a single strong peak at 1.4 eV and the bell-shaped profile centered near 2.2 eV. The maximum cross section at 1.4 eV is comparable to the largest peak of 0→1 vibrational excitation cross section. Our calculation predicted the above strong resonance peak at 1.4 eV (See Figure 8). Unfortunately, more details of their experimental results are not yet published.

The differential cross sections for the vibrational excitation obtained from present calculation are shown in Figures 16-20, where they are compared with the experimental data. These data are again from Ref. 40, but they are not absolutely calibrated, in contrast to the above integral cross sections. The shapes of the differential cross sections, obtained from present theory, are similar to each other around the resonance

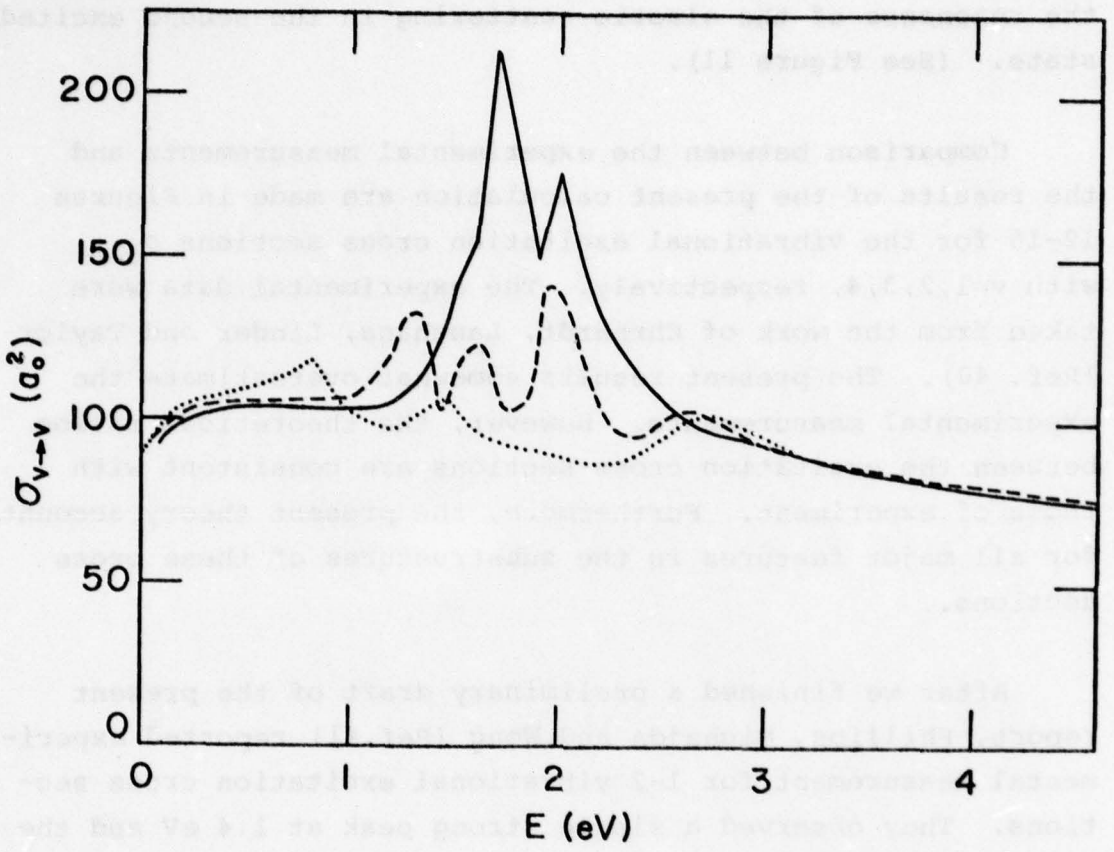

Figure 11. The Vibrationally Elastic Scattering Cross Sections $\sigma_{v\to v}$ for v = 0,1,2; ——— v = 0; ----- v = 1; .... v = 2.

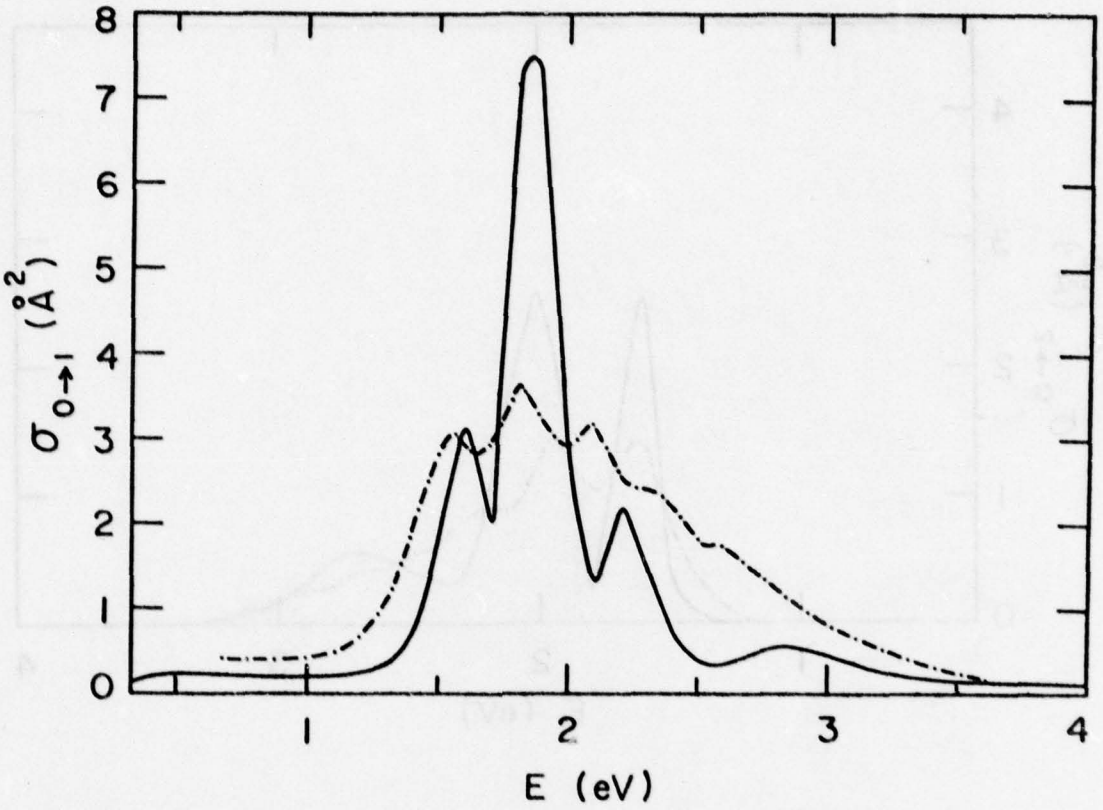

Figure 12. Comparison Between the Experiment and Theory for 0→1 Vibrational Excitation Cross Section; ——— Present Calculation; -·-·-·- Experimental Data Taken from Ref. 40.

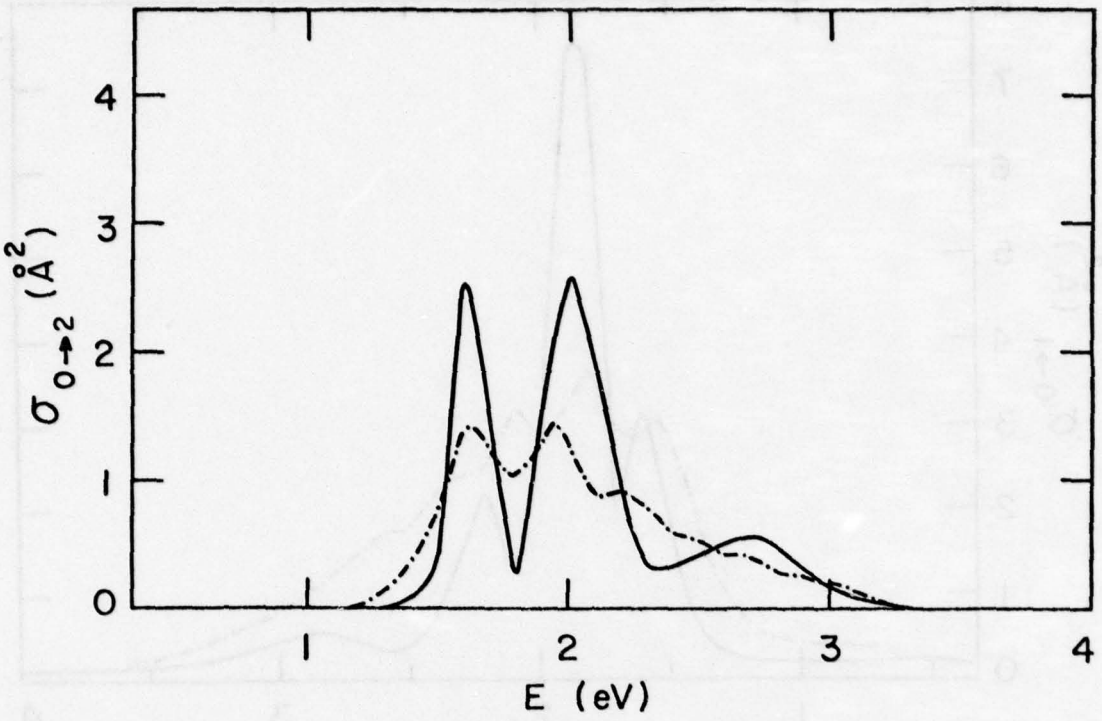

Figure 13. Comparison Between the Experiment and Theory for 0→2 Vibrational Excitation Cross Section; Notations of Curves are the Same as in Figure 12.

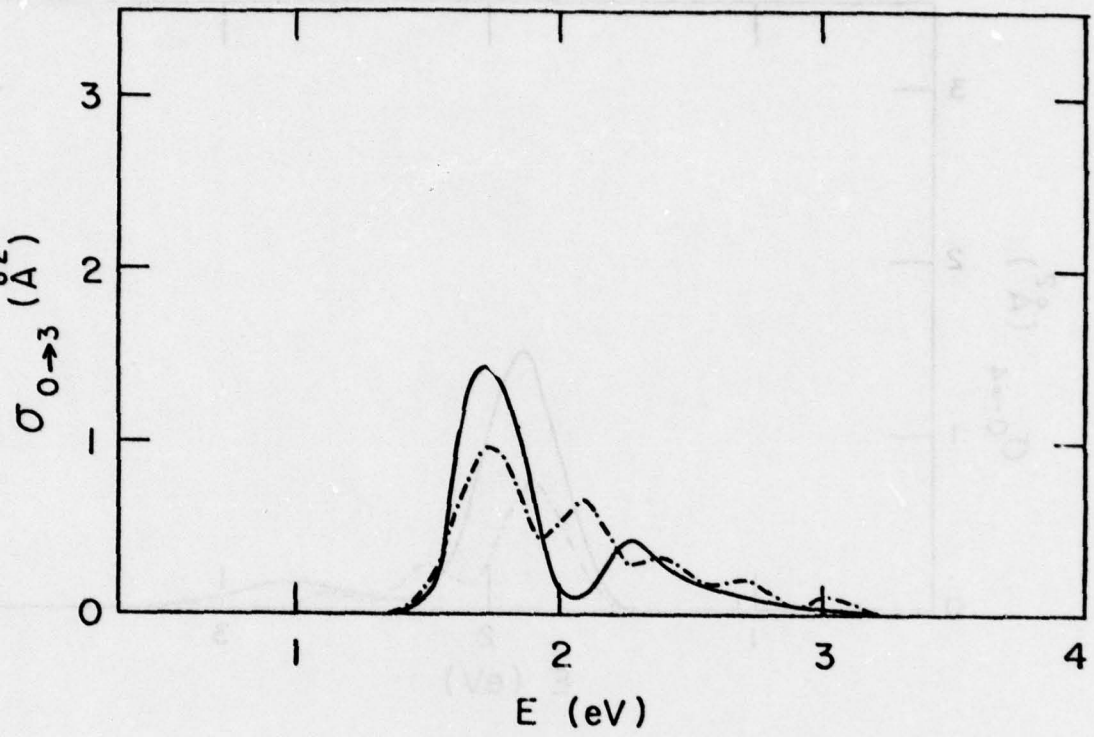

Figure 14. Comparison Between the Experiment and Theory for 0→3 Vibrational Excitation Cross Section; Notations of Curves are the Same as in Figure 12.

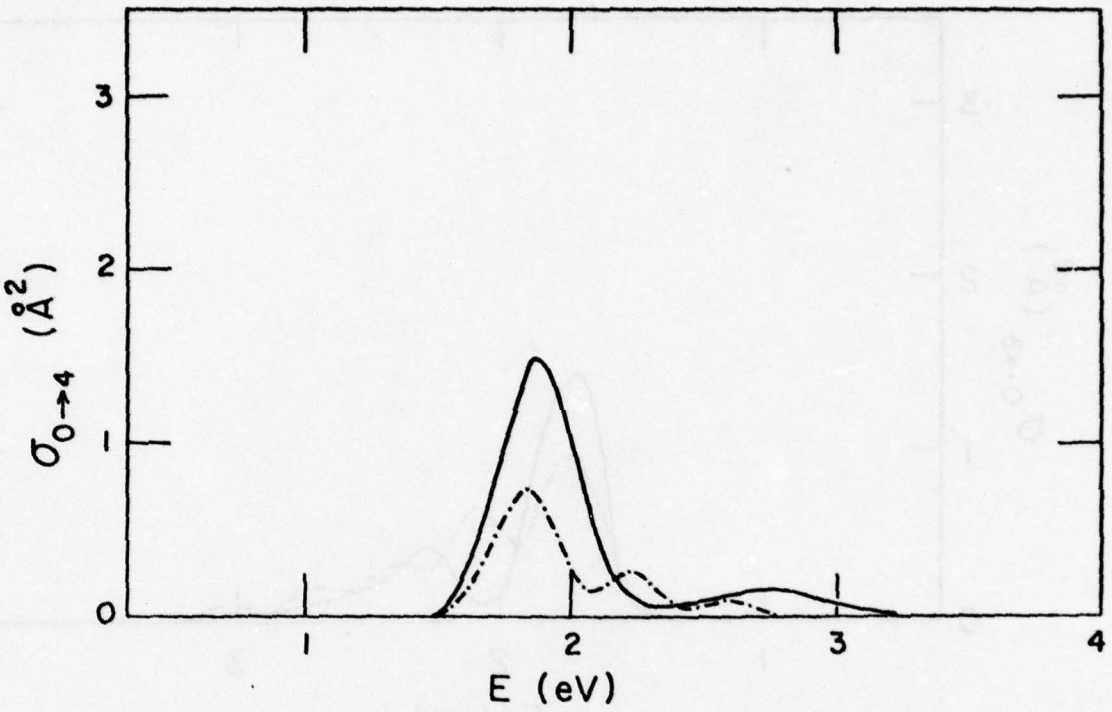

Figure 15. Comparison Between the Experiment and Theory for 0→4 Vibrational Excitation Cross Section; Notations of Curves are the Same as in Figure 12.

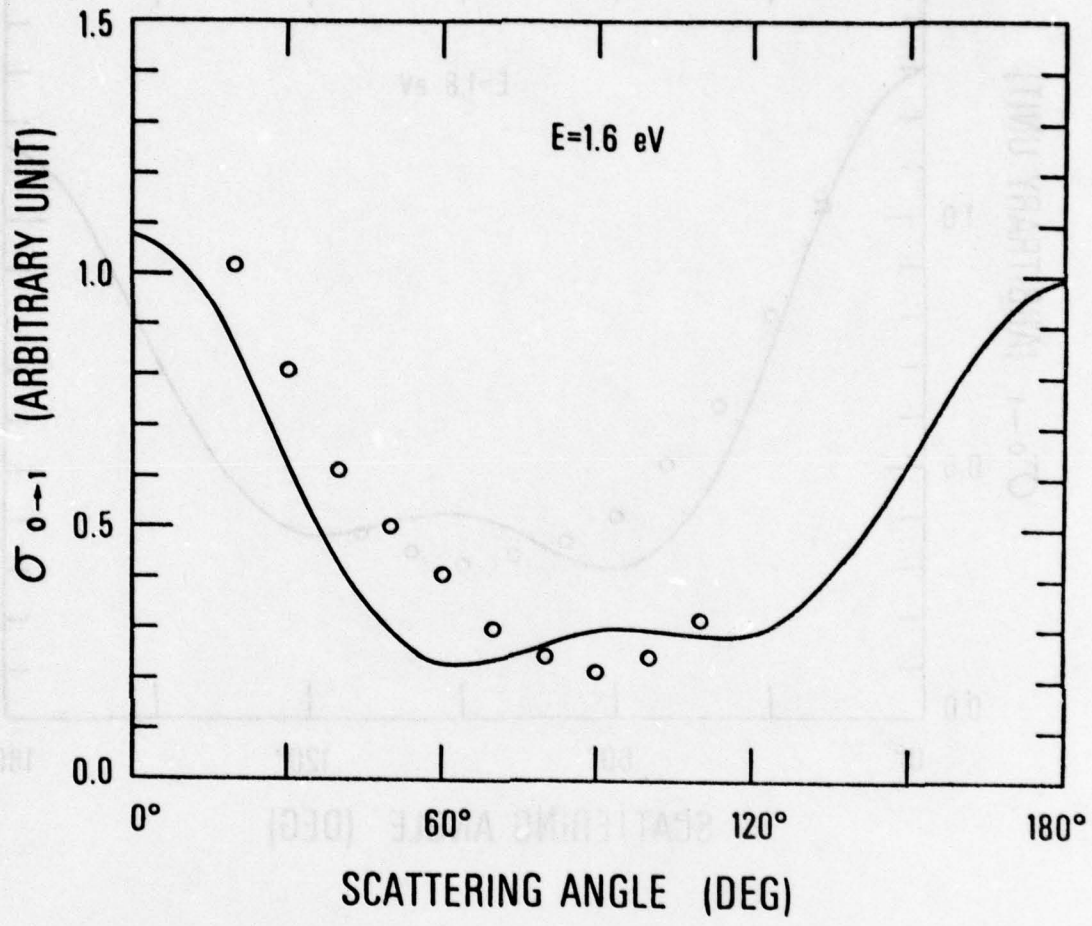

Figure 16. Differential Cross Section for 0→1 Vibrational Excitation at E = 1.6 eV; ——— Present Calculation; oooo Experimental Data Taken from Ref. 40, but These are not Absolutely Calibrated.

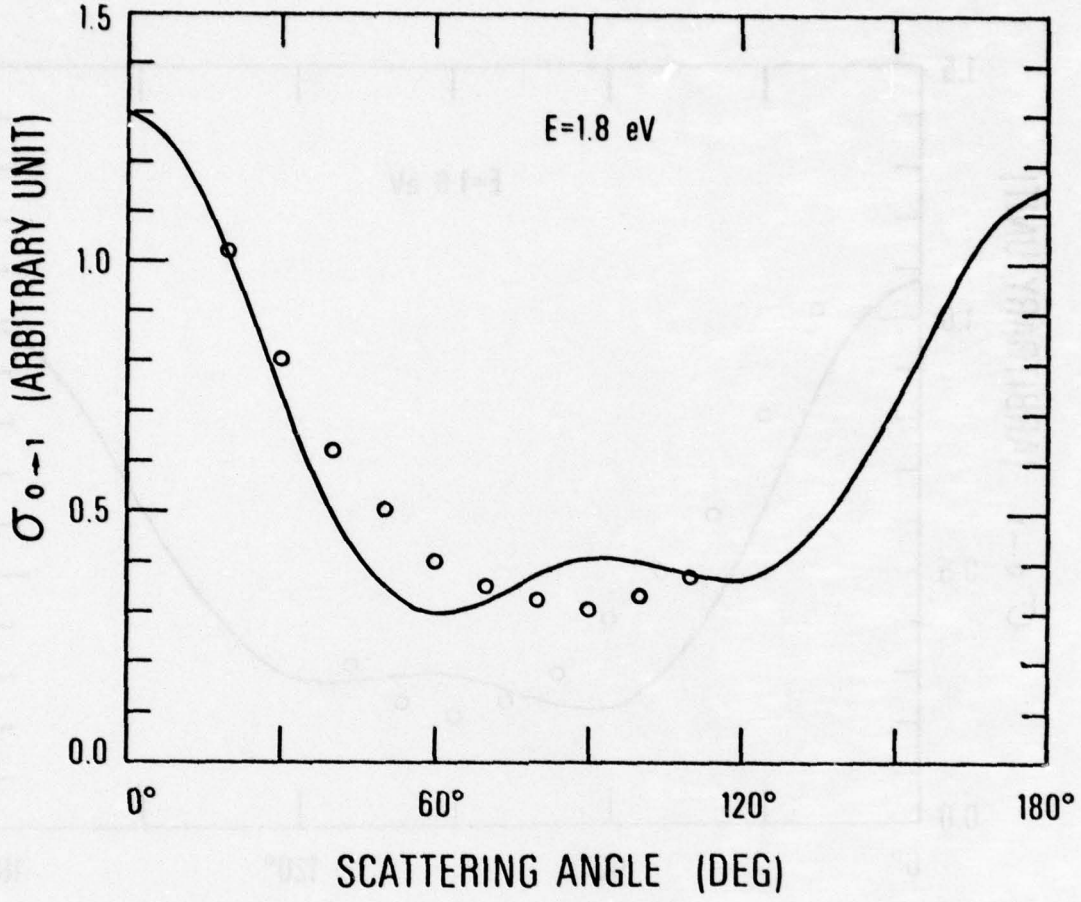

Figure 17. Differential Cross Section for 0→1 Vibrational Excitation at E = 1.8 eV; Notations of Curves are the Same as in Figure 16.

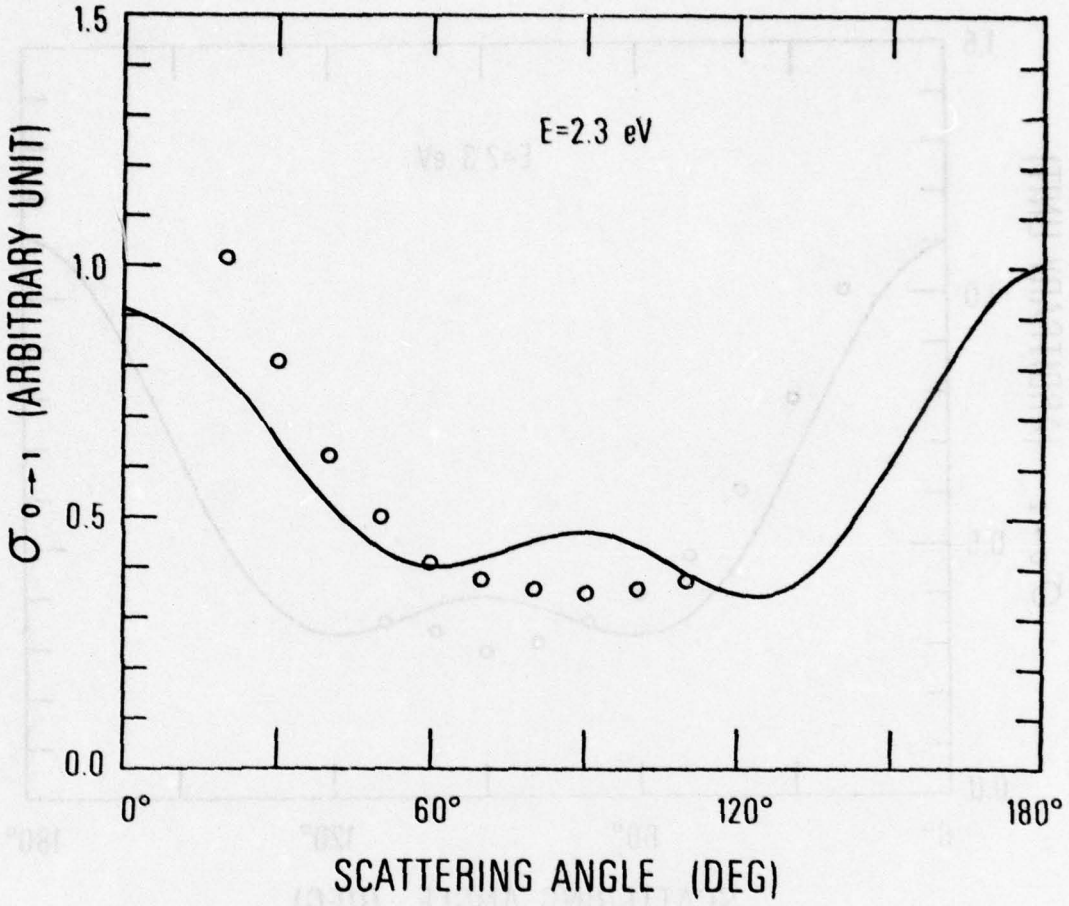

Figure 18. Differential Cross Section for 0→1 Vibrational Excitation at E = 2.3 eV; Notations of Curves are the Same as in Figure 16.

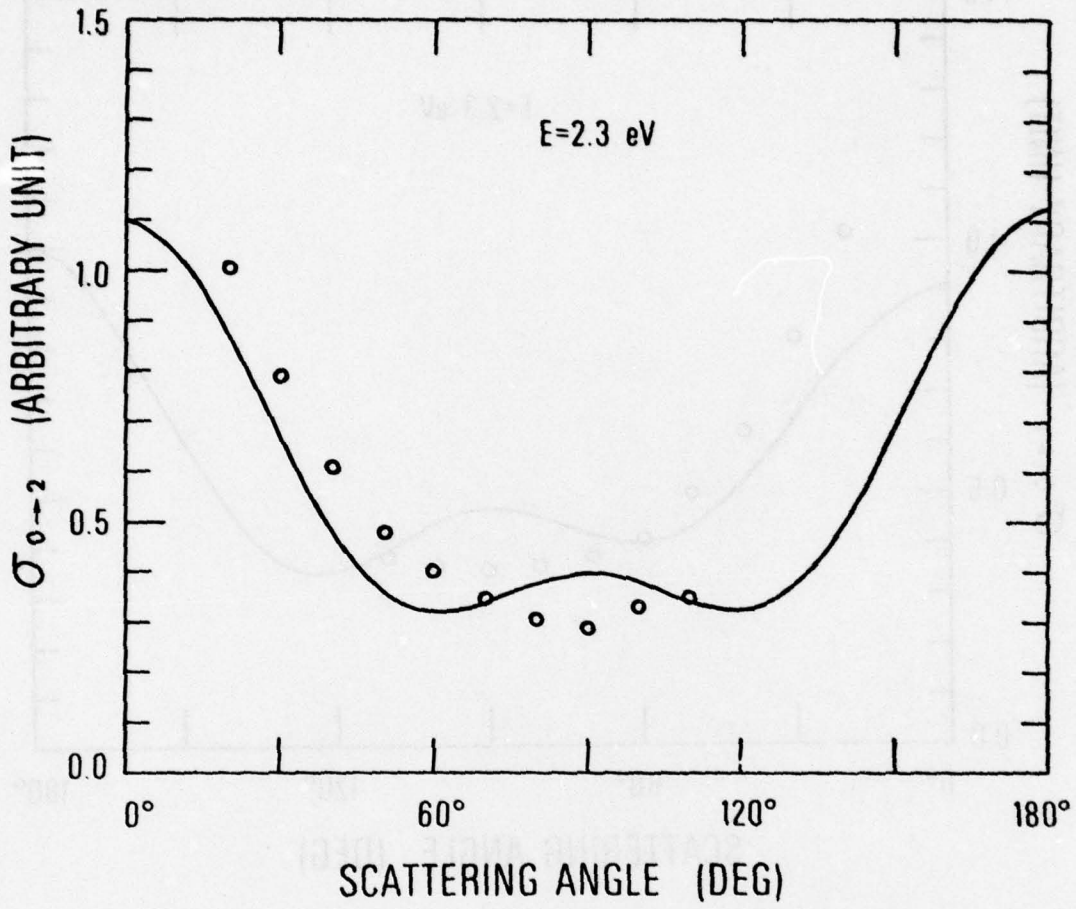

Figure 19. Differential Cross Section for 0→2 Vibrational Excitation at E = 2.3 eV; Notations of Curves are the Same as in Figure 16.

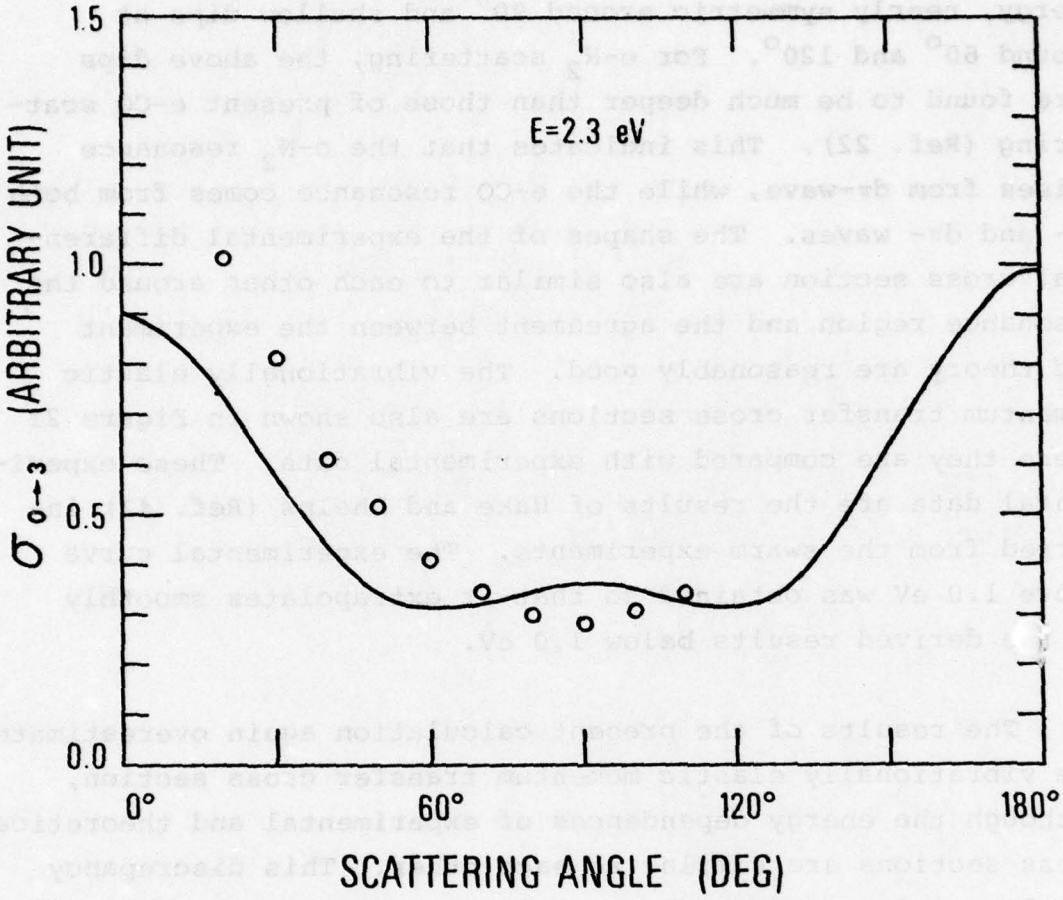

Figure 20. Differential Cross Section for 0→3 Vibrational Excitation at E = 2.3 eV; Notations of Curves are the Same as in Figure 16.

energy, nearly symmetric around 90^0 and shallow dips at around 60^o and 120^o. For e-N_2 scattering, the above dips were found to be much deeper than those of present e-CO scattering (Ref. 22). This indicates that the e-N_2 resonance arises from $d\pi$-wave, while the e-CO resonance comes from both $p\pi$- and $d\pi$- waves. The shapes of the experimental differential cross section are also similar to each other around the resonance region and the agreement between the experiment and theory are reasonably good. The vibrationally elastic momentum transfer cross sections are also shown in Figure 21 where they are compared with experimental data. These experimental data are the results of Hake and Phelps (Ref. 42) inferred from the swarm experiments. The experimental curve above 1.0 eV was obtained so that it extrapolates smoothly to the derived results below 1.0 eV.

The results of the present calculation again overestimate the vibrationally elastic momentum transfer cross section, although the energy dependences of experimental and theoretical cross sections are similar to each other. This discrepancy mainly originates from the non-resonant background waves.

As mentioned earlier, the main emphasis of the present e-CO project is the calculation of the vibrational transitions. Therefore, we were less concerned with the convergence on the partial waves which are important in the elastic scattering, in order to keep the computational efforts within manageable level. Furthermore, the present <u>ab initio</u> dipole moment is about 2.4 times bigger than the experimental one. This will partly cause the above overestimation of the elastic scattering, in particular, in the low energy region below 1.0 eV. In our point of view, the normalization procedure of the potential $V_1^{(stat)}(r,R)$, which contains the dipole potential

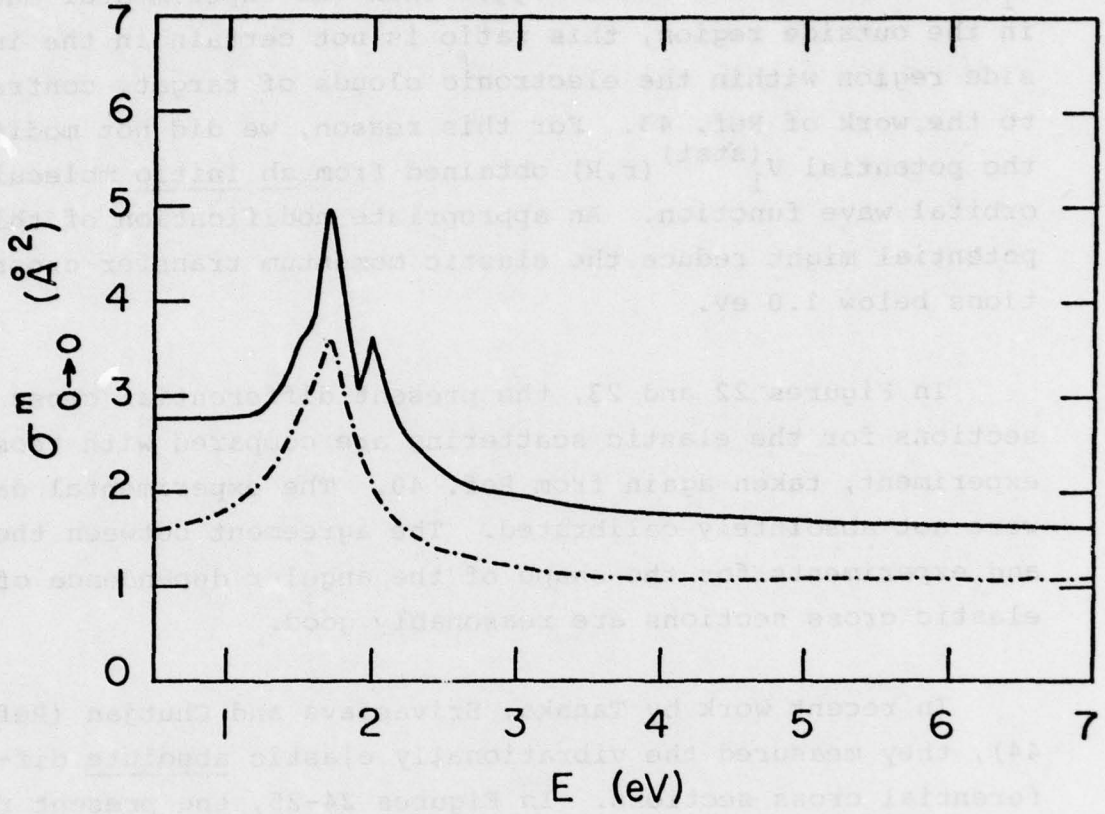

Figure 21. Vibrationally Elastic Momentum Transfer Cross Section; ——— Present Calculation; -·-·-·- Data Inferred from the Swarm Experiment in Ref. 42.

in the long range region, is not quite clear. Although $V_1^{(stat)}(r,R)$ is 2.4 times bigger than the experimental one in the outside region, this ratio is not certain in the inside region within the electronic clouds of target, contrary to the work of Ref. 43. For this reason, we did not modify the potential $V_1^{(stat)}(r,R)$ obtained from ab initio molecular orbital wave function. An appropriate modification of this potential might reduce the elastic momentum transfer cross sections below 1.0 eV.

In Figures 22 and 23, the present differential cross sections for the elastic scattering are compared with those of experiment, taken again from Ref. 40. The experimental data were not absolutely calibrated. The agreement between theory and experiments for the shape of the angular dependence of the elastic cross sections are reasonably good.

In recent work by Tanaka, Srivastava and Chutjan (Ref. 44), they measured the vibrationally elastic absolute differential cross sections. In Figures 24-25, the present results are compared with their data. (Notice the small difference between two experimental data from Ref. 35 and 38 in the shape of forward angles. See Figures 23 and 24). In general, the present results and those of experiments are fairly good in both absolute magnitude and shapes of the differential cross sections.

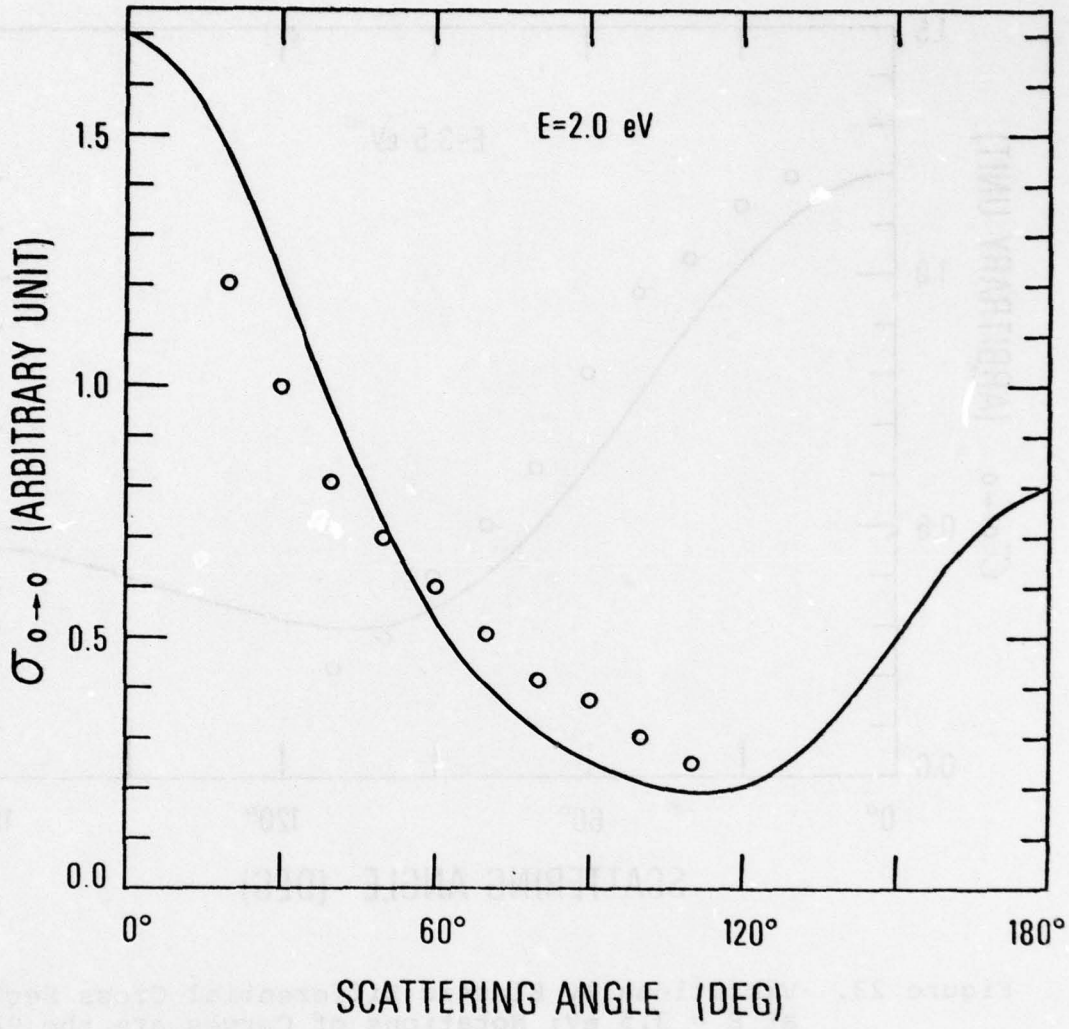

Figure 22. Vibrationally Elastic Differential Cross Section at E = 2.0 eV; ——— Present Calculation; ooooo Experimental Data Taken from Ref. 40, but These are not Absolutely Calibrated.

AD-A071 596 CALIFORNIA UNIV RIVERSIDE DEPT OF PHYSICS F/G 20/8
CALCULATION OF ELECTRON-CARBON MONOXIDE VIBRATIONAL TRANSITION --ETC(U)
APR 79 R T POE, B H CHOI F33615-77-C-2011

UNCLASSIFIED AFAPL-TR-79-2022 NL

2 OF 2
AD A071596

END
DATE FILMED
8-79
DDC

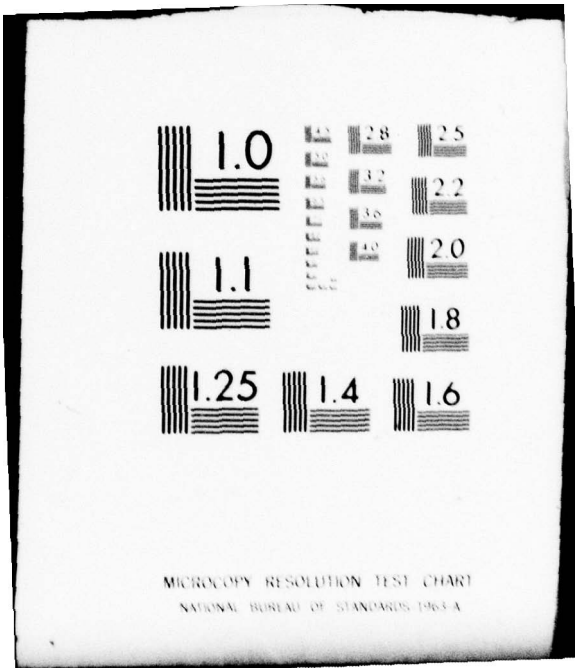
1.0
1.1
1.25
1.4
1.6
2.8
3.2
3.6
4.0
2.5
2.2
2.0
1.8
MICROCOPY RESOLUTION TEST CHART
NATIONAL BUREAU OF STANDARDS 1963-A

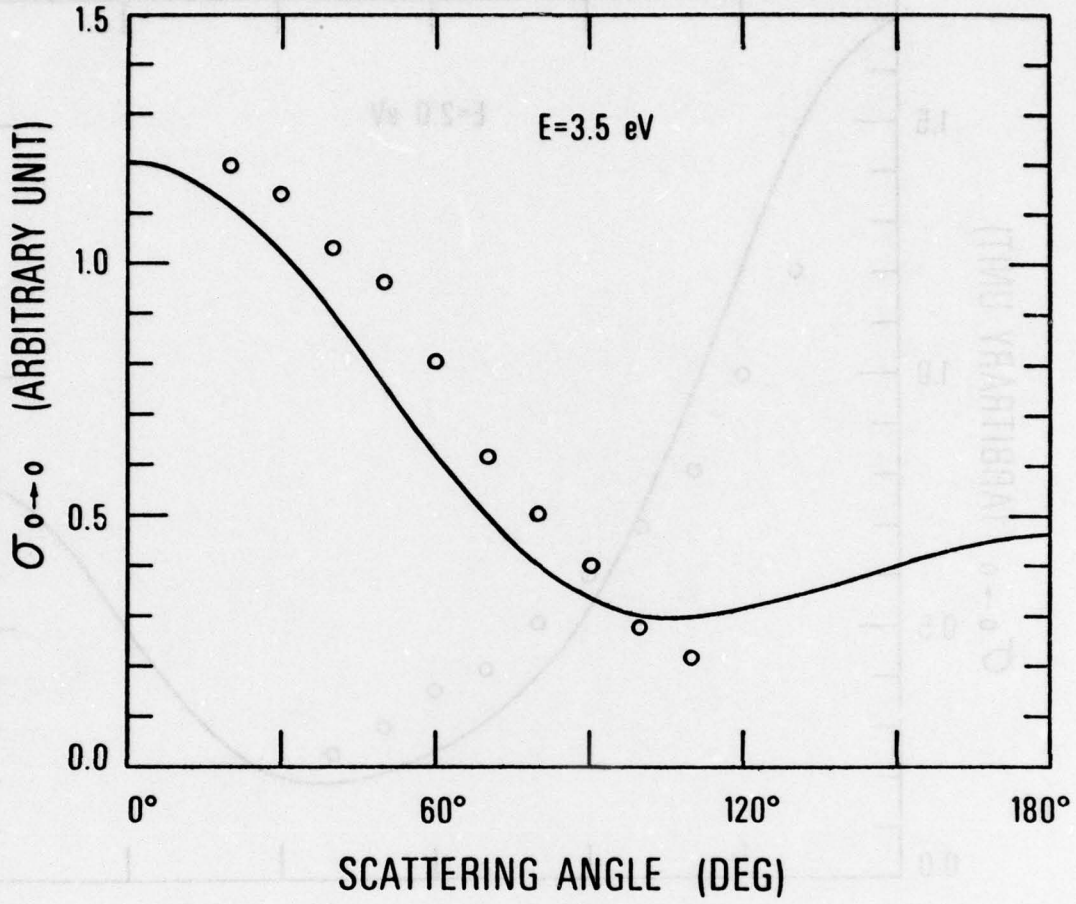

Figure 23. Vibrationally Elastic Differential Cross Section at E = 3.5 eV; Notations of Curves are the Same as in Figure 22.

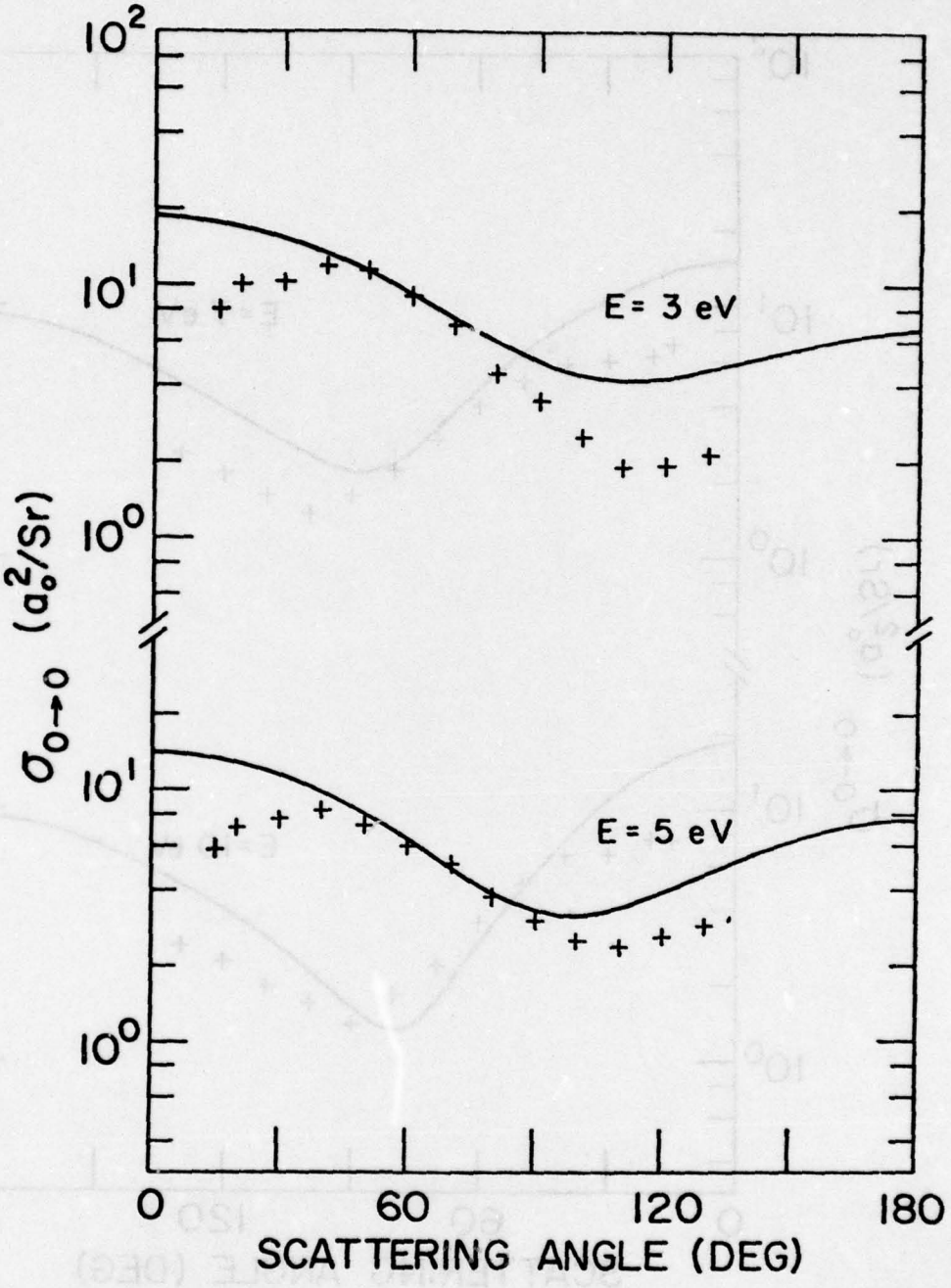

Figure 24. Vibrationally Elastic Differential Cross Section at E = 3.0, 5.0 eV; _____ Present Calculation; ++++ Experimental Data Taken from Ref. 44, and These are Absolutely Calibrated.

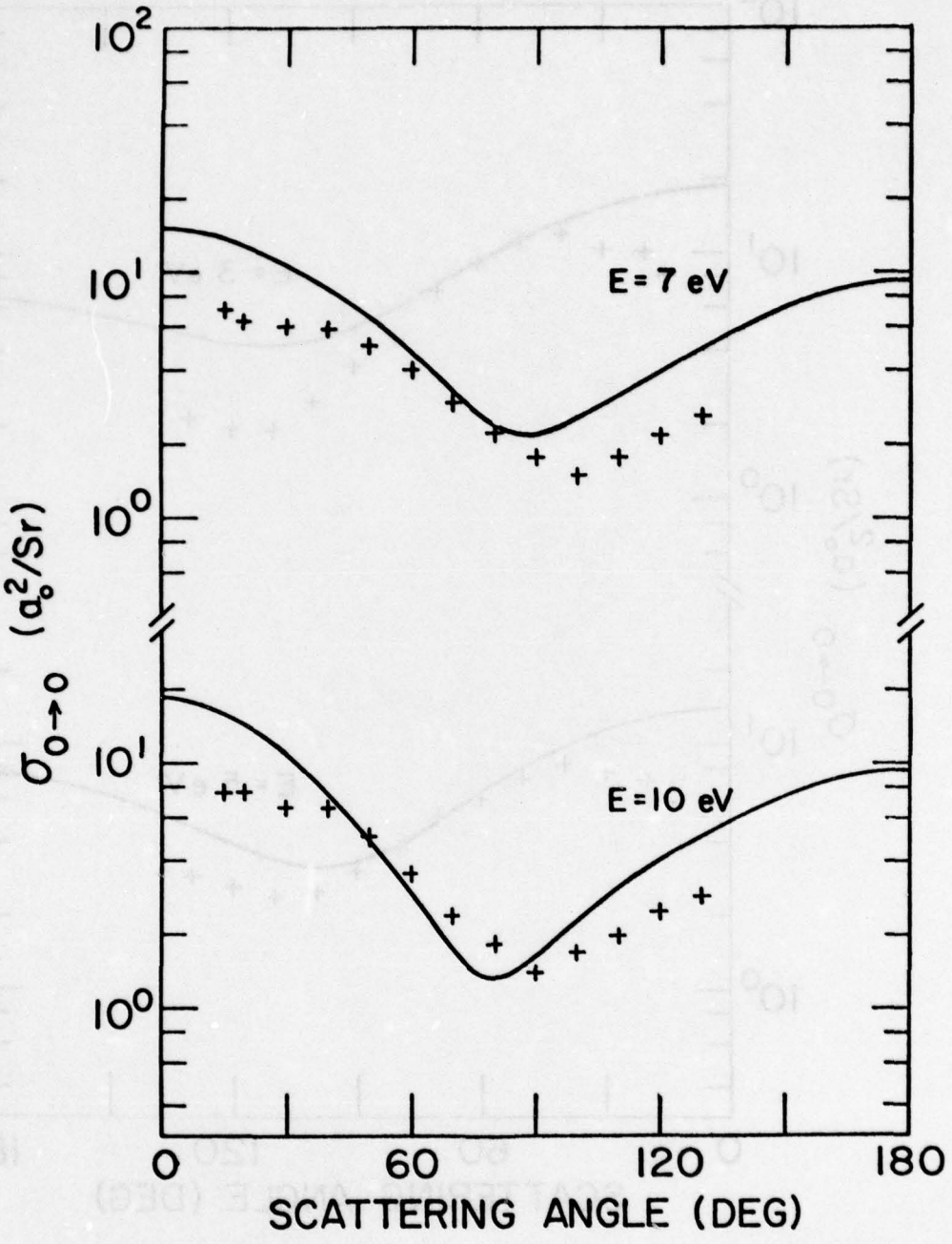

Figure 25. Vibrationally Elastic Differential Cross Section at E = 7.0, 10.0 eV; Notations of Curves are the Same as in Figure 24.

SECTION VI
DISCUSSIONS AND CONCLUSION

We have computed the vibrational transition cross sections of e-CO scattering in the energy range of 0 ~ 10 eV. The hybrid theory, which is an ab initio approach but tractable for the calculation of the vibrational transition cross section, yields reasonably good results when the accurate interaction potentials obtained from molecular orbital wave functions are used. Furthermore, this theory is capable of predicting experimental measurements as demonstrated in the 1→2 vibrational excitation.

In electron-molecule scattering, the rotational motion of target molecule is much slower than the translational motion of incident electron. Therefore, the rotational motion was treated with adiabatic approximation in hybrid theory. In other words, rotational wave functions were not included in the close-coupling calculation and the transition matrix elements were evaluated at each instantaneous direction of the internuclear axis of target. The present results showed that the rotational motion of target molecule is indeed adiabatic and is not quite so important when studying the vibrational transition cross section in which the final rotational states are summed and the initial rotational states are averaged. However, it should be noted that the adiabatic condition for rotational motion cannot be satisfied in the very low energy region such as 0 ~ 1/10000 eV.

Based on the present results, a general trend may be found for those transition cross sections connected to higher vibrational states which were not included in the calculation. For the vibrational transition with large change of vibrational quantum numbers such that $\Delta v > 7$, the corresponding cross sections will be small, at most order of 0.1 a.u. (a_o^2)

for excitation. There will be no sharp substructures of those cross sections in the present energy region. The transition cross sections between the higher vibrational states with $\Delta v=1,2,3$ must be appreciable throughout the whole energy range including threshold region. Those cross sections with $\Delta v=1$ may be on the order of 5 a.u. The cross section will decrease as Δv increases. The elastic scattering cross section ($\Delta v=0$) for higher vibrational state, will be basically given by the background of the above cross section for the ground vibrational state. However, it is generally difficult to obtain rigorous and quantitative predictions due to the irregularity of the energy dependence of transition cross sections.

We have computed the rate coefficients of elastic scattering and vibrational excitations. These are given by

$$k_{v_i \to v_f} = \langle v_e \, \sigma_{v_i \to v_f} \rangle$$

$$= \left(\frac{8}{\pi m}\right)^{\frac{1}{2}} \frac{1}{(kT)^{3/2}} \int_{\varepsilon_f - \varepsilon_i}^{\infty} E_i \sigma_{v_i \to v_f}(E_i) e^{-E_i/kT} \, dE_i$$

for $\varepsilon_f \geq \varepsilon_i$.

Here, m is the mass of electron and v_e is the incident velocity. The E_i and T are the incident energy (E_{inc}) and absolute temperature, respectively. The $\varepsilon_{i,f}$ are the initial and final vibrational energy levels. The rate coefficients of vibrational deexcitation may be obtained from

$$k_{v_f \to v_i} = k_{v_i \to v_f} \times e^{\frac{\varepsilon_f - \varepsilon_i}{kT}}$$

This equation is derived from the following relations of detailed balance and the energy conservations:

$$E_i \, \sigma_{v_i \to v_f}(E_i) = E_f \, \sigma_{v_f \to v_i}(E_f)$$

$$E = E_i + \varepsilon_i = E_f + \varepsilon_f$$

The E_f is the scattered energy.
In TABLE 4, the rate coefficients thus computed are tabulated for kT = 0.5, 1.0 and 1.5 eV. The entries of that table are in units of cm^3/sec. The numbers a-n in the table should read as $ax10^{-n}$. Since energies for which the cross sections were calculated in the present report are not dense enough to perform accurate integration over energy, we made linear interpolation for the cross sections from available ones. Therefore, the entries in the table are approximate values. Yet, the general trend of the vibrational transitions can be more easily found from the above rate coefficients. It is seen that the rates of excitation monotonically decrease as Δv increases. As the temperature increases, the rate coefficients again monotonically increase. But there is a tendency of saturation in high temperature region.

Although the hybrid theory seems to be best suited for the present purpose, it also has some weaknesses as most of other ab initio approaches do. For example, it is difficult to achieve the complete convergence on both partial waves and vibrational states with the size of core memory of the present day computer. If the number of partial waves included is sufficiently large to guarantee the convergence, then only a few vibrational states can be coupled in the calculation. A similar remark also applies to the number of vibrational states included. For this reason, we invested a considerable effort to determine the optimal values of v_{max} and ℓ_{max} (see Eq. (70)). As mentioned earlier, we were less concerned with the convergence on partial

TABLE 4

THE RATE COEFFICIENTS OF ELASTIC SCATTERING AND VIBRATIONAL TRANSITIONS FOR ELECTRON-CARBON MONOXIDE

v_i \ v_f	0	1	2	3	4	5
	kT=0.5					
0	1.4729-7	3.4234-9	1.0951-9	5.3365-10	4.6469-10	1.6074-10
1		1.4287-7	5.9041-9	2.7611-9	1.1259-9	8.0967-10
2			1.3942-7	5.9926-9	2.0535-9	9.7961-10
3				1.3759-7	4.7254-9	1.4264-9
4					1.3576-7	4.9933-9
5						1.3666-7
	kT=1.0					
0	2.1161-7	6.9466-9	2.6392-9	1.2853-9	1.1265-9	4.2100-10
1		1.9416-6	1.0571-8	5.8508-9	2.4898-9	2.0086-9
2			1.8475-7	9.6855-9	4.5533-9	2.1197-9
3				1.7998-7	7.9249-9	2.7236-9
4					1.7694-7	7.5651-9
5						1.7696-7
	kT=1.5					
0	2.3314-7	7.1663-9	2.8070-9	1.3205-9	1.1870-9	4.5676-10
1		2.1376-7	1.0901-8	6.0707-9	2.6407-9	2.1343-9
2			2.0322-7	1.0319-8	5.0428-9	2.2279-9
3				1.9763-7	8.9206-9	3.0076-9
4					1.9312-7	8.7260-9
5						1.9260-7

waves. Therefore, the present results for the elastic scattering cross sections could be less accurate than those of vibrational transition cross sections. For the latter cross sections presented in this report, a reasonable, although not complete, convergence seems to be achieved except for those transitions connected to the highest vibrational states. This arises from the inevitable "boundary effect" for any close-coupling approximation. In general, the transition cross sections with large $\Delta v = |v_i - v_f|$, for example, $\Delta v = v_{max}-1$, $v_{max}-2$, are somewhat sensitive to the number of vibrational states included. However, the contributions of these cross sections are small. The other transition cross sections are not quite as sensitive to the above number. Because of the limitation to the number of vibrational states which can be included in the calculations, it is difficult to compute the cross sections with $\Delta v >> 10$. In any case, these cross sections are very small and another method may be applied to study those transitions.

The use of accurate input potentials is no less important than the problem of convergence. Without the polarization potential, the resonance peak cannot be produced in this low energy region, in spite of the fact that the polarization potential is much smaller than the static potential. This implies that the cross sections are again sensitive to the input potentials in the resonance energy region, while it is not so in the non-resonance region. Furthermore, the exchange effect of the present e-CO vibrationally inelastic scattering seems to be more important than that of e-N_2 case, as we have seen in SECTION V.

The present theory contains only one parameter, that is, the cutoff radius r_c in the polarization potential. That parameter is not entirely phenomenological. It is approximately given by the boundary of the electronic cloud of target molecule. Beyond this radius r_c, the polarization potential

is effective. However, the present molecular structure theory does not yield the precise value of r_c. Thus, we had to determine r_c in an empirical manner as described in SECTION IV.

The use of the orthogonalization approach for the exchange effect (without any other modifications) is somewhat less physical in the sense that the cutoff radius is smaller than the above boundary. Thus the polarization potential is significant inside the electronic cloud of the target molecule and the cross sections are sensitive to r_c. In Ref. 43 where the (elastic) fixed-nuclei calculation was made for e-CO scattering with the orthogonalization approach, Chandra obtained a small cutoff radius, that is, $r_c = 1.6\ a_o$.

On the other hand, the r_c determined from close-coupling calculation with the inclusion of the local exchange potential is about the same as the above boundary. The polarization potential thus obtained is negligible inside the electronic cloud of target. The cross sections become less sensitive to r_c. Moreover, the method of the local exchange potential for the vibrational close-coupling calculation is simpler than the orthogonalization approach and yields better results. Therefore, it seems to be preferable for the present purpose.

However, it should be noted that, inside the electronic density of target, the incident and target electrons more or less experience the same potential. If the exact solutions of the Schrödinger equation can be obtained, the scattering waves should be orthogonal to the orbitals of target molecule. Thus, the orthogonality condition is partly based on physical grounds. When the local exchange potentials are used as in the present calculation, we are not sure how much above orthogonality condition is satisfied, in other words, how small the overlap integration between the scattering waves and the orbitals of target are compared with 1. The addition of the

orthogonality condition to the present local exchange method could improve the results of calculation. Therefore, the study of the vibrational transition with local exchange + orthogonalization approach will be profitable in the future.

In summary, we have successfully carried out a detailed investigation of electron-carbon monoxide vibrational transitions in the low energy region within the framework of the hybrid theory. The present project represents significant advances on two important points. First, on the theoretical side, the hybrid theory represents the most sophisticated ab initio approach that is yet still amenable to practical calculations. The predictiveness of such an ab initio theory is illustrated by the prediction of our theory, and the subsequent confirmation of the Yale experiment, of a sharp resonance at 1.4 eV for v=1→2 transitions (Ref. 41). Secondly, on the practical side, we have developed an efficient state-of-art general computer code for the hybrid theory approach in electron-diatomic molecule scatterings. While much has been learned from the present project, future applications to other important molecular species are necessary to bring about a general theoretical understanding of this important class of electron-molecule vibrational transitions.

We would like to make some remarks on figures and tables. The integral cross section curves of present theory in Figures 5-15 and 21 are based on the points with 0.1 eV increment of the energy. These are joined smoothly to obtain the above curves and it does not affect any main features of the theoretical cross sections. It is sufficient to take three significant figures of the entries in Tables 3 and 4 for practical purposes, where five significant figures are presented.

APPENDIX

USER'S MANUAL OF THE COMPUTER CODE

The computer code named "HYBRID" that computes the cross sections of the vibrational, and the simultaneous vibrational and rotational transitions for low energy e-CO scattering is described in this appendix. It will provide the guidelines for the users of the present code. The formulations on which the above computer program is based are explained in the main text of the present report.

1. Description of Subroutines

MAIN(HYBRID)

This routine controls the overall procedures of the computation. It calls most of the subroutines or function subroutines. Furthermore, all input data are read in this routine. The important input data are the maximum number of vibrational states included, the vibrational energy levels, the vibrational wavefunctions, the range of integration for the coupled differential equation, the maximum number of partial waves, the harmonic component of the static potential, the polarizabilities, the Fermi momenta of the target molecule and the energy of the incident electron.

In addition, the vibrational transition matrix elements are computed, in this routine, from the scattering wave functions obtained in the subroutine COUPLE (see the following).

SUBROUTINE COUPLE

This routine solves the coupled differential equation, that is, the Schrodinger equation. Most of the computer time is spent in this subroutine. The following Stormer's 5-strip algorithm

is used for the present purpose. The coupled differential equation is written as

$$U''(r) = V(r)U(r)$$

Here, V(r) is the NxN symmetric matrix and U(r) is the NxM matrix. The N is the dimension of the coupled differential equation, that is, the number of channels. M is the number of independent solutions. It can be shown that

$$U(r) = 2U(r-h)-U(r-2h) + \sum_{n=1}^{5} C_n V_n(r) + O(h^6)$$

with

$$V_n(r) = V(r-nh)U(r-nh) \quad (n = 1,2,3,4,5)$$

$$C_1 = 299/240,\ C_2 = -11/15,\ C_3 = 97/120$$

$$C_4 = -2/5,\ C_5 = 19/240$$

The h is the integration step size.

SUBROUTINE CROSSV

This routine evaluates the integral and the differential vibrational transition cross sections (including the elastic scattering cross sections) from the vibrational transition matrix thus obtained. All vibrational transition cross sections are printed out here.

SUBROUTINE CROSSVJ

The simultaneous vibrational and rotational transition cross section (for both integral and differential cross section) are evaluated in this routine. It is called in MAIN only when ICVJ≠0 (see subsection 2.) The above cross sections are printed out in this routine.

SUBROUTINE MINVR

This routine computes the inversion matrix A^{-1} for a given real non-singular matrix A. The matrix inversion is needed as a part of algorithm in COUPLE.

SUBROUTINE MINV

The same as MINVR except for a given complex non-singular matrix A. This routine is called in MAIN when the vibrational transition matrix elements are evaluated.

SUBROUTINE SIMQR

This solves the simultaneous linear equation Ax=y for given real non-singular matrix A and column vector y. It is called again in MAIN when the vibrational transition matrix elements are evaluated.

SUBROUTINE BSSL

The spherical Bessel and Neumann functions are generated in this routine for the purpose of matching the scattering solution of the coupled differential equation in the asymptotic region where the interaction potential is negligible. The matching procedure is needed to obtain the vibrational transition matrix elements.

FUNCTION CLEBSH

This function subroutine computes the vector coupling coefficients between two angular momentum eigenfunctions. It is the most frequently called routine in CROSSV and CROSSVJ. It is also called in MAIN when the vibrational matrix elements of the interaction potential are constructed as a preparation of close-coupling calculation.

FUNCTION RACAH

This function subroutine computes the vector recoupling coefficients between three angular momentum eigenfunctions. It is called in CROSSVJ only when the simultaneous vibrational and rotational transition cross sections are evaluated.

FUNCTION GAUSSN

The integrations are performed in this function subroutine using the Gaussian 5-point quadrature formular. The range of integration is divided into equal intervals and the above formular is applied in each interval. It is called in MAIN when the local exchange potential is generated.

The calling sequences of the routines are shown in Figure A-1. Here, [A] → [B] denotes that the routine B is called in the routine A.

2. Input Data Structures

The information on the physical properties of target molecule and the electron-molecule interaction potential are inputted in the present program. These include the vibrational matrix elements for the harmonic components of the static potential with specified maximum component, its mesh points, the vibrational energy levels, the vibrational quantum numbers, the target mass, the ionization potential, the vibrational wave function, the polarizabilities and the local Fermi momentum. Other inputted parameters are those related to the numerical procedures to generate the scattering wave functions by solving coupled differential equation and to compute the cross sections. Most of the input data are read from (input) cards, except the following arrays; VWF (vibrational wave function), VS (the vibrational matrix elements for the harmonic components of static potential) and AKFER (local

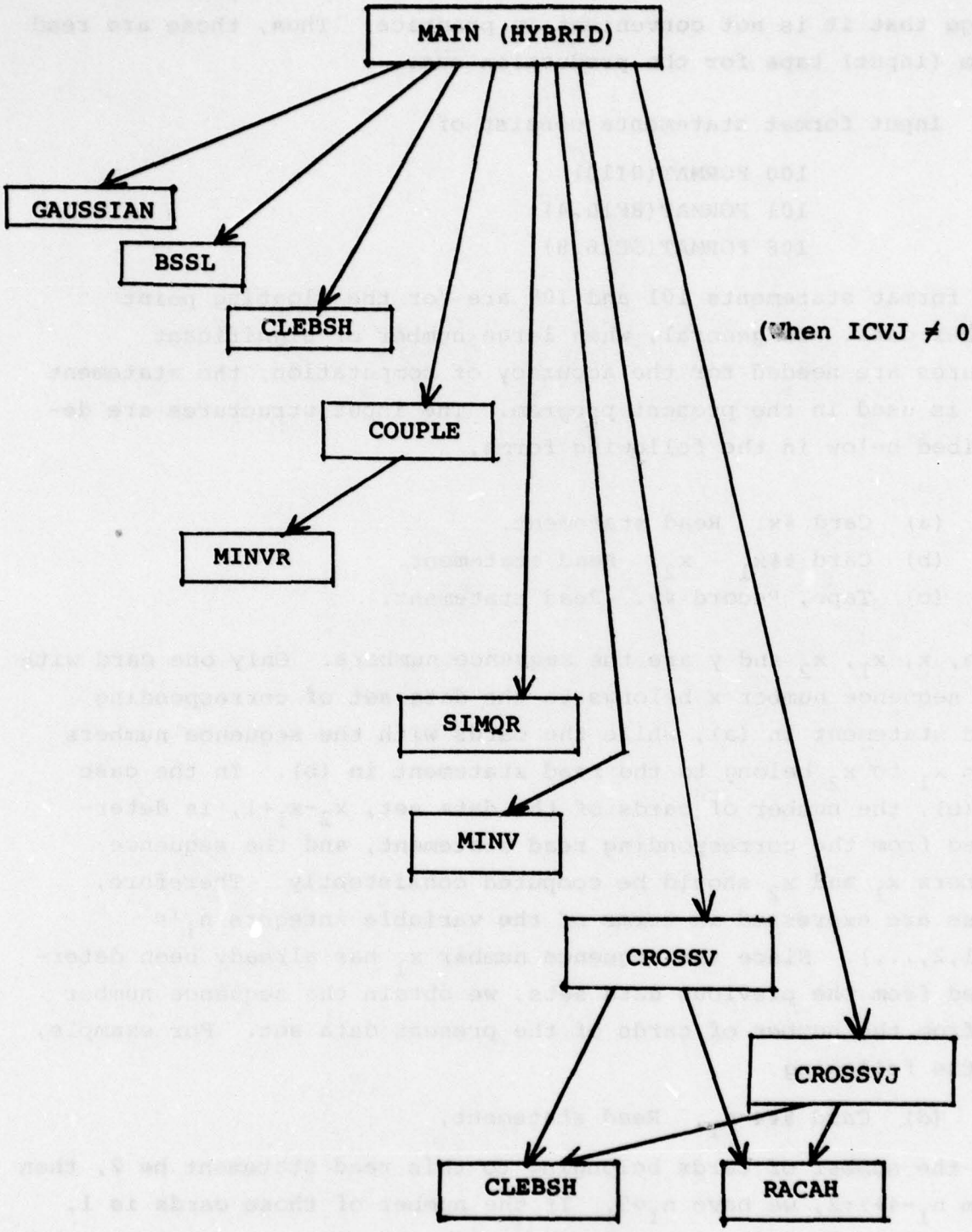

Figure A-1. The Calling Sequence of the Subroutines.

Fermi momentum). These data may be read from cards for the testing purpose, but the numbers of elements of the arrays are so large that it is not convenient in practice. Thus, those are read from (input) tape for the production run.

Input format statements consist of

```
100 FORMAT(8I10)
101 FORMAT(8F10.4)
108 FORMAT(5E16.8)
```

The format statements 101 and 108 are for the floating point number data. In general, when large number of significant figures are needed for the accuracy of computation, the statement 108 is used in the present program. The input structures are described below in the following forms,

(a) Card #x. Read statement.
(b) Card ##x_1 ~ x_2. Read statement.
(c) Tape, Record #y. Read statement.

Here, x, x_1, x_2 and y are the sequence numbers. Only one card with the sequence number x belongs to the data set of corresponding read statement in (a), while the cards with the sequence numbers from x_1 to x_2 belong to the read statement in (b). In the case of (b), the number of cards of the data set, x_2-x_1+1, is determined from the corresponding read statement, and the sequence numbers x_1 and x_2 should be computed consistently. Therefore, these are expressed in terms of the variable integers n_i's (i=1,2,...). Since the sequence number x_1 has already been determined from the previous data sets, we obtain the sequence number x_2 from the number of cards of the present data set. For example, in the following

(d) Card ##4~n_1. Read statement,

let the number of cards belonging to this read statement be 2, then from $n_1-4+1=2$, we have $n_1=5$. If the number of those cards is 1, then $n_1=4$. In this case, (d) is equivalent to

(e) Card #4. Read statement.

Card #1. READ 100, NLEVX, INCO, NTR, LLMAX, KKVS

NLEVX: The maximum number of the vibrational states included.

INCO: The number of times the step sizes are doubled while integrating the coupled differential equation.

NTR: The number of times the readjustments are made to improve the accuracy while solving the coupled diffential equation.

LLMAX: The maximum harmonic component of interaction potential.

KKVS: The number of mesh points for input (interaction) potential.

<sample> 2 3 5 8 50

Card #2. READ 100, (NBO(K), K = 1, INCO)

NBO(K): At these mesh points, the stepsizes are doubled.

<sample> 9 30 50

Card #3. READ 100,(IV(K), K = 1 NTR)

IV(K): At these mesh points, the readjustments are made.

<sample> 60 100 200 350 0

(The last one is always 0 to terminate the readjustment).

Card ##4~n_1. READ 108, EJJ, (EJ(I), I=1, NLEVX)

The number of cards in this data set, n_1-4+1, is given as

$$n_1-4+1 = [(NLEVX+1)/5]$$

Here, [a] denotes the smallest integer n such that $n \geq a$.

EJJ: This variable is $\neq 0$, when the electronic structures of the target and the residual molecule are different. Otherwise, it is =0.

EJ(I): The energy of the Ith vibrational level (in eV). EJ(1)=0.

<sample> 0.00000000E+00 0.00000000E+00 2.65720790E-01

Card #n_1+1. READ 100, (NVF(I), I=1, NLEVX)

NVF(I): The vibrational quantum number for Ith level.

<sample> 0 1

Card #n_1+2. READ 101, TMASS

TMASS: The mass of the target molecule in amu (atomic mass units).

<sample> 28.

Card #n_1+3. READ 101, RNG, STEPNO, RMIN0, RMTCH, RVNG, VX, RCUT

RNG: The whole range of integration for the coupled differential equation (in a.u.).

STEPNO: The number of mesh points for each half oscillation of the scattering wave function.

RMIN0: The starting point of the integration (in a.u.). Usually it is the origin and thus is equal to 0.

RMTCH: The matching point of the integrated solution to the known form of the asymptotic wave function (in a.u.).

RVNG: After this point, the interaction potential is negligibly small and it is set to zero (a.u.).

VX: The (approximate) maximum strength of the interaction potential (in eV).

RCUT: The cut-off radius in the polarization potential (in a.u.)

<sample> 20.5 20. 0.0 20.25 20. 245. 1.945

Card #n_1+4. READ 100, NRL

NRL: The number of equal interval for the range of internuclear separation. The Gaussian 5-point quadruature formular is applied in each interval for integration of the quantities related to the vibrational wave functions.

<sample> 15

Card #n_1+5. READ 101, VRNG, RSTRT.

VRNG: The range of the internuclear separation considered for the vibrational wave function (a.u.).

RSTRT: The smallest internuclear separation (a.u.).

<sample> 0.967 1.75

Card #n_1+6. READ 101, (RT(K), K=1,7)

RT(K): The Kth internuclear separation for which the molecular wave function of the target is given.

<sample> 1.8 1.898 2.015 2.132 2.249 2.366 2.483

Card #n_1+7. READ 100, NNG

NNG: The number of equal interval for the range of the angles between the internuclear axis and the position vector of the incident electron. The Gaussian 5-point quadrature formular is applied in each interval for the integration.

<sample> 12

Card #n_1+8. READ 101, (ENB(K), K=1,7)

ENB(K): The ionization potential (in a.u.) of the target molecule at RT(K).

<sample> 0.52845 0.53698 0.54634 0.55437 0.56053 0.56427 0.56514

Tape, Record #1. DO208 N=1, NLEVX
READ(20,108)(VWF(N,K),K=1,KRL)
208 PRINT 108, ...

VWF(N,K): The vibrational wave function.

Here, KRL = 5*NRL

Card ##n_1+9~n_2. READ 101, (RVS(K), K=1, KKVS)

The number of cards in this data set,

n_2-n_1-9+1 = [KKVS/8]

RVS(K): The Kth mesh point for the input potential.

<sample>

0.0	0.05	0.10	0.15	0.20	0.25	0.30	0.40
0.50	0.60	0.70	0.80	0.90	0.95	1.00	1.025
1.05	1.075	1.10	1.20	1.30	1.40	1.50	1.60
1.70	1.80	1.90	2.00	2.20	2.30	2.40	2.50
2.60	2.80	3.00	3.20	3.40	3.60	3.80	4.00
4.20	4.60	5.00	5.40	5.80	6.20	6.60	7.00
7.40	7.80						

Card ##n_2+1~n_3. READ 108, (ALP0(IJ),1J=1,IJX)

Here IJX = NLEVX*(NLEVX+1)/2.

The number of cards in this data set,

$$n_3-n_2-1+1 = [IJX/5]$$

ALP0(IJ): The 0.5 times the vibrational matrix elements of the spherical polarizabilities.

<sample> 6.66363442E+00 -1.37499560E-01 6.70040101E+00

Card ##n_3+1~n_4. READ 108, (ALP2(IJ),IJ=1,IJX)

The number of cards in this data set,

$$n_4-n_3-1+1 = [IJX/5]$$

ALP2(IJ): The 0.5 times the vibrational matrix elements of the non-spherical polarizabilities.

<sample>1.20439007E+00 -1.18009803E-01 1.23198772E+00

```
Tape, Record #2.  DO39 LL1=1, LLMX1
                  DO 84 IJ=1, IJX
                  READ(21,108)(VS(IJ,LL1,K),K=1,KKVS)
                84 CONTINUE
                  DO 514 IJ=IJX1,55
                  READ(21,108)(U(K),K=1,KKVS)
               514 CONTINUE
                39 CONTINUE
```

Here, LLMX1=LLMAX+1, IJX1=IJX+1

VS(IJ,LL1,K): The vibrational matrix elements of the harmonic components of the static potential.

U(K): Dummy variable. It simply completes the reading of the present record of the tape.

```
Tape, Record #3.  DO 513 II=1,7
                  DO 513 J=1, KKVS
                  READ(22,108)(AKFER(II,J,K),K=1,KNG)
               513 CONTINUE
Here, KNG = 5*NNG
AKFER(II,J,K):  The local Fermi momentum.

Card #n4+1.  READ 100, LMAX,MMN,MMX

     LMAX:  The maximum partial wave for the angular momentum.
      MMN:  The minimum value of the internuclear projection
            of the angular momenta.
      MMX:  The maximum value of the above projection.

<sample>        4          0          2

Card #n4+2.  READ 100, KNNG,IVN,IVX,ICVJ

     KNNG:  The number of the scattering angles for the dif-
            ferential cross section to be evaluated.  The angles
            are divided into equal intervals.
      IVN:  The lowest vibrational energy level for which the
            cross sections are to be computed.
      IVX:  The (possible) highest vibrational energy level for
            which the cross sections are to be computed.
     ICVJ:  If it is = 0, only vibrationally elastic and the
            vibrational transition cross sections are to be com-
            puted.  If it is ≠0, the simultaneous vibrational and
            rotational transition cross section together with the
            above cross sections are to be computed.

<sample>          31         1          10         0
```

Card #n_4+3. READ 100,LAMXV,LAMX

LAMXV: If it is =1, the momentum transfer cross sections are to be calculated. If it is =0, no momentum cross sections can be computed.

LAMX: The maximum harmonic component included when the differential cross sections are evaluated in the vibrational transitions.

<sample> 1 8

Card #n_4+4. READ 100, JBN,JBX,LAMXJ

This data card should be deleted when ICVJ=0.

JBN: The lowest rotational state for which the cross sections are to be computed.

JBX: The highest rotational state for which the cross sections are to be computed.

LAMXJ: The maximum harmonic component included when the differential cross sections are evaluated in the simultaneous vibrational and rotational transitions.

<sample> 1 10 8

Card #n_4+5~n_5. READ 101, E

E: Total energy (the incident energy when the target molecule is in the ground vibrational state) in eV.

The number of cards in this data set, n_5-n_4-5+1, is equal to the number of the energies for which the cross sections to be computed plus one. Any negative energy should be punched on the last card in this data set to terminate the whole program.

<sample> 4.2
-4.2

3. Output Structures

The outputs of the present program are in the form of the print outputs. No cards are punched out. The input cards ##1~n_5 are printed out at the same time when they are read, except the last card (#n_5). The data in Tape, Record #1, which are the vibrational wavefunctions from RSTRT to RSTRT+VRNG, are also printed out. The data in other Record of this Tape are not printed out because the number of elements in those data is very large. For each total energy E, all the cross sections are printed out. They are illustrated as follows:

```
<sample>        E = 4.2000
                    NLEVL = 2
                    IMX   = 593
                    MM    = 0
                    NMAX  = 10
                    MM    = 1
                    NMAX  = 8
                    MM    = 2
                    NMAX  = 6

              EI = 4.2000      VI = 0      VF = 0

     XSECT = 7.76528843E+01      XSECTM = 6.25863523E+01

  0.00000    1.44929E+01    6.00000    1.43962E+01    .....
 24.00000    1.30153E+01   30.00000    1.22427E+01    .....
             ..................................
168.00000    6.50562E+00  174.00000    6.64248E+00    .....

              EI = 4.2000      VI = 0      VF = 1

     XSECT = 3.96312693E-01      XSECTM = 3.99817954E-01

  0.00000    1.32235E-02    6.00000    1.64626E-02    .....
             ..................................
168.00000    8.65896E-02  174.00000    9.24595E-02    .....
```

Here, the variables related to the cross sections are

EI: The incident energy of the electron (eV).

VI: The initial vibrational quantum number.

VF: The final vibrational quantum number.

XSECT: The integral cross section for this transition (a_o^2).

XSECTM: The momentum transfer cross section for this transition (a_o^2).

Note that EI is equal to the total energy E when VI = 0. The entries in Column #1,3,5,7 of the above tabular output are the scattering angles in degree and the entries in Column #2,4,6,8 are the differential cross sections (a_o^2/sr) for this transition.

REFERENCES

(1) Gryzinski, M.: "Two-Particle Collisions. I. General Relations for Collisions in the Laboratory System", Phys. Rev. 138, A302 (1965); "Two-Particle Collisions. II. Coulomb Collisions in the Laboratory System of Coordinates". Ibid., A322 (1965); "Classical Theory of Atomic Collisions. I. Theory of Inelastic Collisions". Ibid., A336 (1965).

(2) Chen, J. C. Y.: "Theory of Subexcitation Electron Scattering by Molecules. I. Formalism and the Compound Negative-Ion States", J. Chem. Phys. 40, 3507 (1964); "Theory of Subexcitation Electron Scattering by Molecules. II. Excitation and De-Excitation of Molecular Vibration". Ibid., 3513 (1964); "Interpretation of the Cross Section for Vibrational Excitation of Molecules by Electrons". Ibid., 45, 2710 (1966); "Direct and Resonance Rotational Excitation of Molecules by Slow Electrons", Phys. Rev. 146, 61 (1966).

(3) Birtwistle, D. T. and Herzenberg A.: "Vibrational Excitation of N_2 by Resonance Scattering of Electrons", J. Phys. B4, 53 (1971).

(4) Gerjuoy, E. and Stein, S.: "Rotational Excitation by Slow Electrons", Phys. Rev. 97, 1671 (1955); "Rotational Excitation by Slow Electrons II", Ibid., 98, 1848 (1955).

(5) Altshuler, S.: "Theory of Low-Energy Electron Scattering by Polar Molecules", Phys. Rev. 107, 114 (1957).

(6) Wijnberg, L.: "Rotational Excitation of Molecules in Collisions with Slow Electrons", J. Chem. Phys. 44, 3864 (1966).

(7) Chang, T. N., Poe, R. T., and Ray, P.: "Glauber-Theory Approach for Molecular Vibrational Excitations", Phys. Rev. Lett. 31, 1097 (1973).

(8) Takayanagi, K. and Geltman, S.: "Excitation of Molecular Rotation by Slow Electrons", Phys. Rev. 138, A1003 (1965).

(9) Dalgarno, A. and Henry, R. J. W.: "The Rotational Excitation of Molecular Hydrogen by Slow Electrons", Proc. Phys. Soc. (London) 85, 679 (1965).

(10) Ardill, R. W. B. and Davison, W. D.: "Exchange Effects in the Rotational Excitation of Molecular Hydrogen by Slow Electrons", Proc. Roy. Soc. (London) A304, 465 (1968).

(11) Lane, N. F. and Geltman, S.: "Rotational Excitation of Diatomic Molecules by Slow Electrons: "Application to H_2", Phys. Rev. 160, 53 (1967).

(12) Henry, R. J. W. and Lane, N. F.: "Polarization and Exchange Effects in Low-Energy Electron-H_2 Scattering", Phys. Rev. 183, 221 (1969) .

(13) Itikawa, Y. and Takayanagi, K.: "Rotational Transition in Polar Molecules by Electron Collisions: Applications to CN and Hcℓ", J. Phys. Soc. Japan, 26, 1254 (1969).

(14) Temkin, A. and Vasavada, K. V.: "Scattering of Electrons from H_2^+: The Method of Polarized Single-Center Orbitals", Phys. Rev. 160, 109 (1967); Temkin A., Vasavada, K. V., Chang, E.S. and Silver, A.: "Scattering of Electrons from H_2^+. II", Ibid., 186, 57 (1969).

(15) Hara, S.: "A Two-Center Approach in the Low Energy Electron-H_2 Scattering", J. Phys. Soc. Japan, 27, 1009 (1969).

(16) Burke, P. G. and Chandra, N.: "Electron-Molecule Interactions III. A Pseudo-Potential Method for e^--N_2 Scattering", J. Phys. B5, 1696 (1972).

(17) Burke, P. G., Mackey, I. and Shimamura, I.: "R-Matrix Theory of Electron-Molecule Scattering", J. Phys. B10, 2497 (1977).

(18) Schneider, B. I.: "R-Matrix Theory for Electron-Molecule Collisions Using Analytic Basis Set Expansions. II. Electron-H_2 Scattering in the Static-Exchange Model", Phys. Rev. A11, 1957 (1975); Schneider, B. I. and Hay, P. J.: "Elastic Scattering of Electron from F_2: An R-Matrix Calculation". Ibid., A13, 2049 (1976).

(19) Chase, D. M.: "Adiabatic Approximation for Scattering Processes", Phys. Rev. 104, 838 (1956).

(20) Hara, S.: "Rotational Excitation of H_2 by Slow Electrons", J. Phys. Soc. Japan, 27, 1592 (1969).

(21) Temkin, A. and Faisal, F. H. M.: "Adiabatic Theory of Rotational Excitation of Non-Σ States", Phys. Rev. A3, 520 (1971); Chang, E. S. and Temkin, A.: "Rotational Excitation of Diatomic Molecules by Electron Impact", Phys. Rev. Lett. 23, 399 (1969).

(22) Chandra, N. and Temkin, A.: "Hybrid Theory and Calculation of e-N_2 Scattering", Phys. Rev. A13, 188 (1976); "Hybrid Theory Calculation of Simultaneous Vibration-Rotation Excitation in e-N_2 Scattering"; Ibid., A14, 507 (1976); "Hybrid Theory Calculation of Electron-N_2 Scattering at 5 and 10 eV", J. Chem. Phys. 65, 4537 (1976).

(23) Morrison, M. A. and Lane, N. F.: "Vibrational Excitation in e-CO_2 Collisions", Bull. Am. Phys. Soc., Vol. 23, No. 9, p. 1082 (DEAP, Nov. 1978).

(24) Faisal, F. H. M. and Temkin, A.: "Application of the Adiabatic-Nuclei Theory to Vibrational Excitation", Phys. Rev. Lett. 28, 203 (1972).

(25) Siegel, J., Dehmer, J. L., Dill, D., and Welch, J.: "Integrated and Differential Elastic and Vibrationally Inelastic Cross Sections for e-N_2 Scattering", Bull. Am. Phys. Soc., Vol. 23, No. 9, p. 1082 (DEAP, Nov. 1978).

(26) Choi, B. H. and Poe, R. T.: "Vibrational and Rotational Transitions in Low-Energy Electron-Diatomic-Molecule Collisions. II. Hybrid Theory and Close-Coupling Theory: An ℓ_z,-Conserving Close-Coupling Approximation", Phys. Rev. A16, 1831 (1977).

(27) Edmonds, A. R.: Angular Momentum in Quantum Mechanics, Princeton University Press (Princeton, 1957).

(28) Harris, F. E. and Michels, H. H.: "Multicenter Integrals in Quantum Mechanics. I. Expansions of Slater-Type Orbital, About a New Origin", J. Chem. Phys. 43, S165 (1965).

(29) Faisal, F. H. M.: "Electron-Molecule Interactions. I. Single-Centre Wave Functions and Potentials", J. Phys. B3, 636 (1970).

(30) Chandra, N.: "Low-Energy Electron Scattering from CO", Phys. Rev. A12, 2342 (1975).

(31) McLean, A. D. and Yoshimine, M.: "Computation of Molecular Properties and Structure", IBM J. Res. Dev. Suppl. 12, 206 (1967).

(32) Levine, I. N.: "Accurate Potential-Energy Function for Diatomic Molecules", J. Chem. Phys. 45, 827 (1966).

(33) Bridge, N. J. and Buckingham, A. D.: "The Polarization of Laser Light Scattered by Gases", Proc. Roy. Soc. (London), Ser. A295, 334 (1966).

(34) Lippincott, E. R. and Nagarajan, G.: "Absolute Raman Intensities of Symmetrical Stretching Modes in Some Molecules and Ions from Delta-Function Model of Chemical Binding", Bull. Soc. Chim. Belges, 74, 551 (1965).

(35) Hirschfelder, J. O., Curtiss, C. F. and Bird, R. B.: Molecular Theory of Gases and Liquids, (John Wiley and Sons, Inc., N.Y., 1954).

(36) Choi, B. H. and Tang, K. T.: "Inelastic Collisions Between an Atom and a Diatomic Molecule. I. Theoretical and Numerical Considerations for the Close-Coupling Approximation", J. Chem. Phys. 63, 1775 (1975).

(37) Slater, J. C.: Quantum Theory of Atomic Structure, Vol. 1, Appendix 19 (McGraw Hill, N.Y. 1960); Ibid., Vol. 2, Appendix 22 (McGraw Hill, N.Y. 1960); Quantum Theory of Matter, Ch. 17 (McGraw Hill, N.Y. 1968).

(38) Hara, S.: "The Scattering of Slow Electrons by Hydrogen Molecules", J. Phys. Soc. Japan, 22, 710 (1967).

(39) Morrison, M. A., Collins, L. A., and Lane, N. F.: "Theoretical Study of Low-Energy Electron-CO_2 Scattering", Chem. Phys. Lett. 42, 356 (1976); Morrison, M. A. and Collins, L. A.: "Exchange in Low-Energy Electron-Molecule Scattering: Free-Electron-Gas Model Exchange Potential and Applications to e-H_2 and e-N_2 Collisions", Phys. Rev. A17, 918 (1978).

(40) Ehrhardt, H., Langhans, L. Linder, F., and Taylor, H. S.: "Resonance Scattering of Slow Electrons from H_2 and CO Angular Distributions", Phys. Rev. A17, 918 (1978).

(41) Phillips, J. M., Michejda, J. A. and Wong, S. F.: "Resonant Electron Scattering from Vibrationally Excited CO", Bull. Am. Phys. Soc., Vol. 23, No. 9, p. 1081 (DEAP, Nov. 1978).

(42) Hake, R. D. and Phelps, A. V.: "Momentum-Transfer and Inelastic-Collision Cross Sections for Electrons in O_2, CO and CO_2", Phys. Rev. 158, 70 (1967).

(43) Chandra, N.: "Low-Energy Electron Scattering from CO. II. Ab Initio Study Using the Frame-Transformation Theory", Phys. Rev. A16, 80 (1977).

(44) Tanaka, H., Srivastava, S. K. and Chutjian, A.: "Absolute Elastic Differential Electron Scattering Cross Sections in the Intermediate Energy Region. IV. CO". J. Chem. Phys. 69, 5329 (1978).

(45) Choi, B. H., Poe, R. T., Sun, J. C., and Shan, Y.: "Two-Potential Approach for Electron-Molecular Collisions at Intermediate and High Energies; Application to e-N_2 Scattering", Phys. Rev. A19, 116 (1979).

*U.S.Government Printing Office: 1979 — 657-002/686